Journal of Molecular Modeling

Short contacts involving Germanium and Tin in crystal structures: Experimental evidence of tetrel bond

--Manuscript Draft--

Manuscript Number:	JMMO-D-17-00807R1
Full Title:	Short contacts involving Germanium and Tin in crystal structures: Experimental evidence of tetrel bond
Article Type:	TC Festschrift P. Politzer
Keywords:	Tetrel bond; Crystal engineering; σ-Hole interactions; Supramolecular interactions.
Corresponding Author:	Giuseppe Resnati Politecnico di Milano Dipartimento di Chimica Materiali e Ingegneria Chimica Giulio Natta ITALY
Corresponding Author Secondary Information:	
Corresponding Author's Institution:	Politecnico di Milano Dipartimento di Chimica Materiali e Ingegneria Chimica Giulio Natta
Corresponding Author's Secondary Institution:	
First Author:	Patrick Scilabra
First Author Secondary Information:	
Order of Authors:	Patrick Scilabra
	Vijith Kumar
	Maurizio Ursini
	Giuseppe Resnati
Order of Authors Secondary Information:	
Funding Information:	
Abstract:	Modelling indicates the presence of a region of lowest electronic density, a σ-hole, on Group 14 elements and this offers a rationalization for the ability of these elements to act as electrophilic sites and to form attractive interactions with nucleophiles. Many papers describe theoretical investigations of interactions involving carbon and silicon, less frequently the heavier Group 14 elements. The purpose of this review is to fill the current lack of experimental evidences on interactions formed by Germanium and Tin with nucleophiles. A survey of crystal structures in the Cambridge Structural Database is reported here. It reveals that close contacts between Ge or Sn and lone pair possessing atoms are quite common, they can occur both intra- and intermolecularly, and they are usually on the extension of the covalent bond formed by the tetrel with the most electron withdrawing substituent. Several examples are discussed wherein germanium and tin atoms bear four carbon residues or wherein halogen, oxygen, sulfur, or nitrogen substituents replace one, two, or three such carbon residues. These short contacts are assumed as the result of attractive interactions between the involved atoms and afford experimental evidences of the ability of Germanium and Tin to work as electrophilic sites, namely to act as tetrel bond (TB) donors. This ability can govern and control the conformation and the packing of organic derivatives in the solid state. TB can thus be considered a promising and robust tool for crystal engineering.
Response to Reviewers:	The manuscripted was revised after the reviewers' comments.

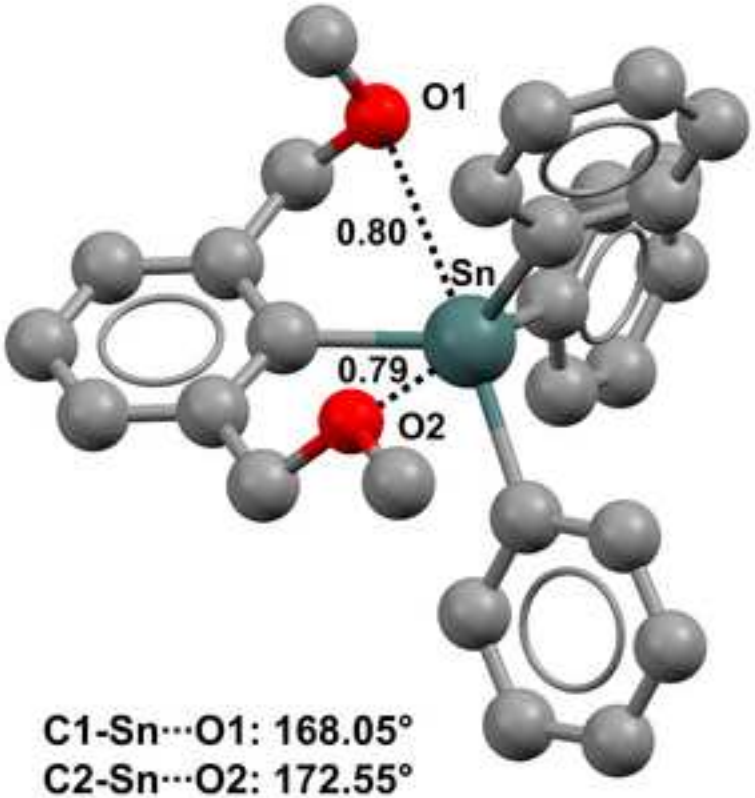

C1-Sn···O1: 168.05°
C2-Sn···O2: 172.55°

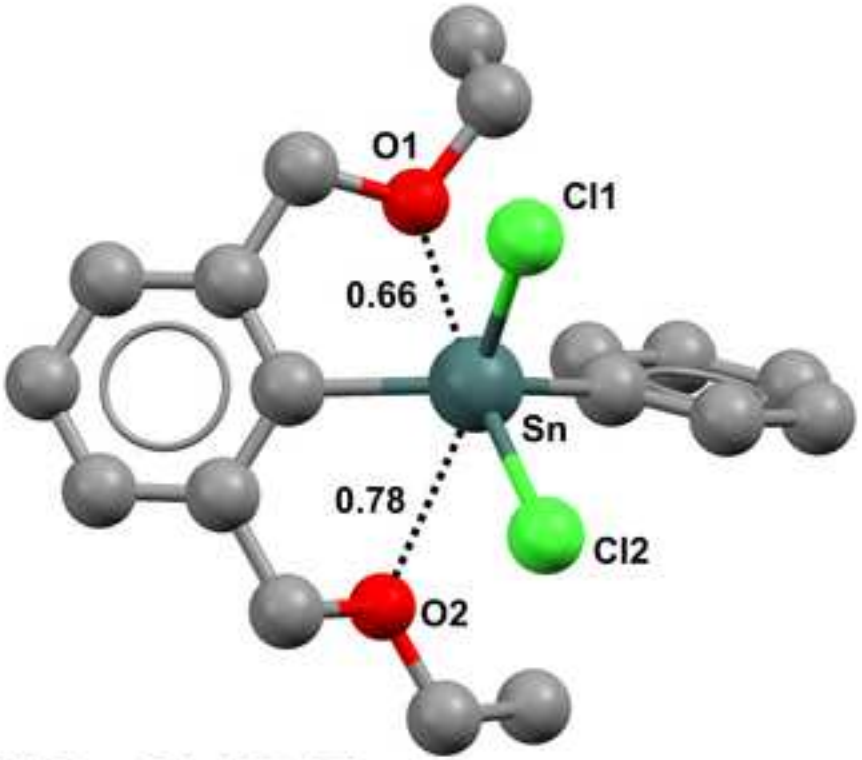

Cl1-Sn···O1: 167.65°
Cl2-Sn···O2: 155.14°

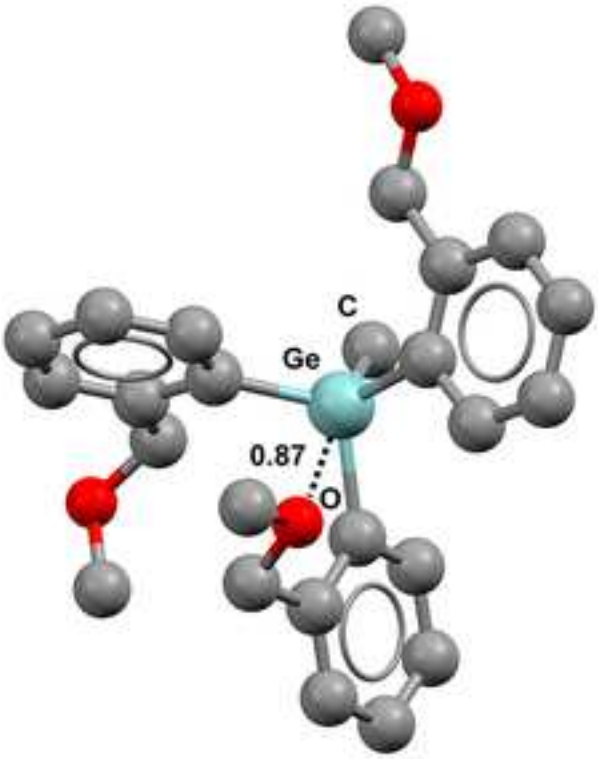

C-Ge···O: 171.79°

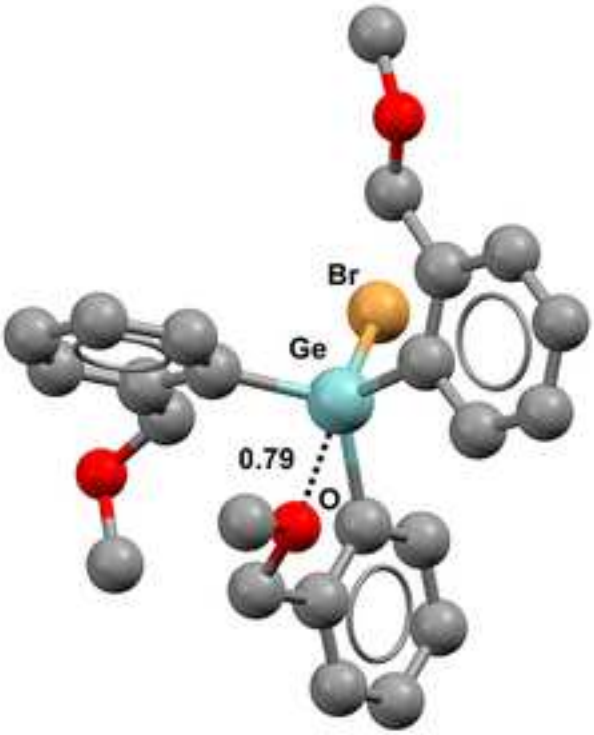

Br-Ge···O: 172.64°

Cl-Ge···O: 173.24°

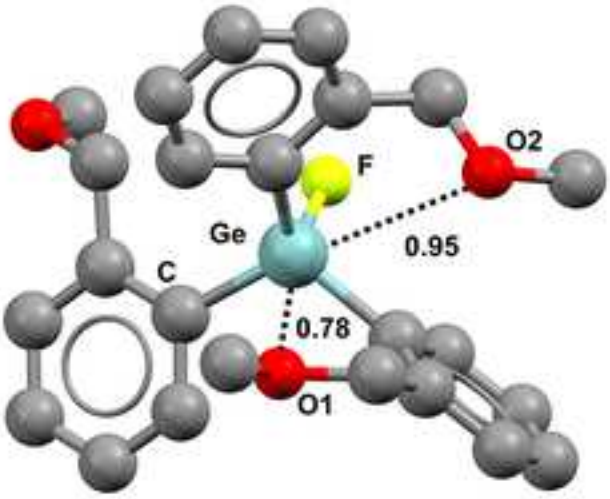

F-Ge···O1: 168.50°
C-Ge···O2: 169.90°

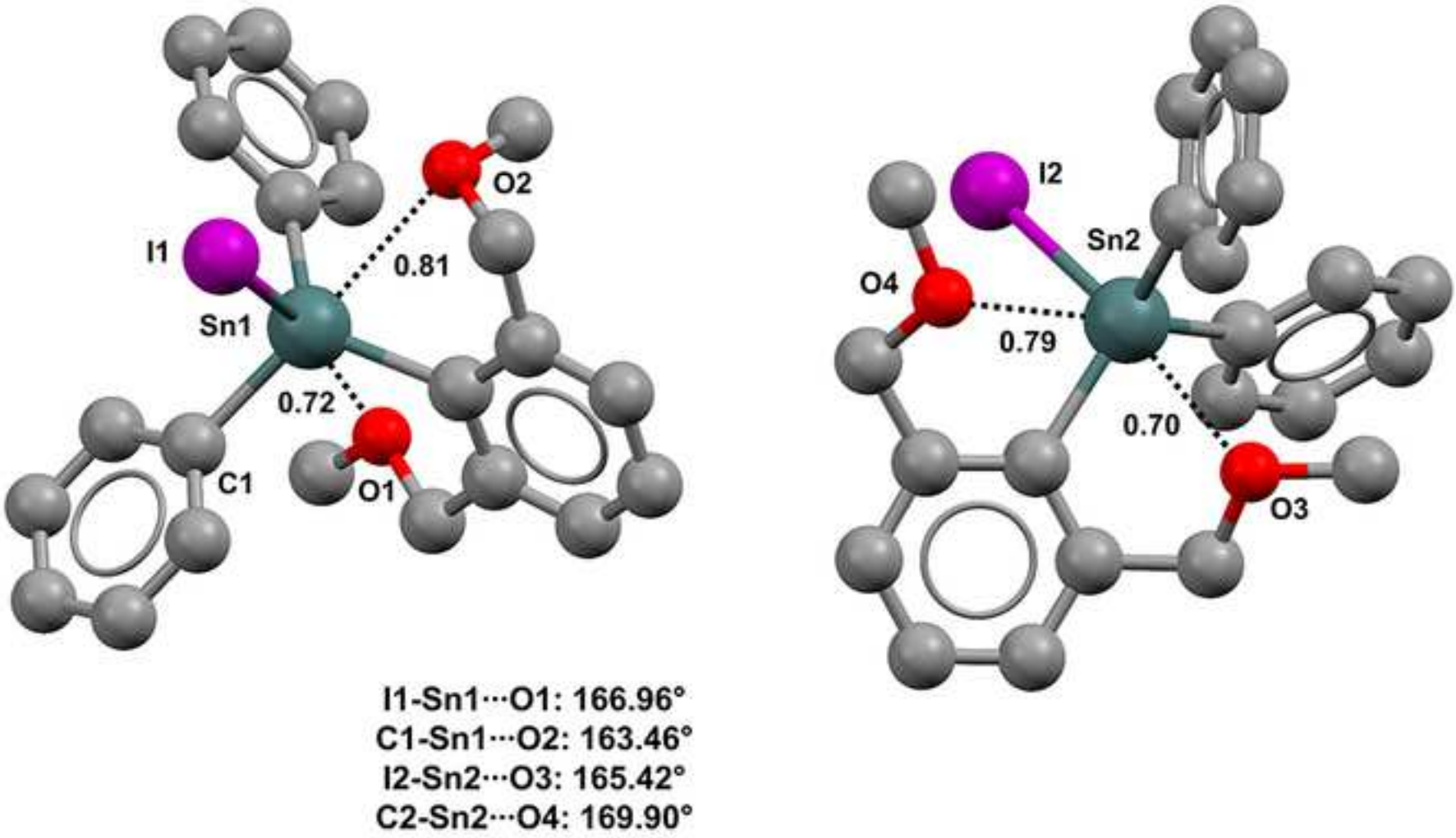

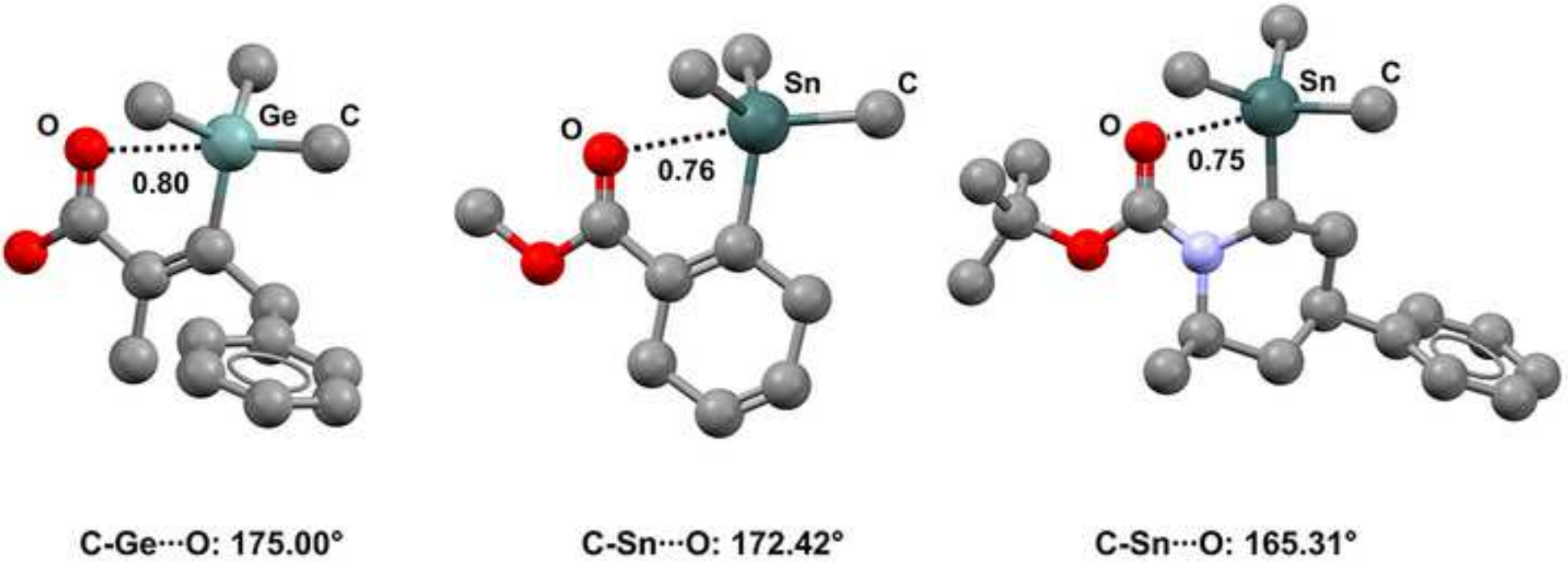

C-Ge···O: 175.00°

C-Sn···O: 172.42°

C-Sn···O: 165.31°

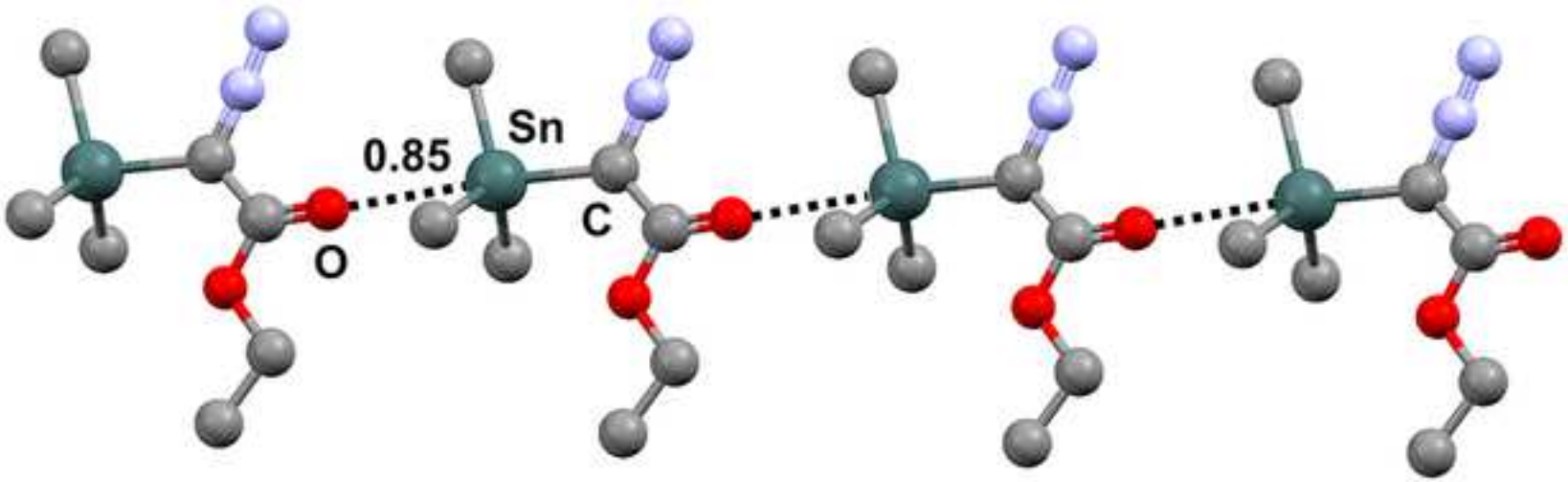

C-Sn···O: 176.46°

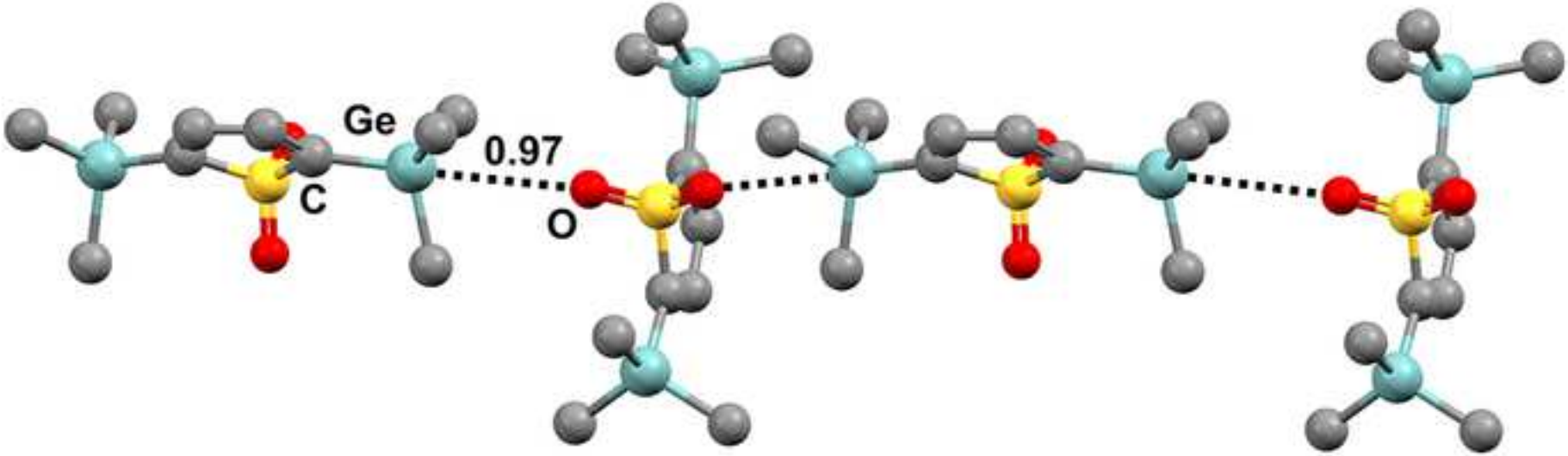

C-Ge···O: 179.77°

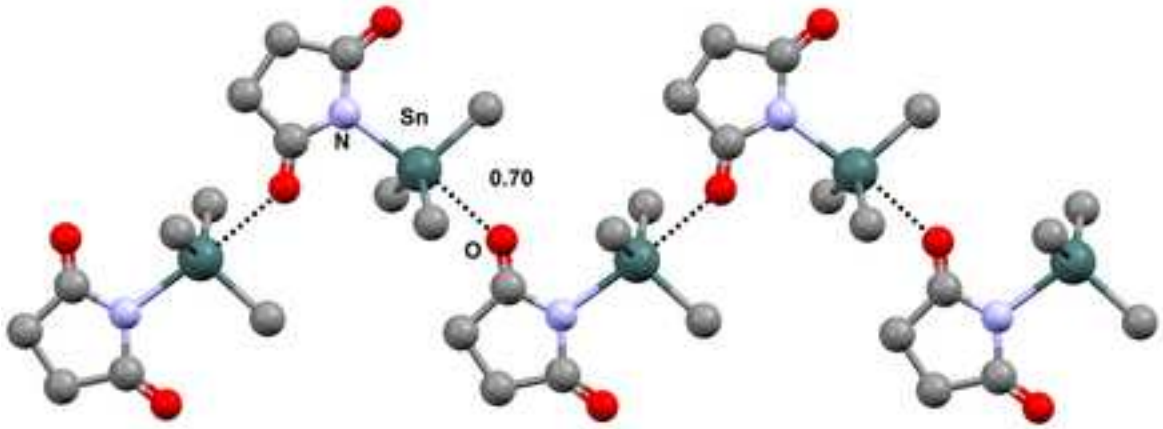

N-Sn···O: 173.44°

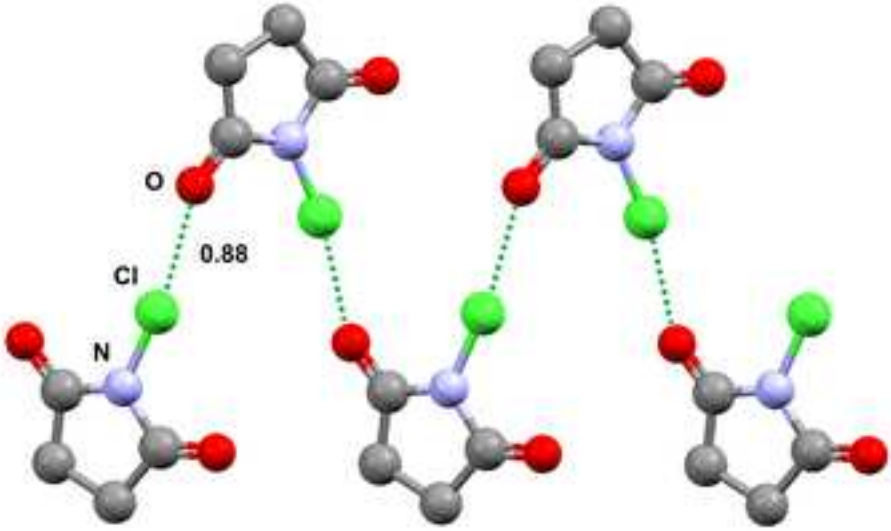

N-Cl···O: 168.87°

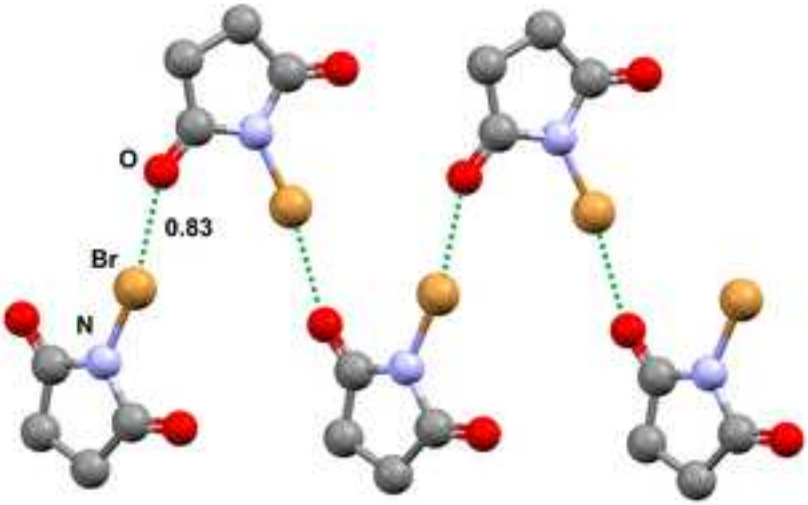

N-Br···O: 169.54°

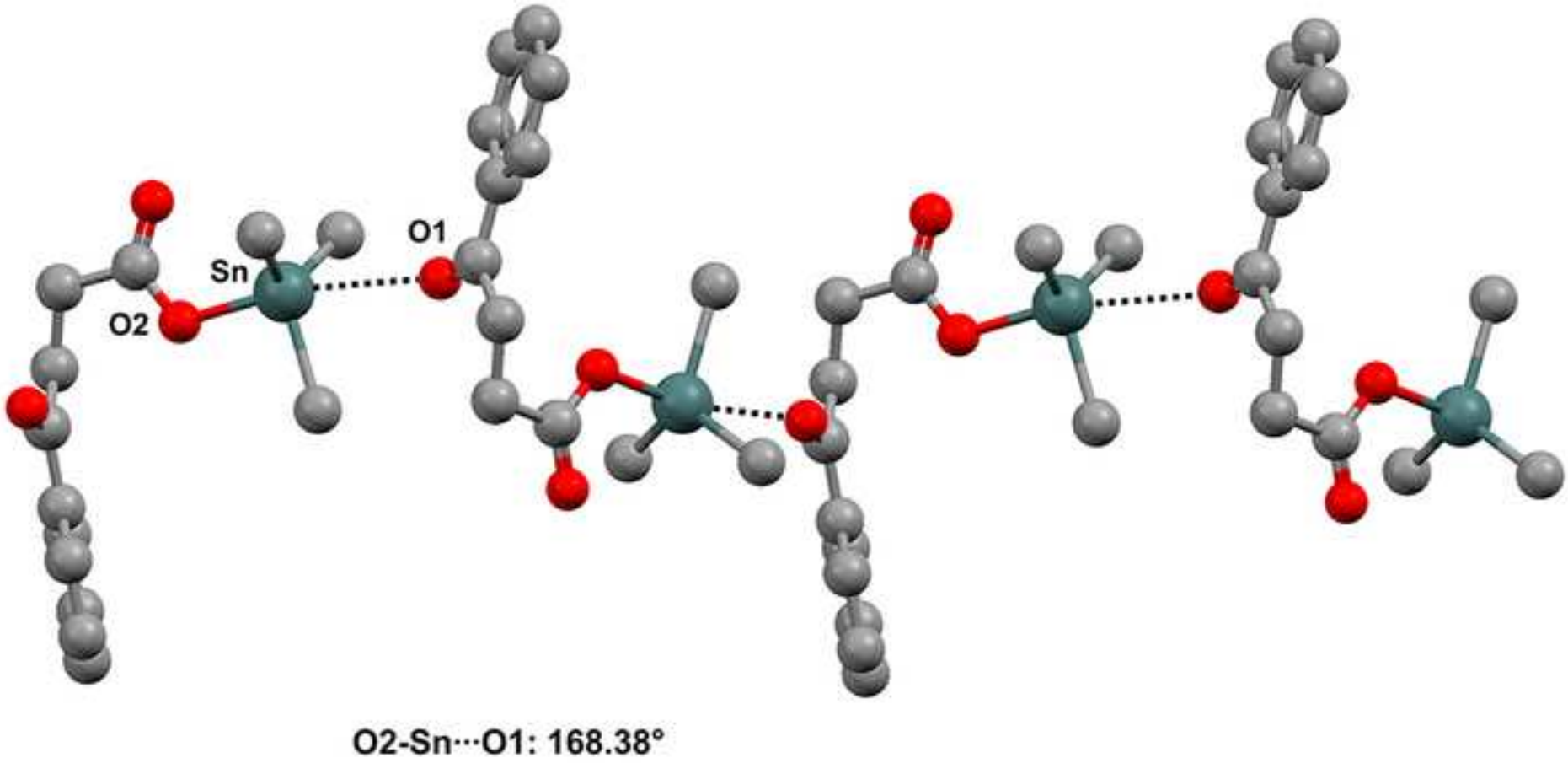

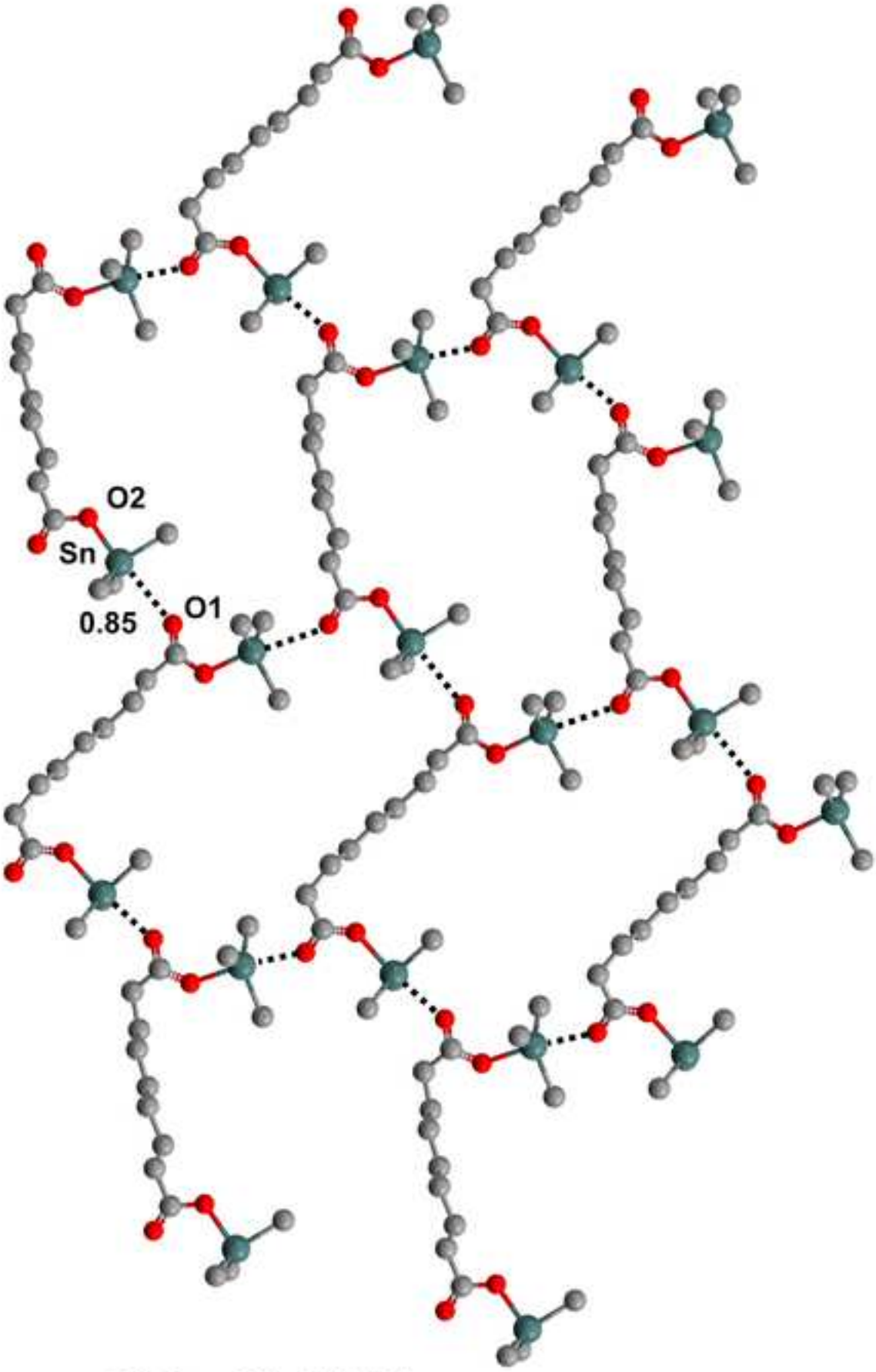

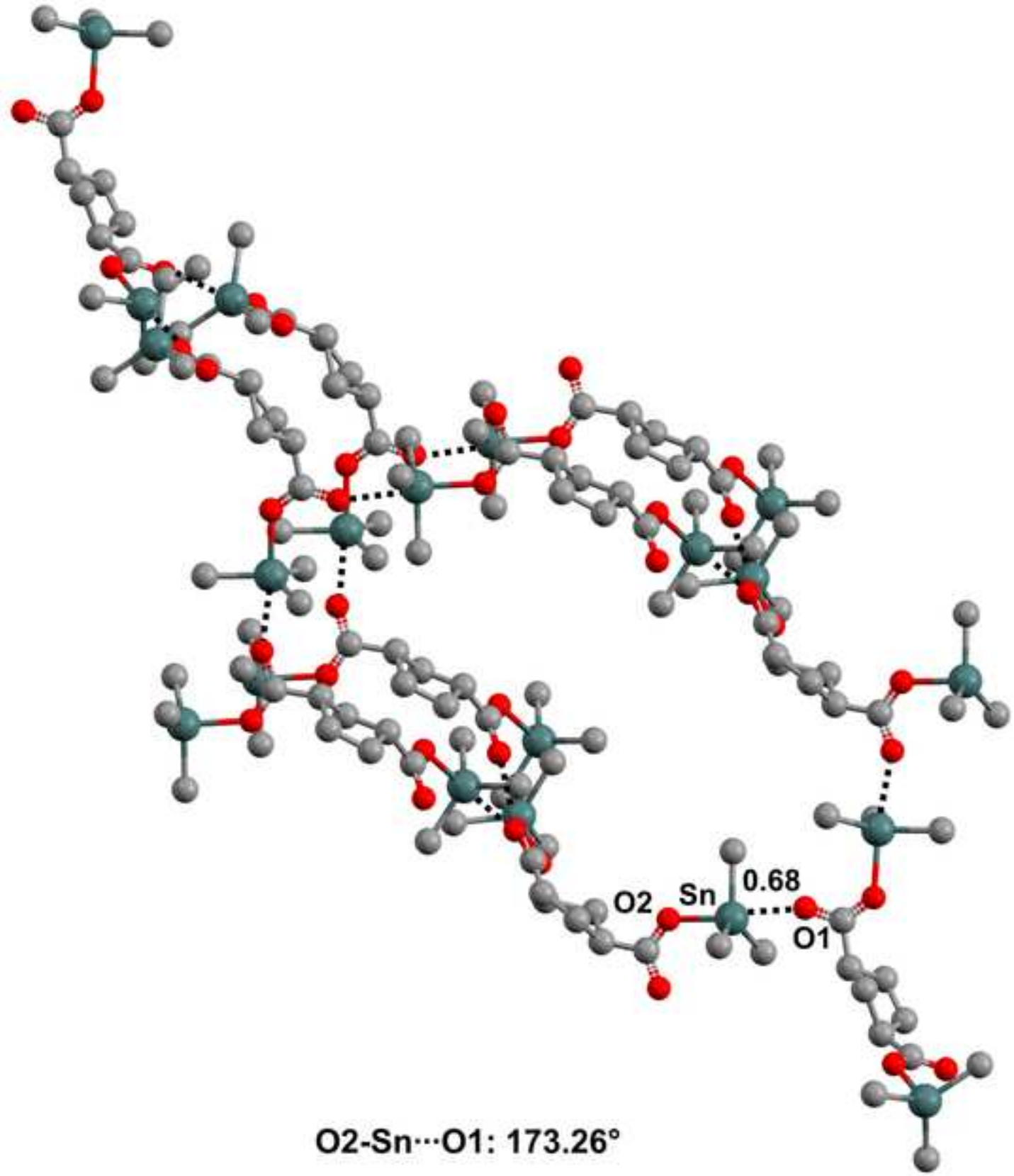

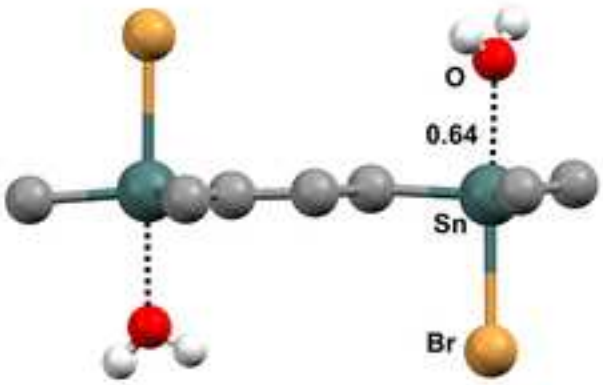

Br-Sn···O: 174.77°

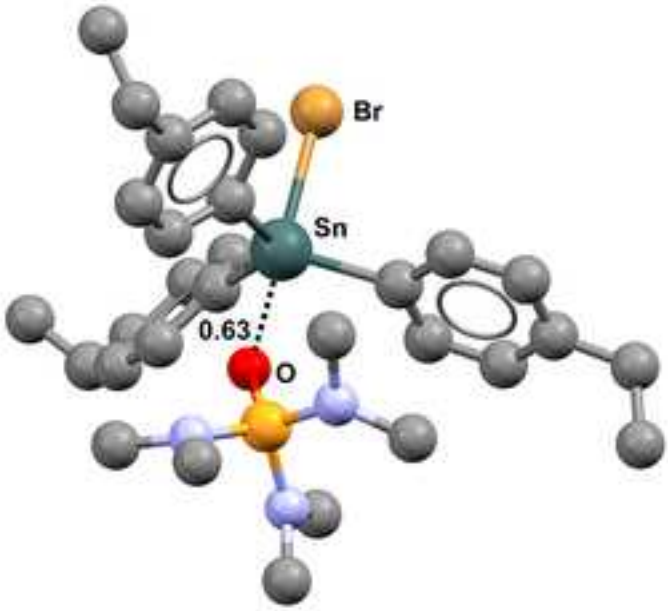

Br-Sn···O: 179.19°

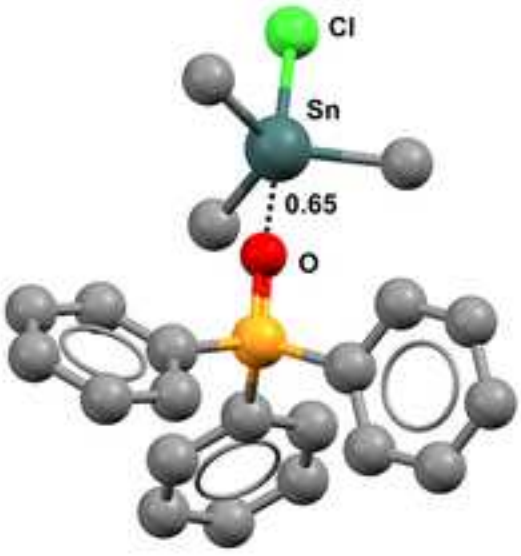

Cl-Sn···O: 177.40°

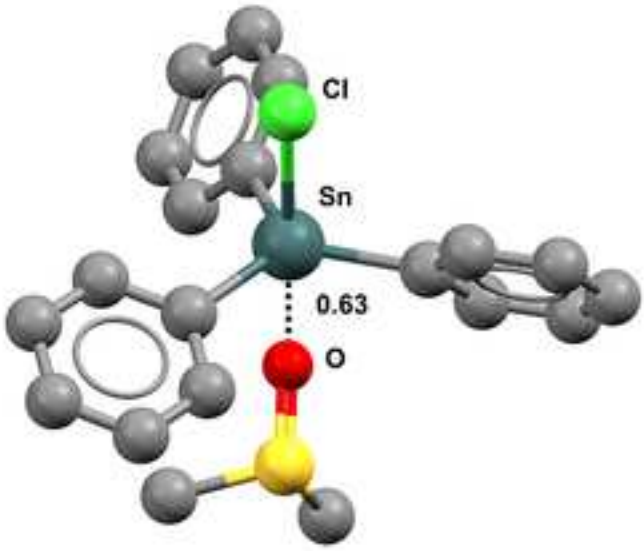

Cl-Sn···O1: 179.00°

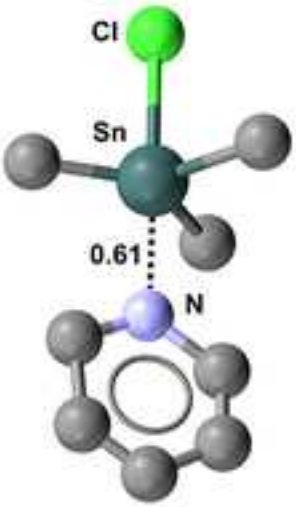

Cl-Sn···N: 179.18°

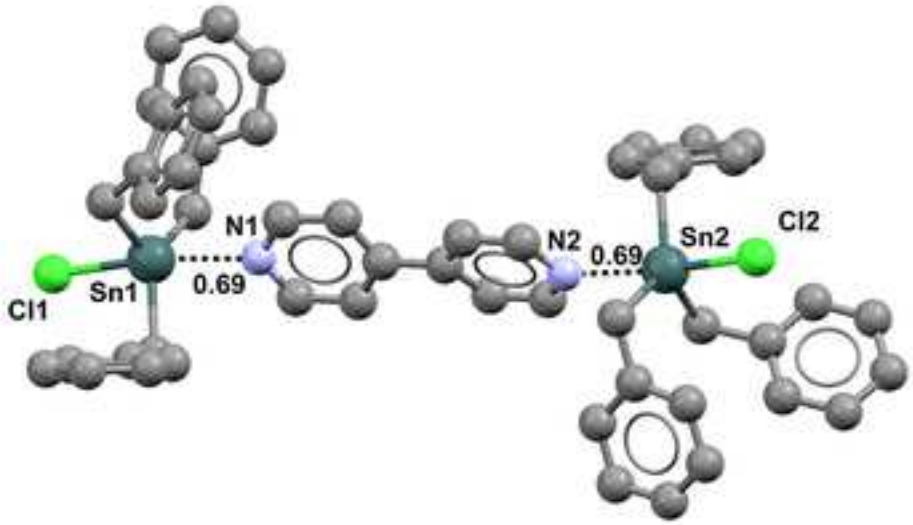

Cl1-Sn1···N1: 169.62°
Cl2-Sn2···N2: 171.48°

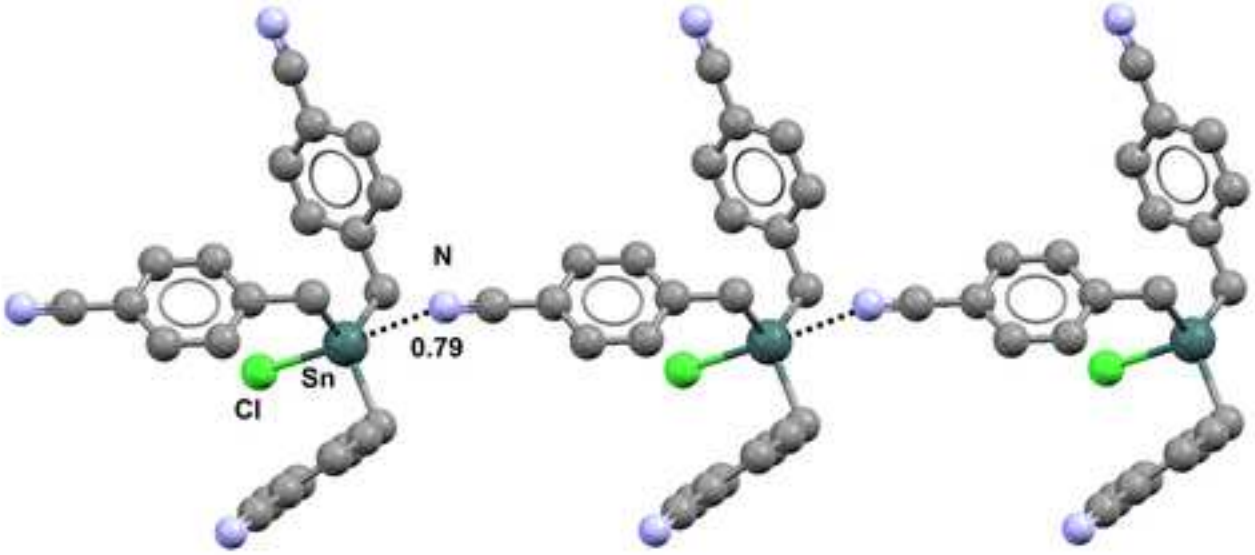

Cl-Sn···N: 175.06°

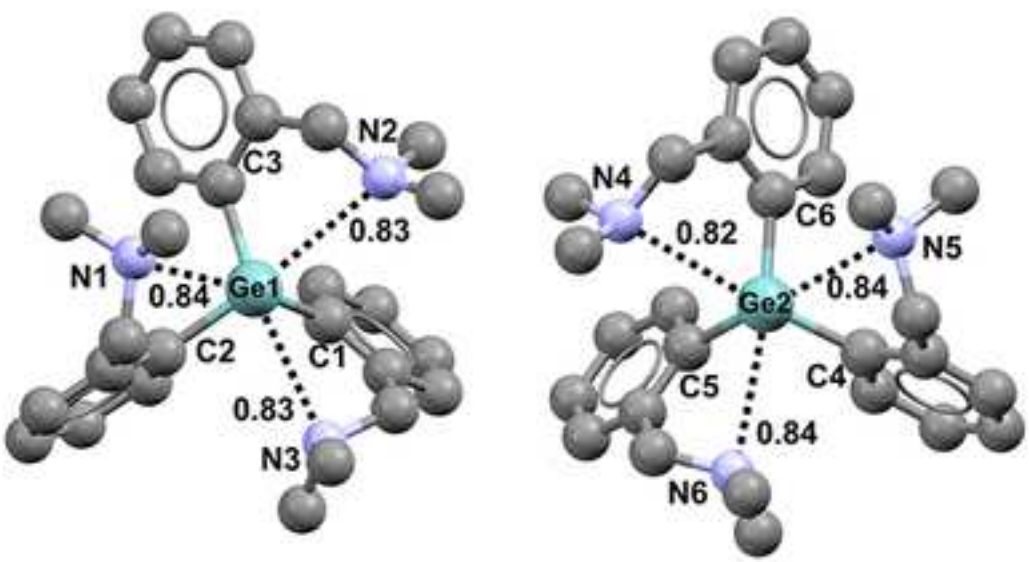

C1-Ge1···N1: 173.89°
C2-Ge1···N2: 173.90°
C3-Ge1···N3: 172.66°
C4-Ge2···N4: 174.37°
C5-Ge2···N5: 176.79°
C6-Ge2···N6: 172.45°

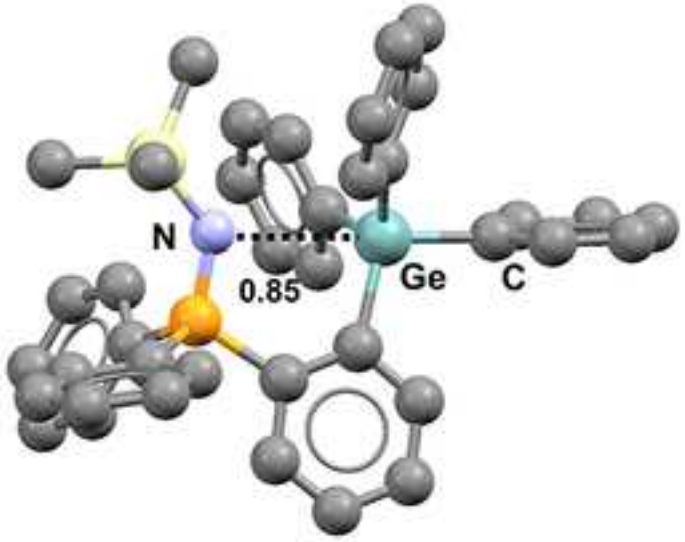

C-Ge···N: 173.79°

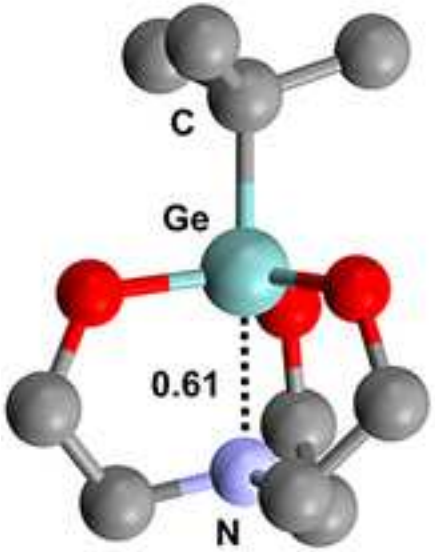

C-Ge···N: 180.00°

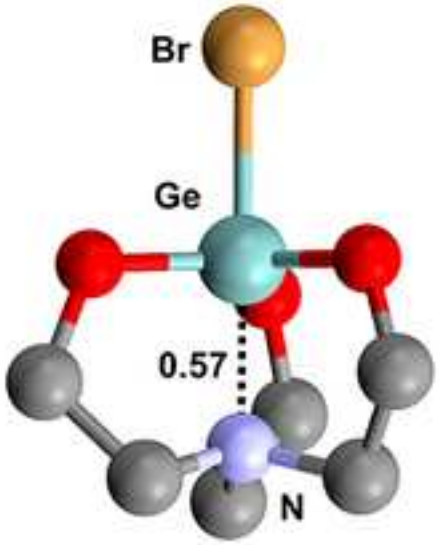

Br-Ge···N: 179.73°

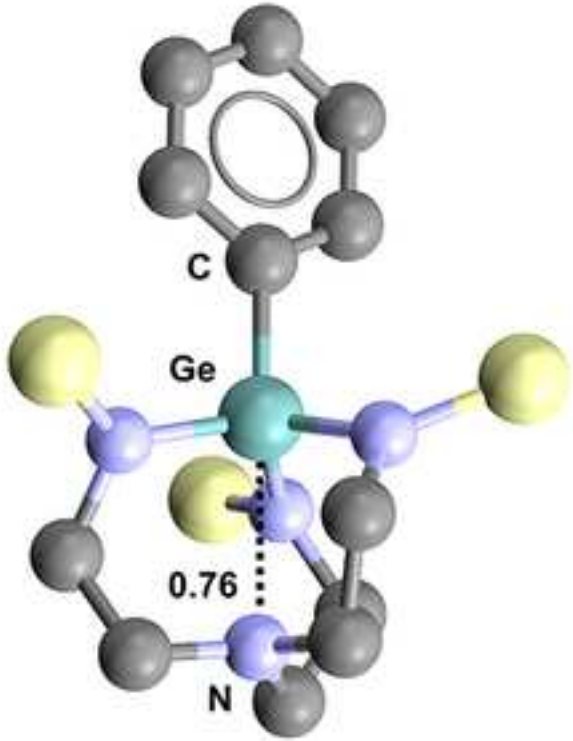

C-Ge···N: 176.39°

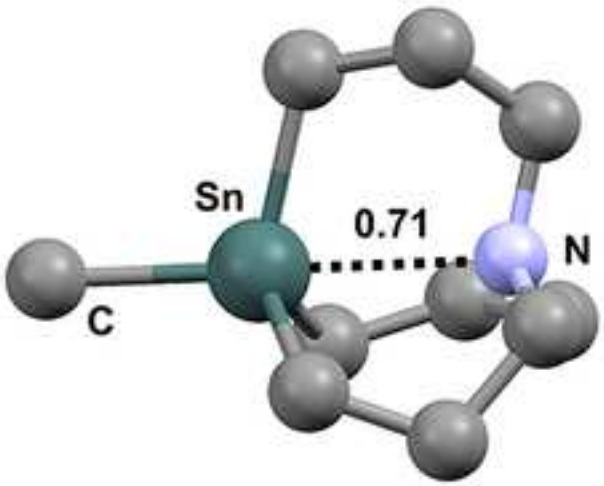

F-Sn···N: 179.57°

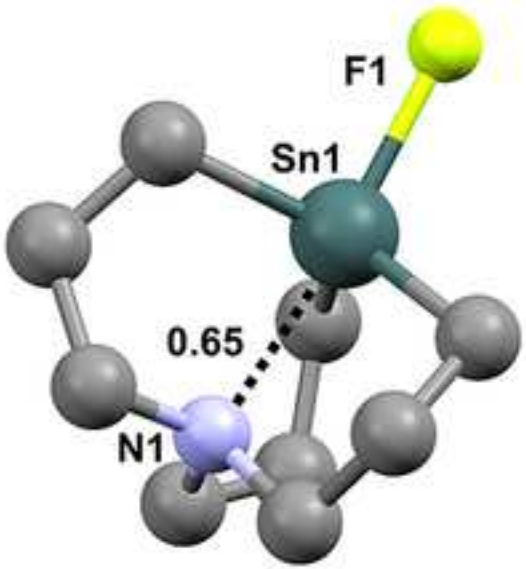

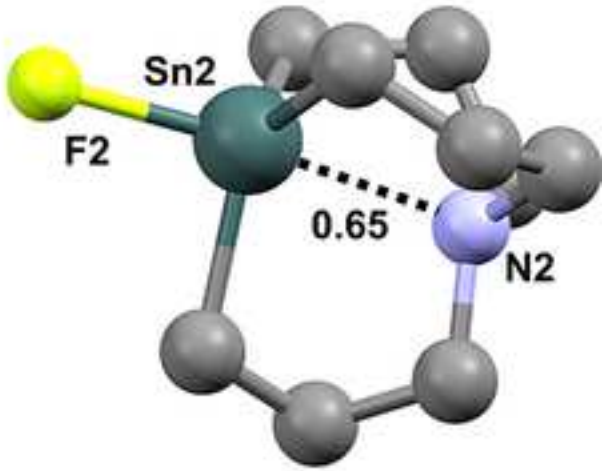

F1-Sn1···N1: 173.96°
F2-Sn2···N2: 172.73°

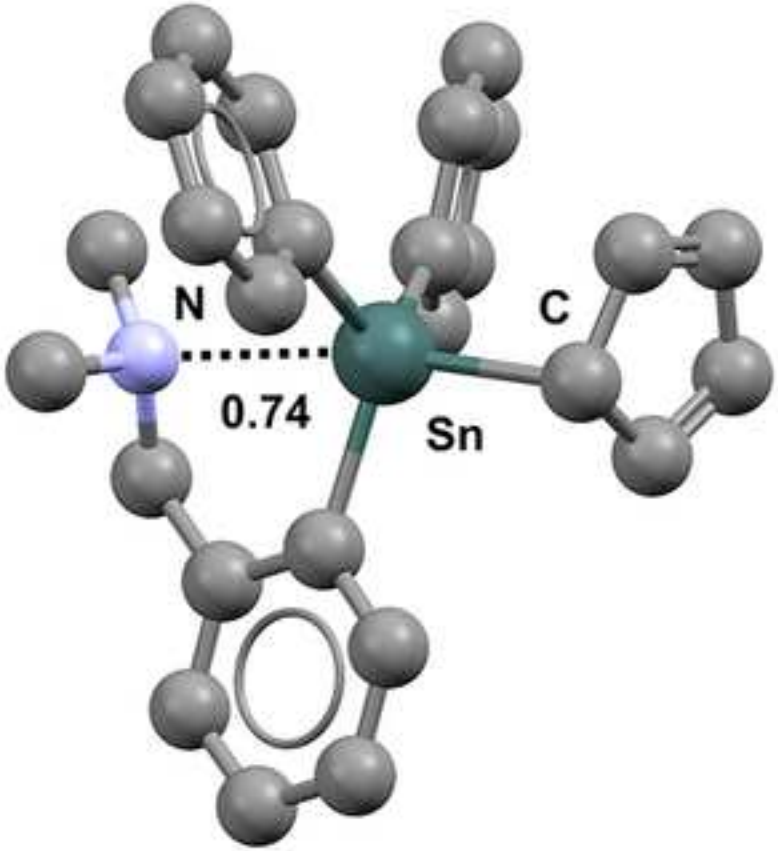

C-Sn···N: 171.08°

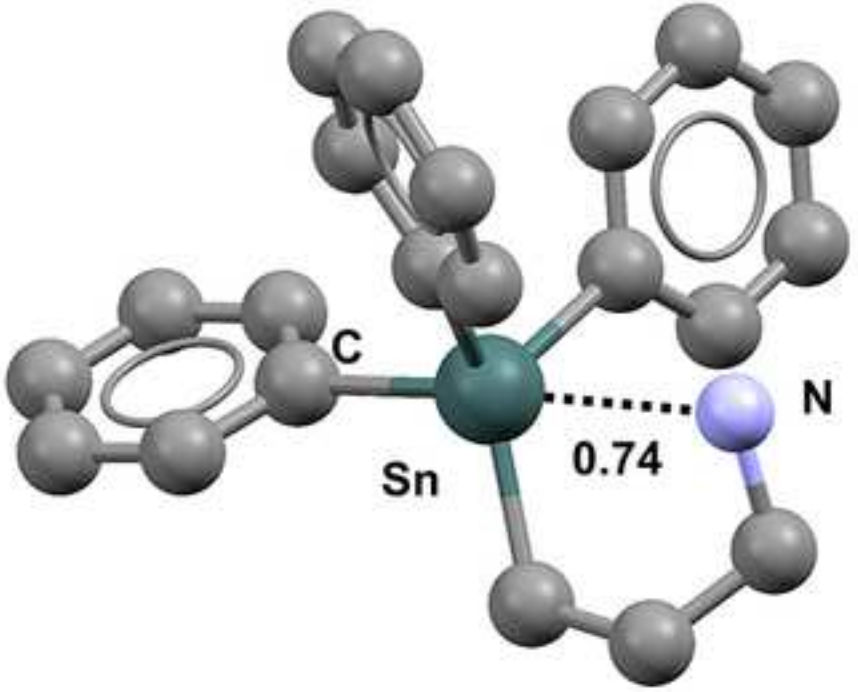

C-Sn···N: 175.81°

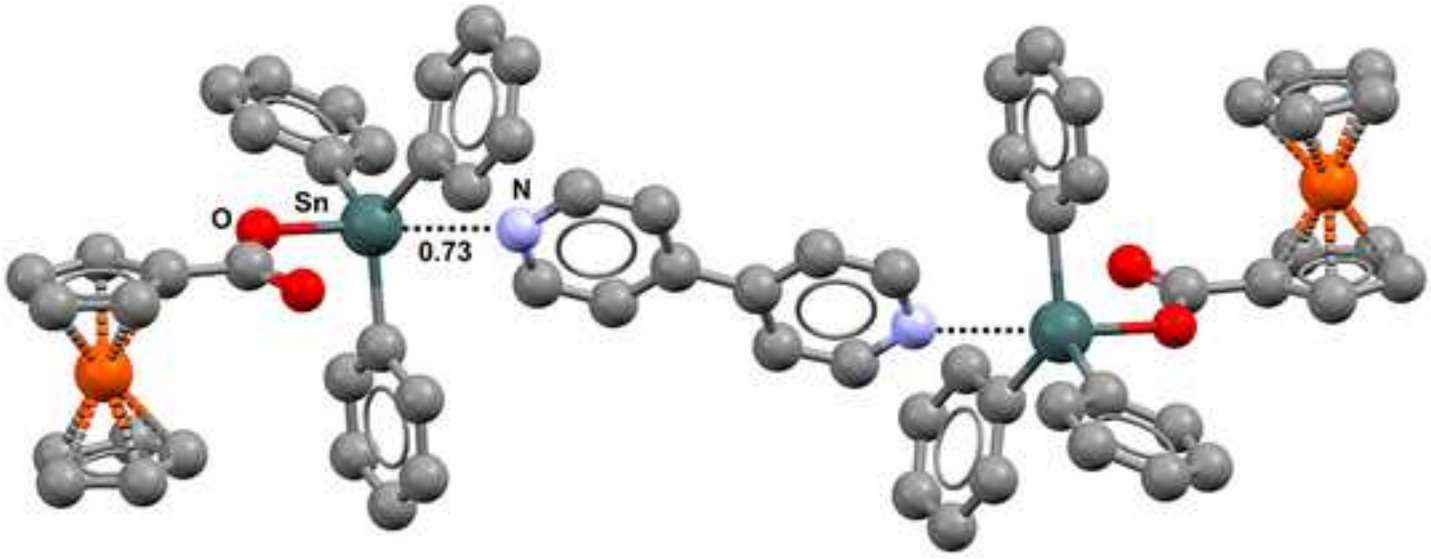

O-Sn···N: 175.85°

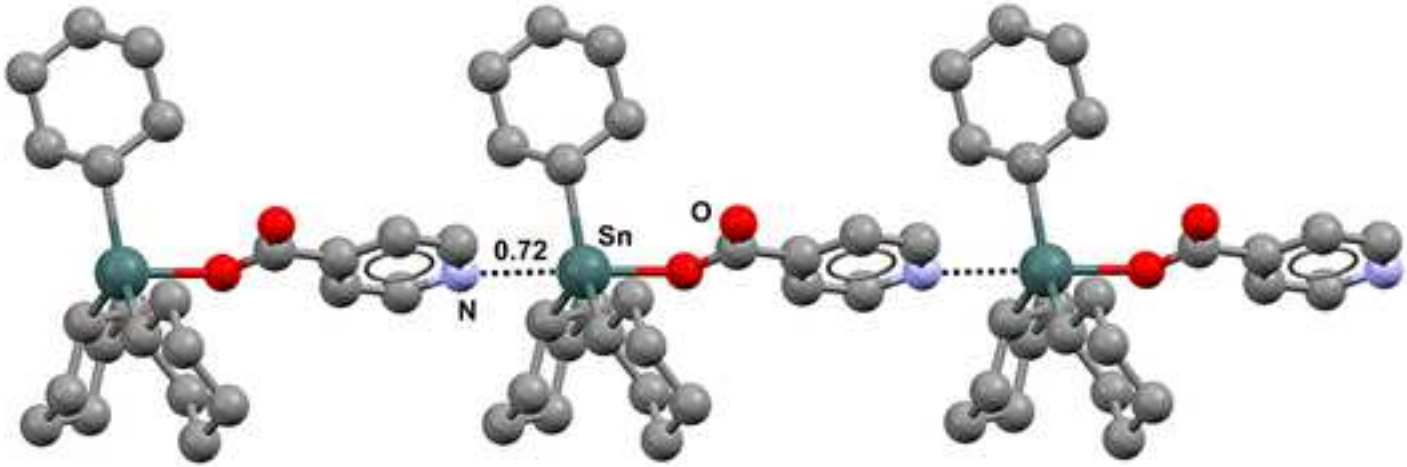

O-Sn···N: 179.45°

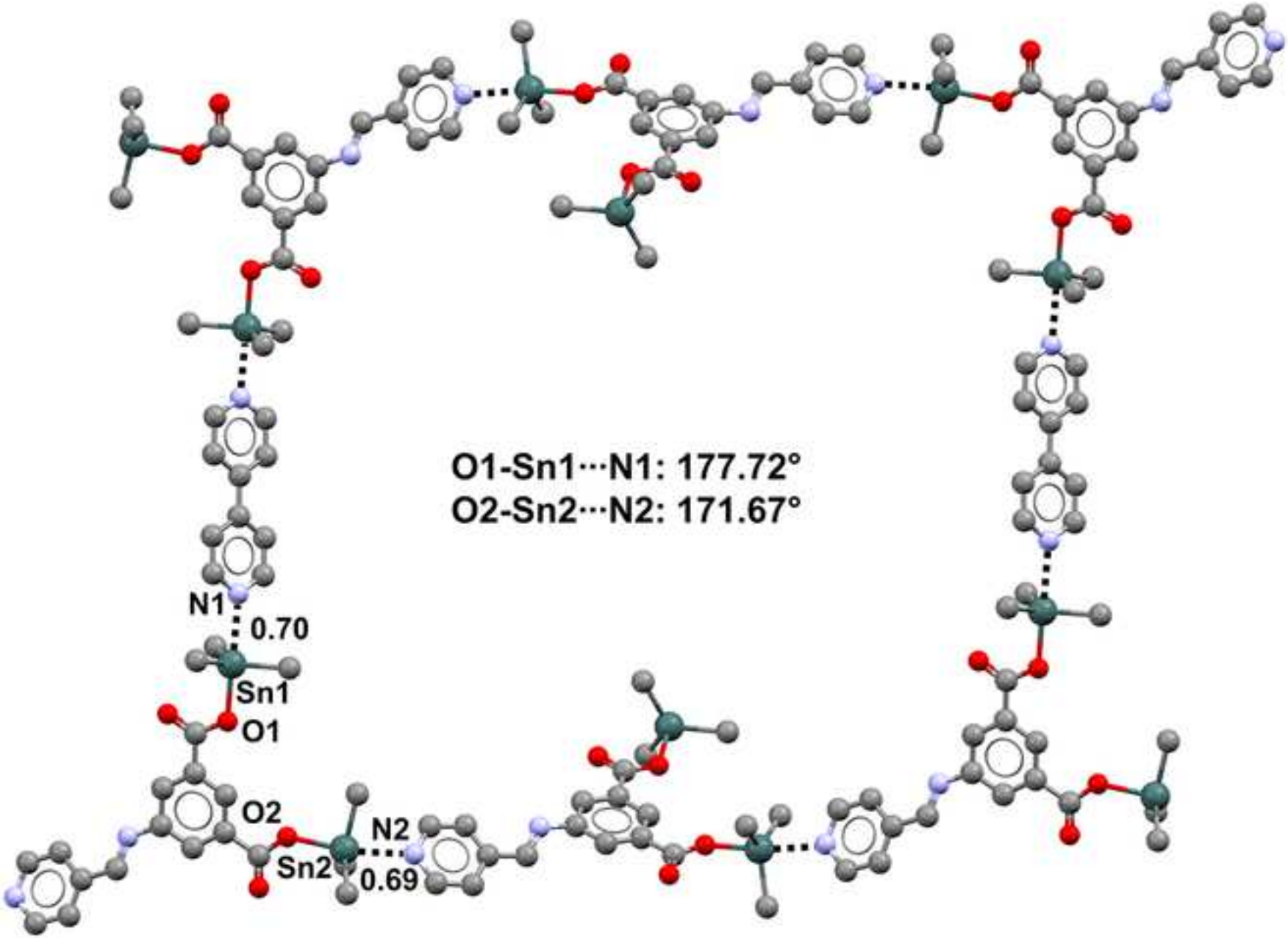

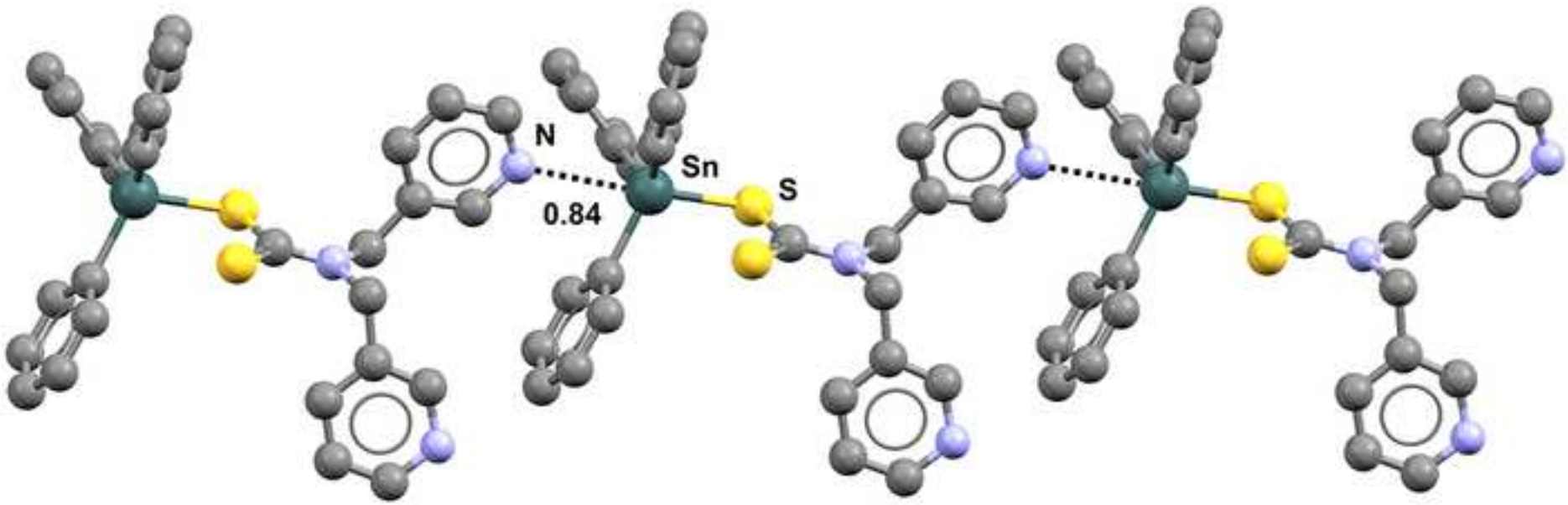

S-Sn···N: 174.50°

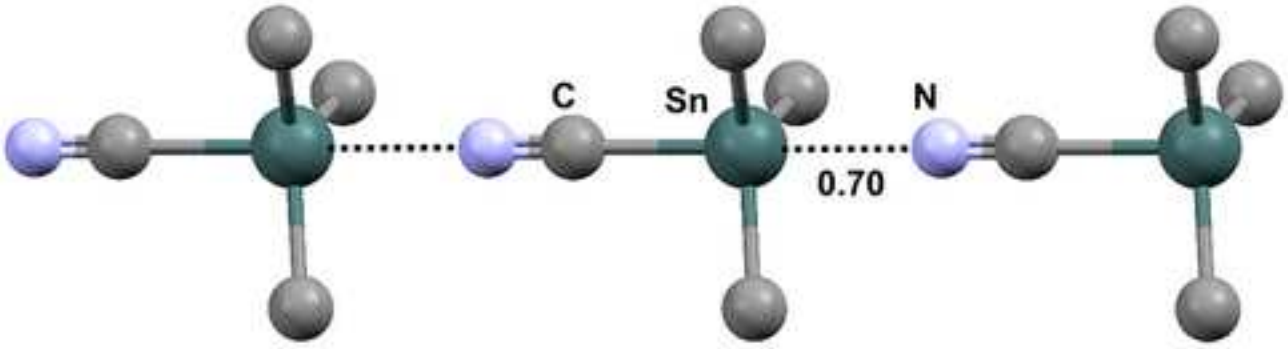

C-Sn···N: 178.68°

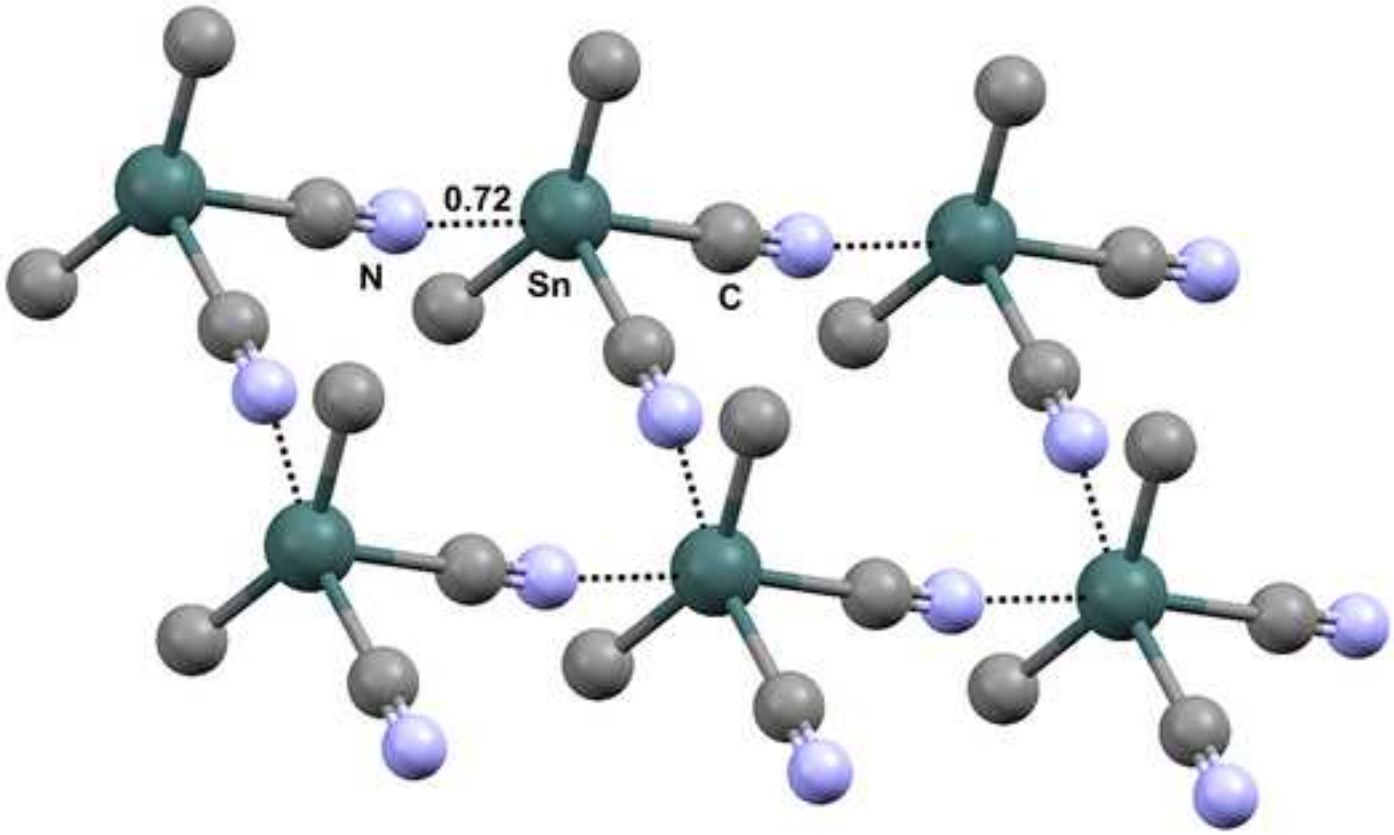

C-Sn···N: 167.88°

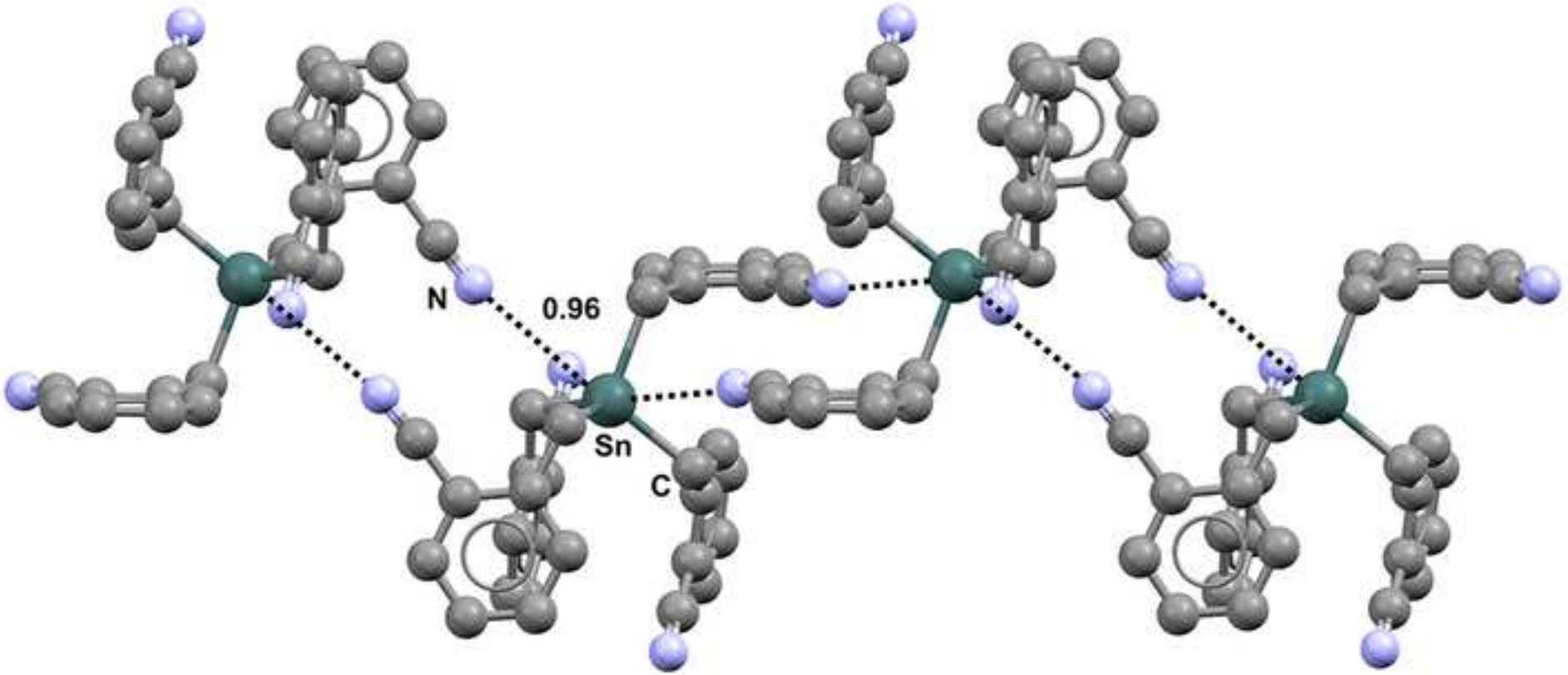

C-Sn···N: 178.46°

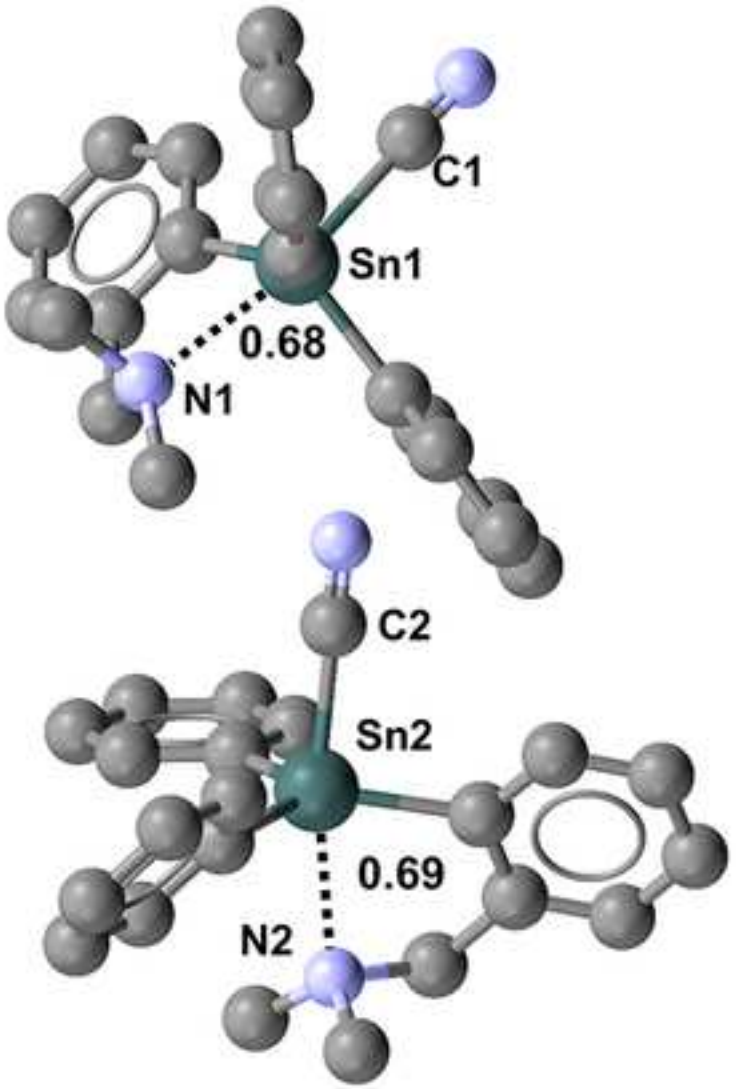

C1-Sn1···O1: 168.20°
C2-Sn2···O2: 169.44°

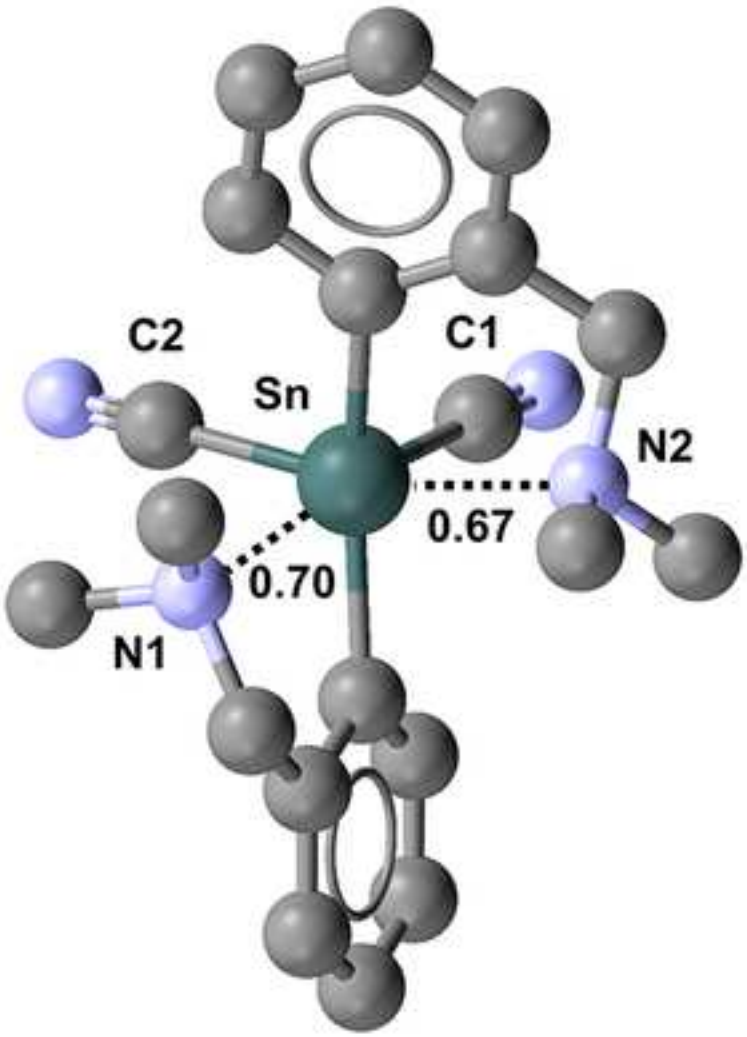

C1-Sn···O1: 168.56°
C2-Sn···O2: 165.95°

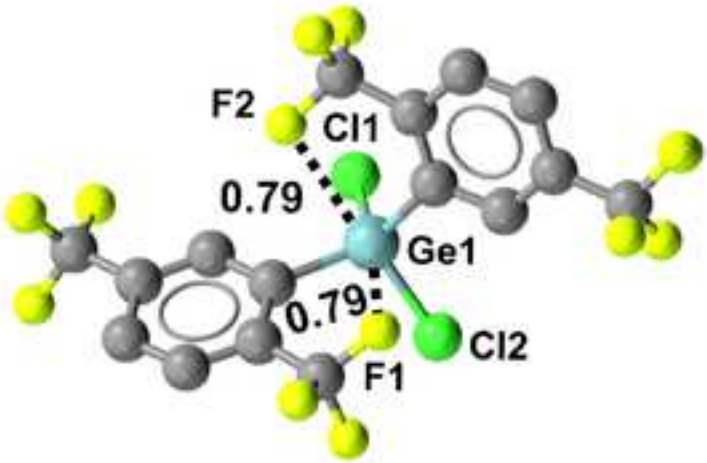

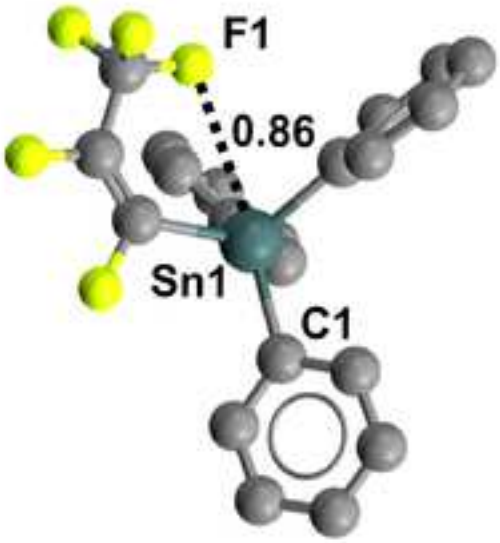

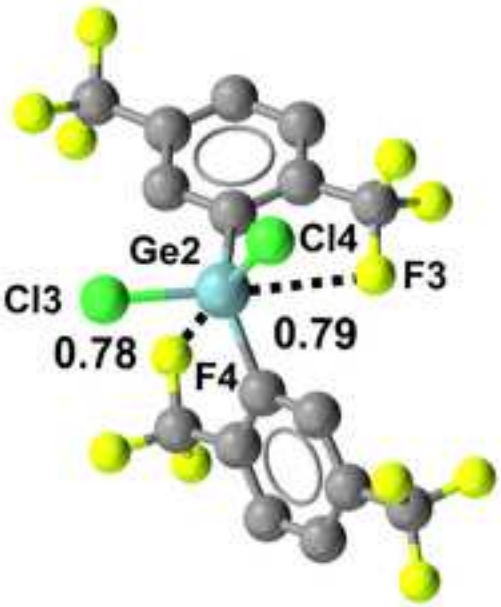

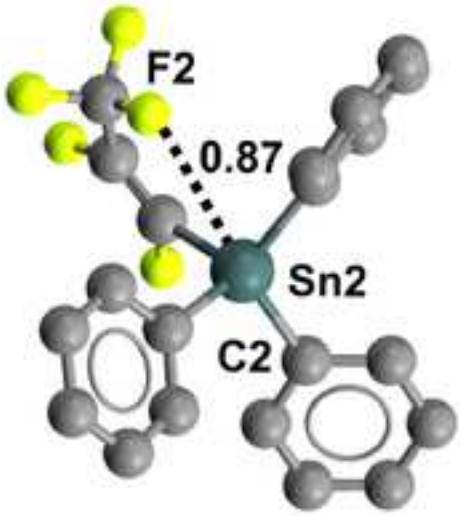

Cl1-Ge1···F1: 175.19°
Cl2-Ge1···F2: 174.93°
Cl3-Ge2···F3: 176.15°
Cl4-Ge2···F4: 175.71°

C1-Sn···F1: 160.68°
C2-Sn···F2: 155.74°

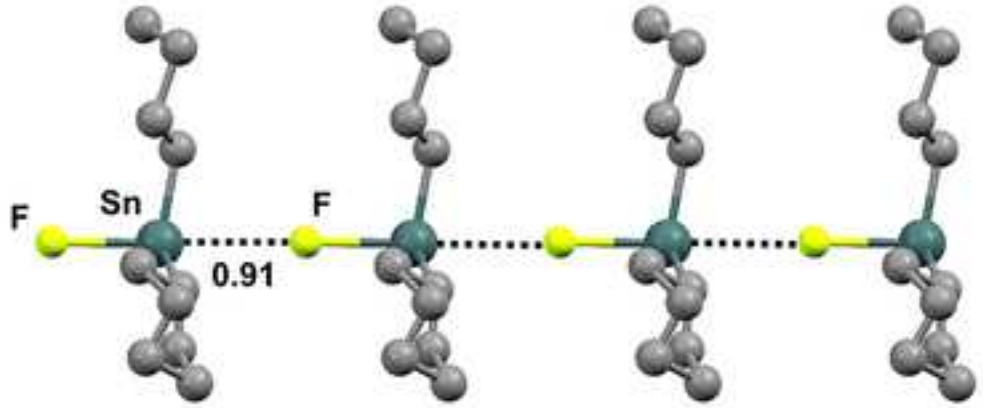

F-Sn···F: 178.85°

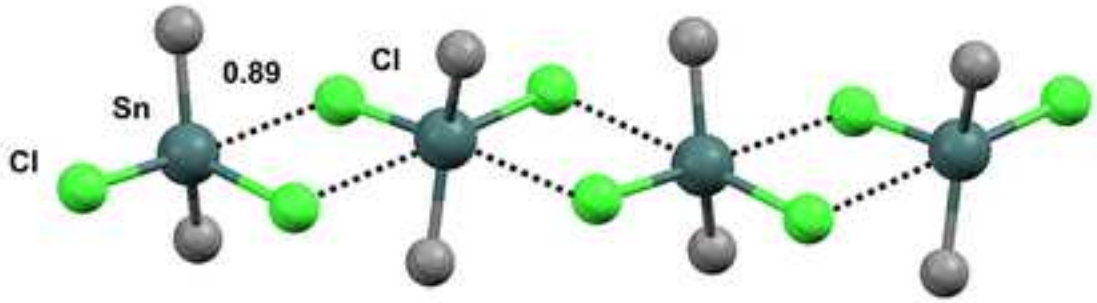

Cl-Sn···Cl: 178.59°

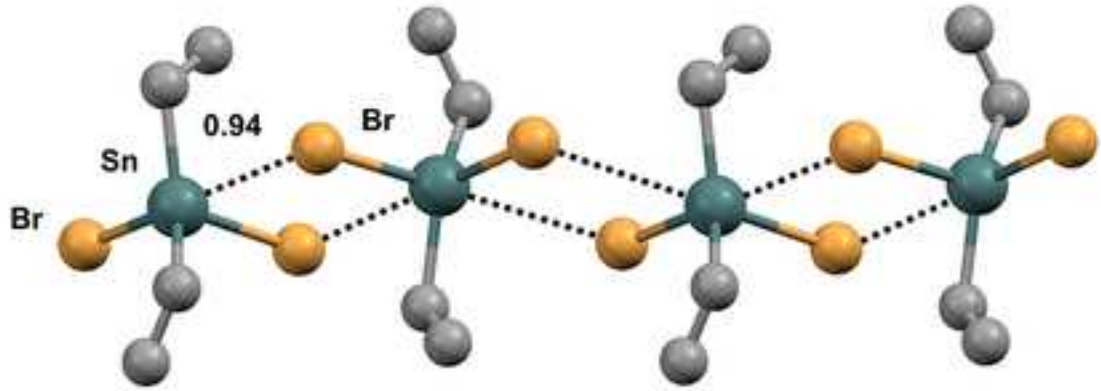

Br-Sn···Br: 179.55°

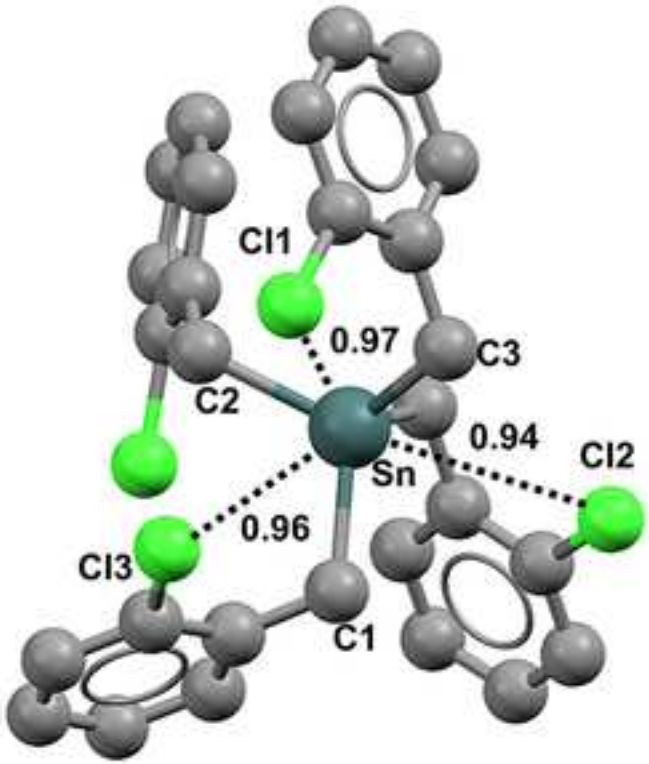

Cl1-Sn···C1: 158.54°
Cl2-Sn···C2: 164.09°
Cl3-Sn···C3: 155.47°

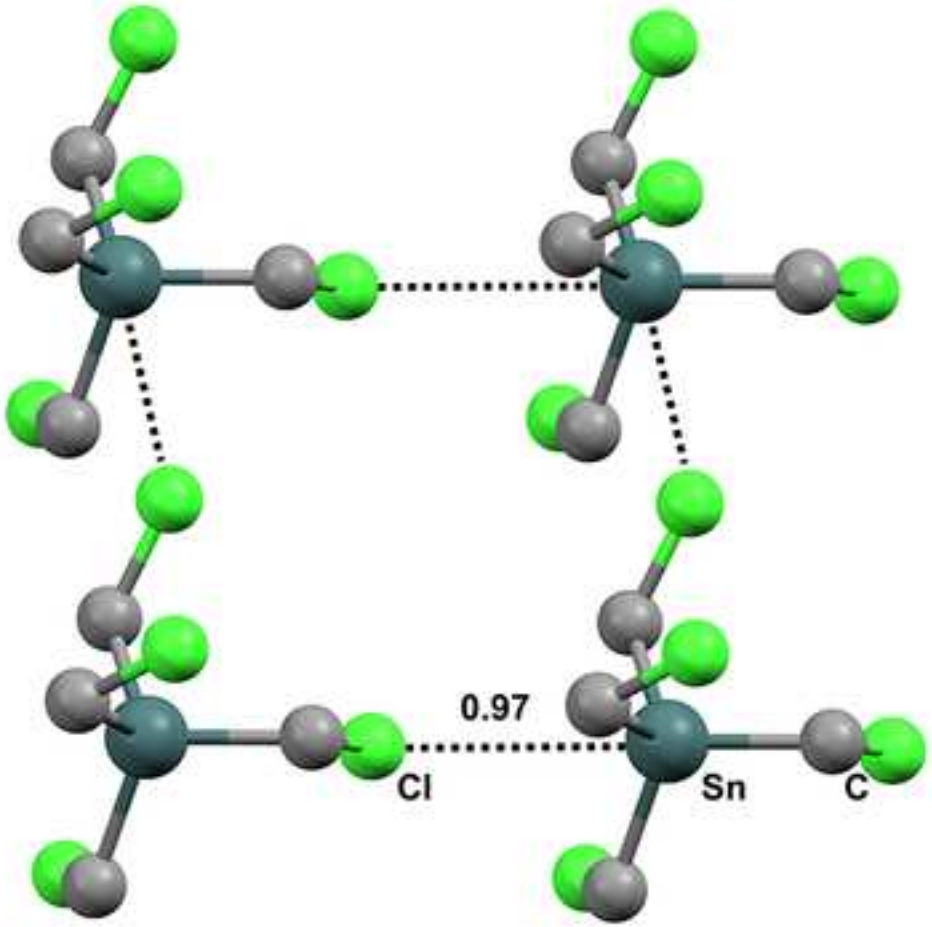

Cl-Sn···C: 175.71°

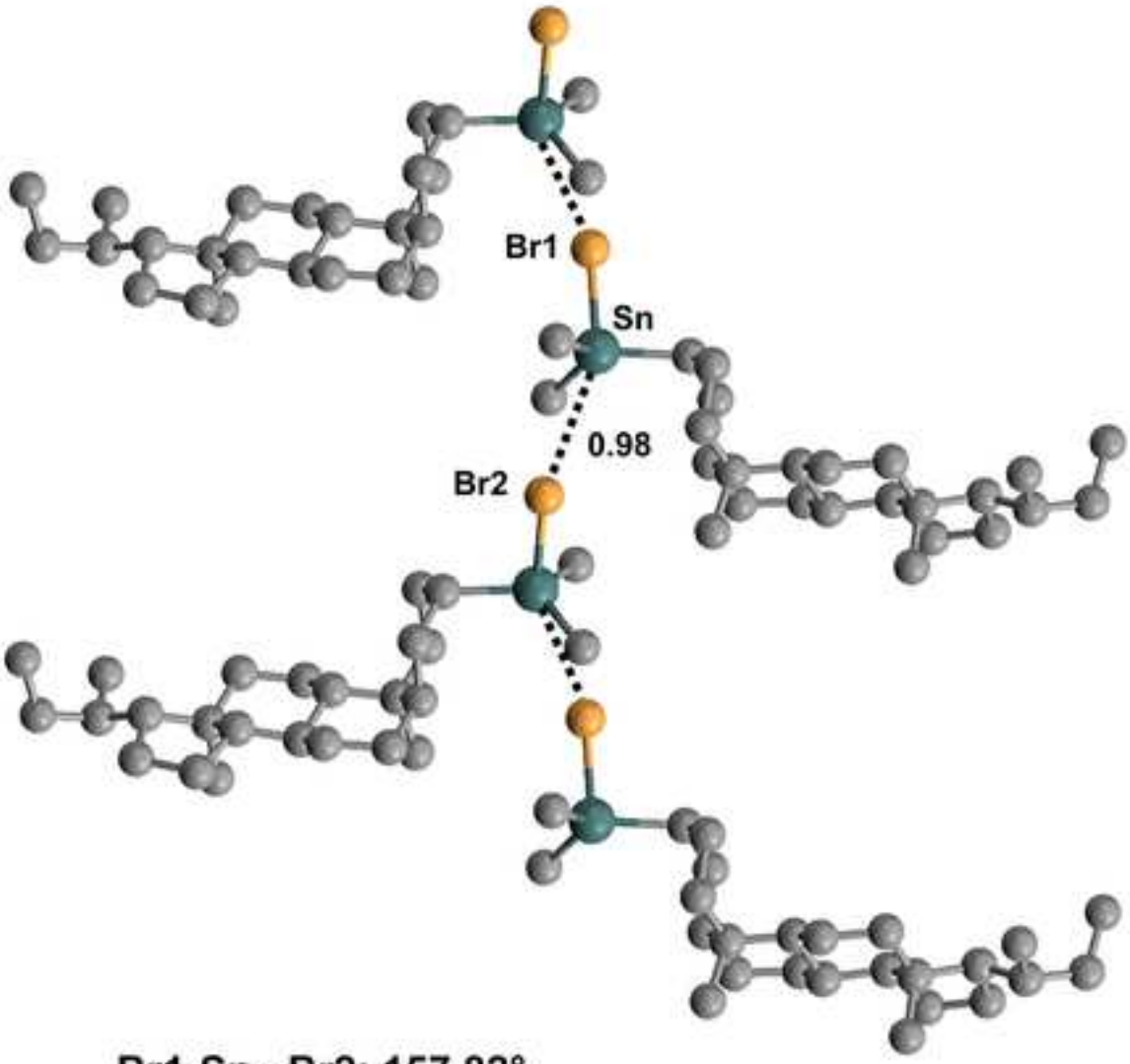

Br1-Sn···Br2: 157.82°

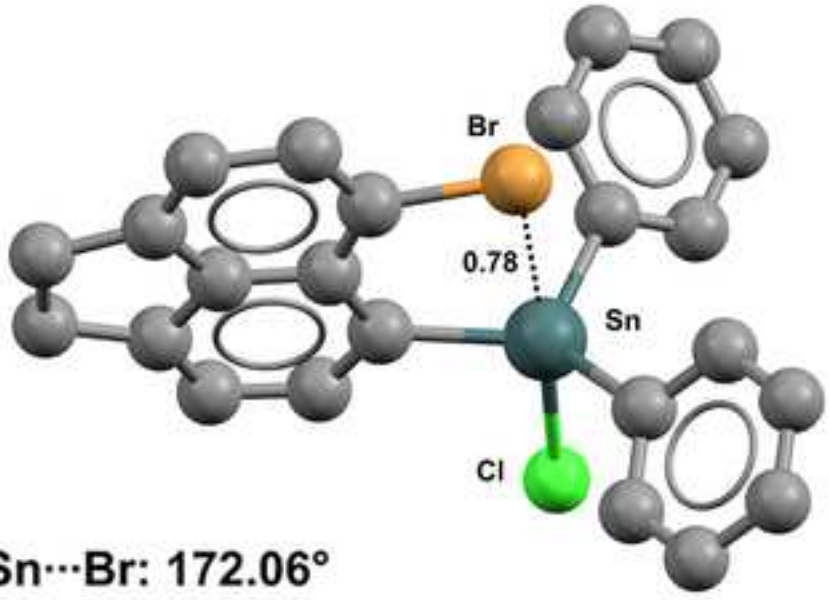

Cl-Sn···Br: 172.06°

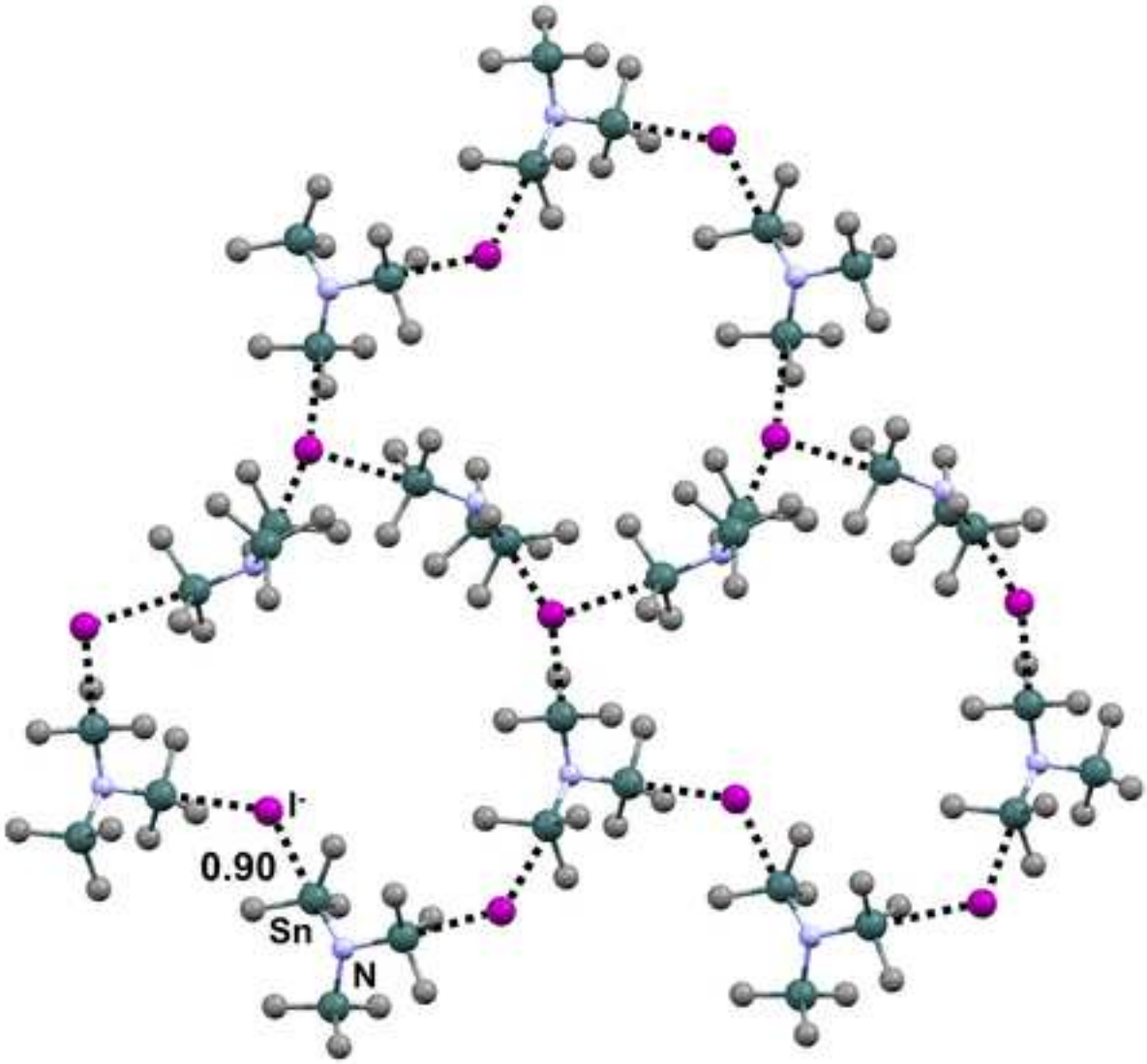

N-Sn···I-: 175.64°

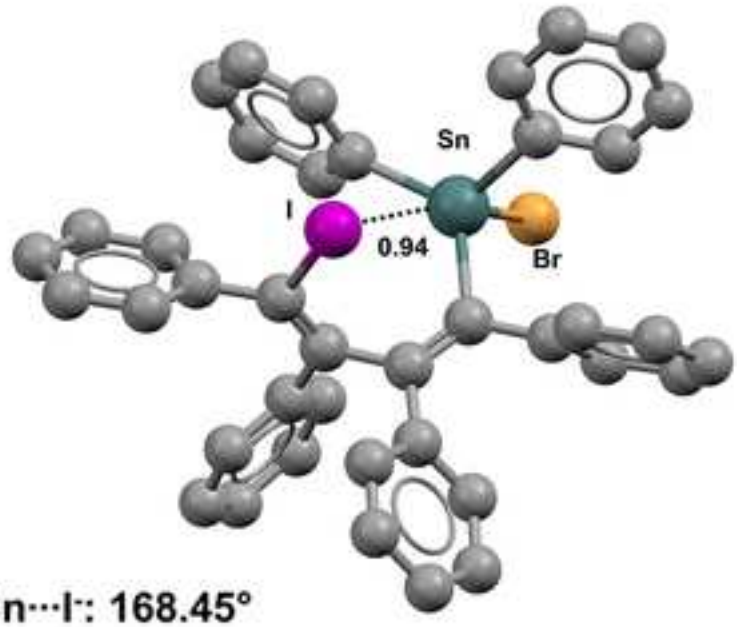

Br-Sn···I-: 168.45°

Abstract graphic

Click here to download Abstract graphic graphicalabstract_JMM.tif

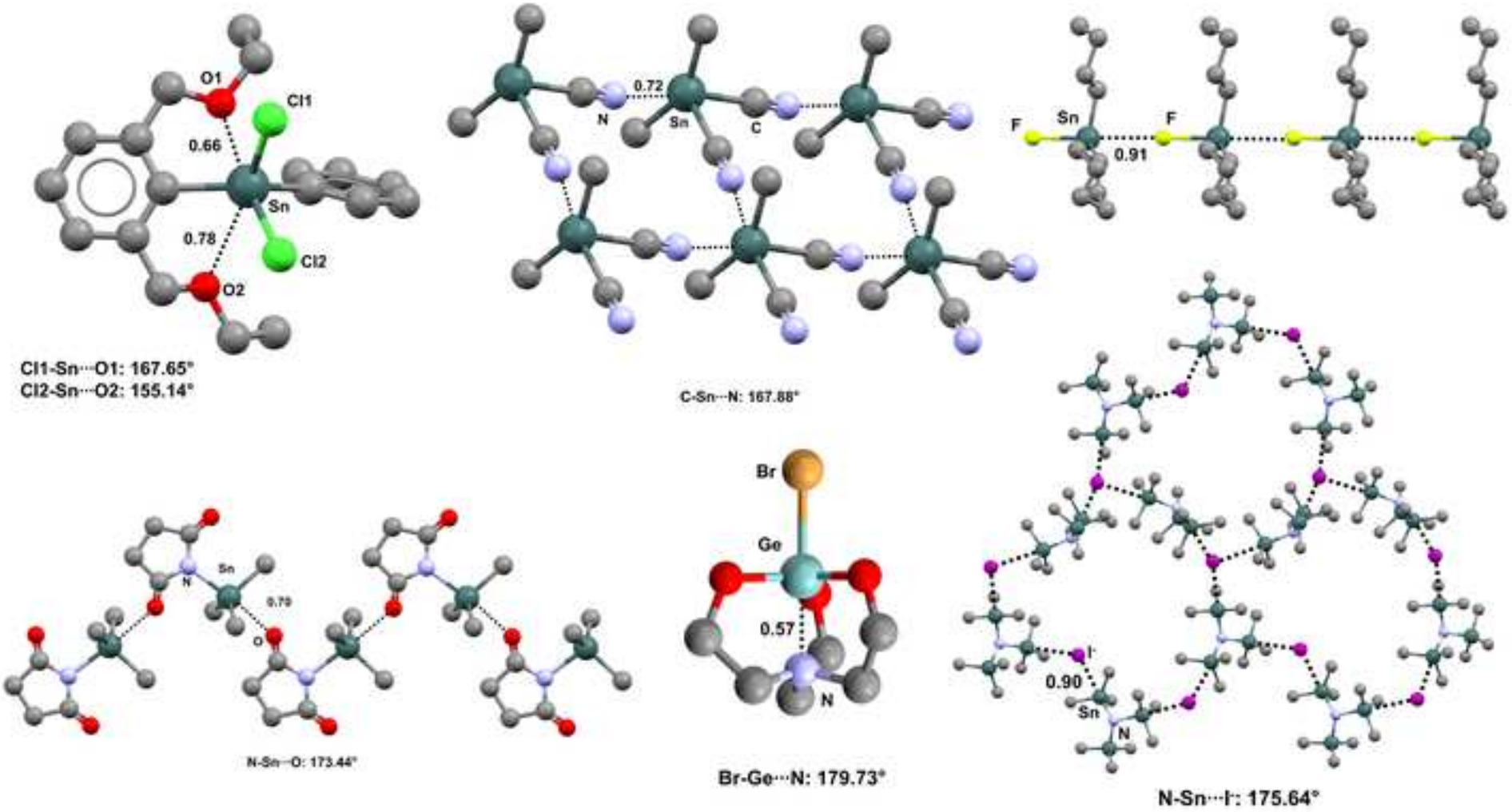

Short contacts involving Germanium and Tin in crystal structures: Experimental evidence of tetrel bond

Patrick Scilabra, Vijith Kumar, Maurizio Ursini, Giuseppe Resnati*

NFMLab - D.C.M.I.C. "Giulio Natta", Politecnico di Milano, Via L. Mancinelli 7, 20131 Milan, Italy.

Keywords: Tetrel bond; Crystal engineering, σ-Hole interactions; Supramolecular interactions.

Abstract

Modelling indicates the presence of a region of lowest electronic density, a σ-hole, on Group 14 elements and this offers a rationalization for the ability of these elements to act as electrophilic sites and to form attractive interactions with nucleophiles. Many papers describe theoretical investigations of interactions involving carbon and silicon, less frequently the heavier Group 14 elements. The purpose of this review is to fill the current lack of experimental evidences on interactions formed by Germanium and Tin with nucleophiles. A survey of crystal structures in the Cambridge Structural Database is reported here. It reveals that close contacts between Ge or Sn and lone pair possessing atoms are quite common, they can occur both intra- and intermolecularly, and they are usually on the extension of the covalent bond formed by the tetrel with the most electron withdrawing substituent. Several examples are discussed wherein germanium and tin atoms bear four carbon residues or wherein halogen, oxygen, sulfur, or nitrogen substituents replace one, two, or three such carbon residues. These short contacts are assumed as the result of attractive interactions between the involved atoms and afford experimental evidences of the ability of Germanium and Tin to work as electrophilic sites, namely to act as tetrel bond (TB) donors. This ability can govern and control the conformation and the packing of organic derivatives in the solid state. TB can thus be considered a promising and robust tool for crystal engineering.

This paper belongs to Topical Collection P. Politzer 80th Birthday Festschrift

---

* *Corresponding author:* Tel.: +39 02 2399 3032; Fax: +39 02 2399 3180

E-mail address: giuseppe.resnati@polimi.it

Contents

Introduction

A comprehensive knowledge of all the different interactions (i.e., weak bonds) that a molecule can give rise to is a fundamental prerequisite for the control and design of the conformation and the packing that it adopts in the crystal. The interatomic distances slightly below the sum of the van der Waals radii of involved atoms (hereinafter named short contacts) are usually, while not always, the result of attractive interactions between the involved atoms. To register the systematic occurrence of short contacts in crystalline solids is thus highly informative of the attractive interactions that atoms and molecular moieties can give rise to. Short contacts play a crucial role in the properties of matter, especially in condensed phases, and their knowledge and control enables for designing and optimizing the functional properties of materials, either synthetic or natural [1–3].

The hydrogen bond (HB) is by far the most frequently occurring and widely studied interaction [4, 5]; π–π [6], cation-π [7], anion-π [8], and aurophilic bondings [9] are other week bonds which have traditionally received attention. σ-Hole interactions [10–12] are quite recent entries in the set of the week bonds [13–15], but after the seminal papers of P. Politzer *et al.* [16, 17] they rapidly gained a position under the spotlight of the studies in the field [15, 18–20]. A covalently bonded atom characteristically has a region of lower electron density, the "σ-hole", which is usually along the extension of the covalent bond and opposite to the atom. The electrostatic potential at this region is frequently positive and a σ-hole bonding is the result of the attractive interaction between this positive region (electrophilic site, donor of the interaction) and a negative site (nucleophilic site, acceptor of the interaction, e.g. a lone pair possessing atom or an anion). In general, the largest number of σ-holes that an atom can have, and which may drive the formation of attractive interactions, is equal to the number of the covalent bonds it is involved in. The more electron withdrawing the group(s) covalently bound to a given atom are, the more extended and more positive the σ-hole(s) opposite to the bond(s) become [21], and the stronger and shorter the formed σ-hole interaction(s) become. A distinctive feature of σ-hole interactions is their directionality, a consequence of the rather focused location of region(s) with positive electrostatic potential. In an R–A···B interaction, where A is the atom with the positive σ-hole potential and B is the nucleophile, the angle R–A···B is generally between 155° and 180°.

Experimental evidences and theoretical calculations consistently show that most elements of Groups 14-18 of the periodic table form σ-hole bondings. A growing consensus is emerging in the chemists community to name these interactions from the name of the Group of the Periodic Table the electrophilic atom belongs to [22, 23]. The halogen bond (XB) [10, 24], namely the interaction

wherein an element of Group 17 is the electrophilic site, is the best know subset of σ-hole interactions; the chalcogen bond has been studied in silico [25, 26] and in both the solid [27], liquid [28], and gas phases [29]; the pnictogen bond received mainly attention in silico [30] and in the solid [31]; and the aerogen bond (AB) is the most recent member of this type of interactions [32a].

The tetrel bond (TB), namely the interaction wherein a Group 14 element is the electrophile, has received non-minor attention, probably in relation to its huge impact, e.g., its possible role in S_N2 reactions and hydrophobic interactions [13, 32b]. Convincing evidence of the non-occasional ability of carbon to attractively interact with lone pair possessing atoms begun to be reported more than forty years ago. In 1975 Johnson *et al.* calculated that in the water/carbon dioxide dimer the arrangement bonded via a short C···O contact is more stable than the arrangement bound through a short H···O contact [33a] and in 1984 Klemperer *et al.* confirmed, via microwave spectra analyses, that the equilibrium geometry of the adduct features a tetrel bond, namely the tetrel bonded $O_2C\cdots OH_2$ geometry is preferred over the hydrogen bonded HO–H···O=CO geometry [33b]. During the nineteen eighties, tetrel bond was shown to overcome hydrogen bond in driving the formation of other lowest energy complexes formed by carbon dioxide, for instance with HBr [33c] and HCN [33d]. Most papers on the ability of tetrels to function as electrophiles describe theoretical investigations of interactions involving carbon [34] and silicon [35, 36a,b], less frequently the heavier Group 14 elements [37]. Experimental studies of TBs are quite limited [29, 38–40] and to the best of our knowledge they never focused on interactions involving germanium or tin. We thus decided to analyse structures in the Cambridge Structural Database (CSD) in order to assess if organic derivatives of these two elements show the presence of TBs in crystalline solids. We looked for systems wherein germanium and tin are forming short contacts with nucleophilic sites. Directionality being a characteristic of σ-hole interactions, a particular attention was paid in this survey to the geometrical features of the observed short contacts and their linearity was considered an experimental evidence that they can be rationalization as TBs.

In this paper we discuss a selected number of crystalline structures of organic derivatives of germanium and tin wherein these elements form TBs, i.e., short and linear contacts with lone pair possessing heteroatoms. Structurally simple and poorly functionalized molecular systems have been preferentially analyzed as the Ge/Sn···nucleophile interactions occurring in these systems are more likely a straightforward product of the features of the two involved sites, contributions from other parts of the molecule(s) being probably minor. A wider coverage of organic Ge and Sn derivatives presenting TBs in the solid is given in the references. The interactions lengths will be analysed by using the normalized contact (Nc), defined as the ratio between experimentally observed separation of interacting atoms and the sum of their respective van der Waals radii [41, 42]. Nc values allow a

linear comparison between contacts involving different atoms. While the number of CSD structures where Ge/Sn···nucleophile interactions are present is not large enough to enable for definitive, general, and in depth generalizations, the survey of CSD reported here shows that the formation of attractive interactions between organic Ge and Sn sites and a donor of electron density can become a structural determining factor in crystalline solids. Intra- and intermolecular TBs are observed and they can affect the preferred conformation of a molecule and/or the network of intermolecular interactions in the crystal packing. Importantly, cases collected here give convincing experimental evidence that TBs tend to be more linear than PBs [31].

Oxygen atoms as TB acceptors

The conformation adopted by (2,6-bis(methoxymethyl)phenyl)-triphenyl-tin (Refcode MUBVOU) in the crystal (Fig. 1, left) seems to be determined by two intramolecular Sn···O TBs [44]. One interaction is slightly shorter than the other, the two Nc values being 0.76 and 0.78. Shorter σ-hole interactions usually tend to be more linear and consistent with this characteristic the two C–Sn···O angles in TBs mentioned above are 168.05° and 172.55°, respectively. As discussed above, another common feature of σ-hole interactions is that for a given donor of σ-hole interactions, the more electron withdrawing a covalently bonded residue is, the more positive the σ-hole it give rise to is, and the shorter and stronger the interactions with incoming nucleophiles are. Interestingly, in an analogue of the compound discussed above wherein two chlorine atoms substitute for two phenyl rings, the two intramolecular TBs are much shorter, namely in (2,6-bis(ethoxymethyl)phenyl)-dichloro-phenyl-tin (Refcode LIVHOO) the Nc values for the Sn···O TBs are 0.66 and 0.78 (Fig. 1, right) [43].

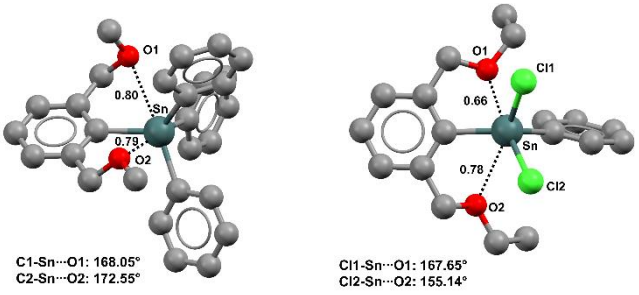

Fig. 1 Ball and stick representation (Mercury 3.9) of (2,6-bis(methoxymethyl)phenyl)-triphenyl-tin (MUBVOU, left) and of a (2,6-bis(ethoxymethyl)phenyl)-dichloro-phenyl-tin (LIVHOO, right). TBs are black dotted lines, hydrogens have been omitted for clarity. Nc values are reported close to the respective interactions. Color code: Grey, carbon; green, chlorine; red, oxygen; dark teal, tin.

It is extensively documented that the propensity of an halogen atom to form XBs increases with its molecular weight [10] and that the heavier halogens usually form stronger and shorter XBs than the lighter ones, both features being independent of the used XB acceptor. Similar trends are observed when elements of Groups 16 and 15 form CBs and PBs, respectively. In all cases this is probably due to the fact that the polarizability in a Group increases with the molecular weight of the element and a high polarizability favours the anisotropic distribution of the electron density in an atom, and thus the strength of σ-hole interactions. It is no surprise [45] that methyl-tris((2-methoxymethyl)phenyl)germane (Refcode IMUTEP) shows only one C–Ge···O contact and that the corresponding Nc value (0.87) is greater than Nc values of the structurally similar tin derivatives MUBVOU and LIVHOO [46] (Fig. 2, top left).

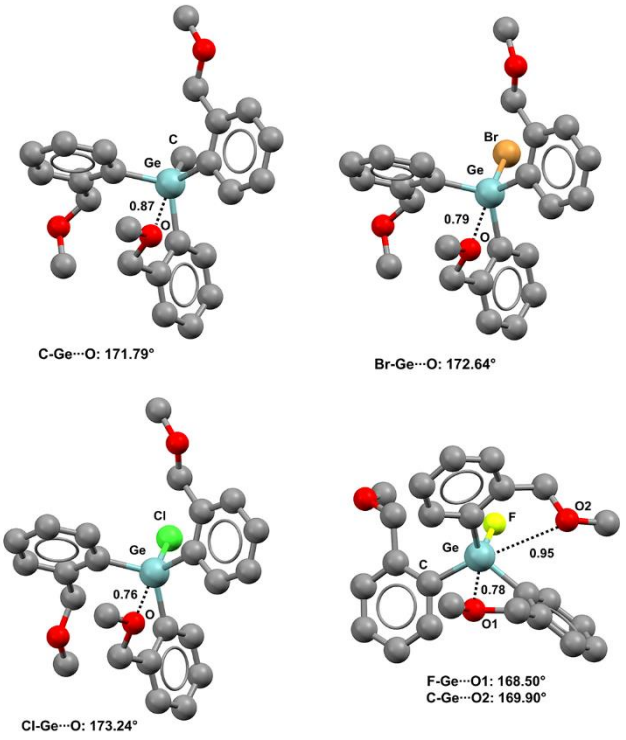

Fig. 2 Ball and stick representation (Mercury 3.9) of methyl-tris((2-methoxymethyl)phenyl)germane (IMUTEP, top left), bromo-tris((2-methoxymethyl)phenyl)germane (IMUTAL, top right), chloro-tris((2-methoxymethyl)phenyl)germane (IMUSUE, bottom left), and of fluoro-tris((2-methoxymethyl)phenyl)germane (IMUSOY, bottom right). TBs are black dotted lines, hydrogens have been omitted for clarity. Nc values are reported close to the respective interactions. Color code: Grey, carbon; brown, bromine; green, chlorine; yellowish green, fluorine; red, oxygen; light teal, germanium.

Bromine is more electronegative than carbon and in bromo-tris((2-methoxymethyl)phenyl)germane (Refcode IMUTAL) the Br–Ge···O TB is shorter (Nc = 0.79) than the C–Ge···O in IMUTEP (Fig. 2, top right) [46]; chlorine is more electronegative than bromine and in chloro-tris((2-methoxymethyl)phenyl)germane (Refcode IMUSUE) the Cl–Ge···O TB is even shorter (Nc = 0.76) (Fig. 2, bottom left). Also in these three structures the linearity of TBs correlates with their lengths

(C–Ge···O, Br–Ge···O, and Cl–Ge···O angles are 171.79°, 172.64°, and 173.24°, respectively). In fluoro-tris((2-methoxymethyl)phenyl)germane(IV) (Refcode IMUSOY) a fluorine has substituted for the methyl of IMUTEP and depletion of electron density at germanium becomes high enough that two TBs are present in the crystal (Fig. 2, bottom right). An F–Ge···O and a C–Ge···O TB are present and, consistent with the relative electronegativity of fluorine and carbon, the former interaction is shorter and more directional than the latter one (Nc values for Ge···O separations are 0.78 and 0.95, respectively). Also, a tin bonded iodine atom can promote the formation of short contacts (Fig. 3). Two independent molecules are present in the unit cell of crystalline iodo-(2,6-bis(methoxymethyl)phenyl)diphenyl-tin (Refcode RAKBOV) and in both of them the conformation is locked by an I–Sn···O and a C–Sn···O intramolecular TB. Former interactions are shorter and more directional than latter ones (Nc values are 0.70, 0.72 for I–Sn···O separations and 0.79, 0.81 for C–Sn···O separations; mean I–Sn···O angles are 166.19° and mean C–Sn···O angles are 166.68°).

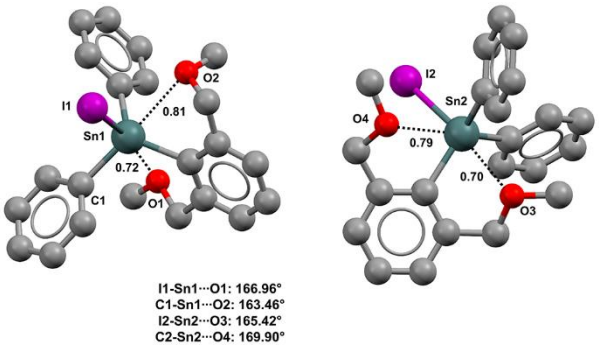

Fig. 3 Ball and stick representation (Mercury 3.9) of the two molecules of the unit cell of iodo-(2,6-bis(methoxymethyl)phenyl)diphenyl-tin (RAKBOV). TBs are black dotted lines, hydrogen atoms have been omitted for clarity. Nc values are reported close to the respective interactions. Color code: Grey, carbon; red, oxygen; purple, iodine; dark teal, tin.

Carbonyl oxygen atoms can act as effective TB acceptors. In (*Z*)-2-methyl-4-phenyl-3-(trimethylgermanyl)but-2-enoic acid (Refcode QIBDOV) [47] a short C-Ge···O contact is present in both conformations adopted by the compound in the crystals (Fig. 4, left) (Nc for Ge···O separations is 0.80, C–Ge···O angles are 174.17°, 175.00°) and a shorter TB occurs in a trimethylstannyl-carbomethoxy derivative (Refcode KASYOS) [48] where a quite similar tin based tecton is present (Nc for C–Sn···O separation is 0.76) (Fig. 4, mid). Similar TBs are given by the carbonyl oxygen of carbamates (e.g., *trans*-*N*-*t*-butyloxycarbonyl-2-methyl-6-(trimethylstannyl)-4-phenyl)piperidine, Refcode EABFES; Nc = 0.75 and C–Sn···O angle is 165.31°; Fig 4, right) [49, 50], and several other carbonyl derivatives, e.g., amides [51], aldehydes [52, 53], and ketones [54].

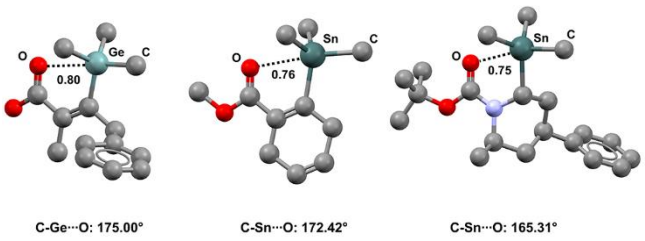

Fig. 4 - Ball and stick representation (Mercury 3.9) of one of the two independent molecules in the unit cell of (*Z*)-2-methyl-4-phenyl-3-(trimethylgermanyl)but-2-enoic acid (QIBDOV, left), (2-carbomethoxy-1,4-cyclohexadien-1-yl)-trimethyl-tin (KASYOS, mid) and *trans*-*N*-*t*-butyloxycarbonyl-2-methyl-6-(trimethylstannyl)-4-phenyl)piperidine (EABFES, right) derivatives. TBs are black dotted lines, hydrogen atoms have been omitted for clarity. Nc values are reported close to the respective interactions. Color code: Grey, carbon; red, oxygen; light blue, nitrogen; light teal, germanium; dark teal, tin.

Both intra- and intermolecular TBs are found in the CSD wherein a carbonyl oxygen is working as the TB acceptor and discrete adducts [55] or infinite chains (one-dimensional networks, 1D nets) can be generated. In ethyl trimethytin-diazoacetate (Refcode SIWRAR) [56], the diazoacetate residue is expected to form a σ-hole on tin more positive than the σ-holes formed by the methyl groups. Consistent with this expectation, a tetrel bonded infinite chain is present in the crystal of the compound (Fig. 5, top) wherein the carbonyl oxygen gets close to tin atom along the extension of the N_2C–Sn covalent bond (the Sn···O separation is 312.5 pm which corresponds to an Nc value of 0.85, the C–Sn···O angle is 176.46°). Similarly, the most positive σ-hole on germanium in 2,5-bis(trimethylgermyl)thiophene-1,1-dioxide (Refcode QAHXIG) [57] is expected opposite to the O_2SC–Ge covalent bond and an infinite chain (Fig. 5, bottom) is formed wherein the suphonyl oxygens gets close to germanium on the extension of the O_2SC–Ge covalent bonds after a particularly linear geometry (the Ge···O separation corresponds to an Nc value of 0.97 and the C–Ge···O angle is 179.77°).

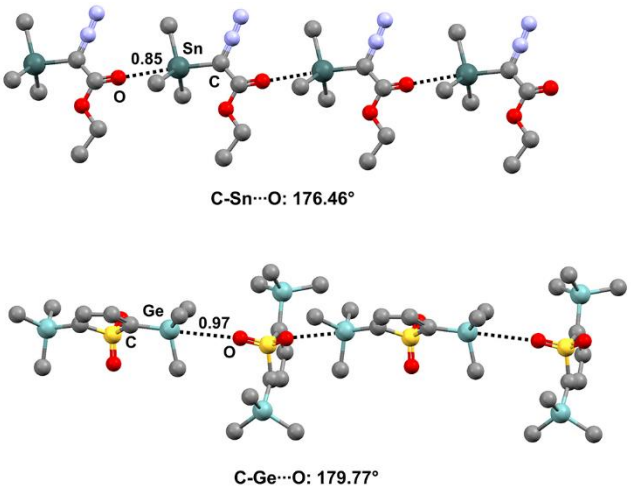

Fig. 5 – Ball and stick representation (Mercury 3.9) of 1D chains generated by ethyl trimethytin-diazoacetate (SIWRAR, top) and 2,5-bis(trimethylgermyl)thiophene-1,1-dioxide (QAHXIG, bottom). TBs are black dotted lines, hydrogen atoms have been omitted for clarity. Nc values are reported close to the respective interactions. Color code: Grey, carbon; red, oxygen; light blue, nitrogen; yellow, sulphur; light teal, germanium; dark teal, tin.

N-triethylstannylsuccinimide (Refcode FUSZIC) [58] works as a self-complementary module and forms tetrel bonded infinite chains (one-dimensional networks, 1D nets) (Fig. 6, top). Consistent with the expected involvement of an sp^2 lone pair of the carbonyl oxygen as the nucleophilic site entering the elongation of the N–Sn covalent bond, the Sn···O=C angle is 138.28° and the tin atom is approximately in the succinimide plane (the distance between the mean square plane through the seven heavy atoms of the succinimide moiety and the tetrel bonded tin atom is 219 pm). The halogen bonded infinite chains formed by *N*-chloro- and N-bromosuccinimide (Refcodes CSUCIM01 and NBSUCA, respectively) [59] are also reported in Fig. 6 (mid and bottom in the order) in order to make apparent the analogous supramolecular features of TB and XB.

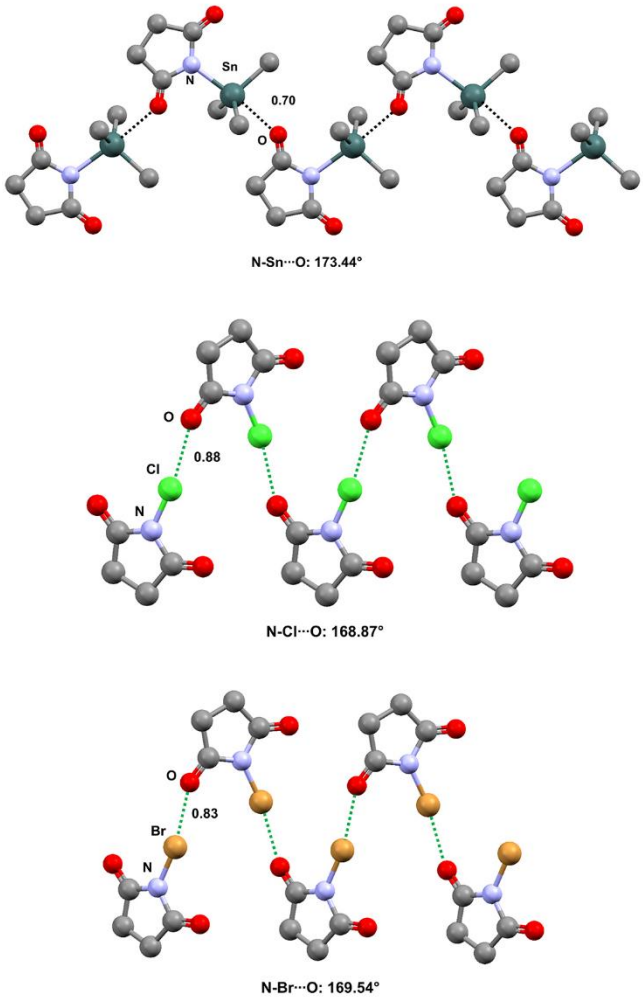

Fig. 6 Ball and stick representation (Mercury 3.9) of the 1D network formed by *N*-triethylstannylsuccinimide (FUSZIC) thanks to N–Sn···O TBs (top), by N-chlorosuccinimide (CSUCIM) thanks to N-Cl···O XBs (mid), and by *N*-bromosuccinimide (NBSUCA) thanks to N–Br···O XBs (bottom). The three methyl groups of the ethyl residues of *N*-triethylstannylsuccinimide and hydrogen atoms have been deleted for sake of simplicity. TBs and XBs are black dotted lines and green dotted lines, respectively. Color code: Grey, carbon; red, oxygen; purple, iodine; brown, bromine; dark teal, tin.

In several structures of the CSD, the tin atom of a trialkyl-alkanoyl-tin moiety (namely in R_3Sn–OC(O)R' derivatives) shows the presence of a TB with a carbonyl oxygen opposite to the Sn–O covalent bond and one-dimensional [60], two-dimensional [61], or three-dimensional [62] networks are formed depending on the overall structure of the compounds (Figs. 7-9).

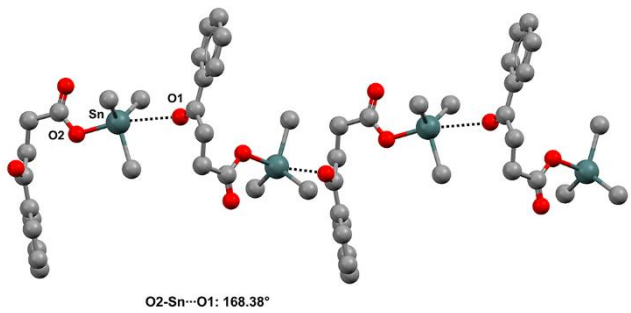

Fig. 7 Ball and stick representation (Mercury 3.9) of the 1D network wherein the ketone oxygen of O-tricyclohexyltin-4-oxo-4-phenylbutanoate (APAZIB) functions as the TB acceptor site. Hydrogen atoms and five of the cyclohexyl carbons have been deleted for sake of simplicity. Color code: Grey, carbon; red, oxygen; dark teal, tin.

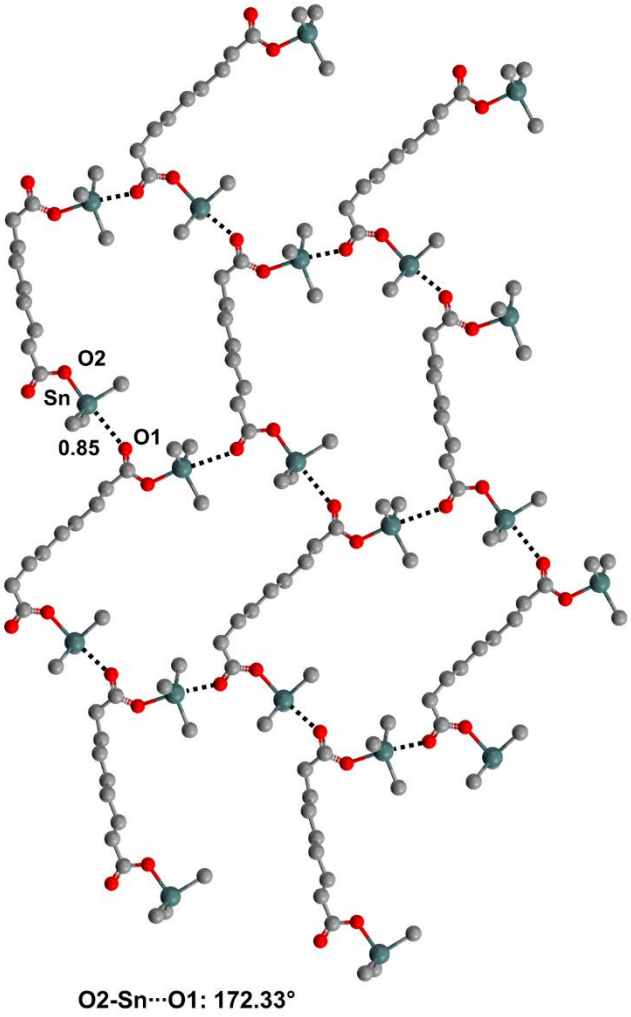

Fig. 8 Ball and stick representation (Mercury 3.9) of the two-dimensional network formed by bis(tricyclohexyltin)nonanoate (CUXSOF). Five atoms of the cyclohexyl residues bound to tin have been deleted for sake of simplicity. Color code: Grey, carbon; red, oxygen; dark teal, tin.

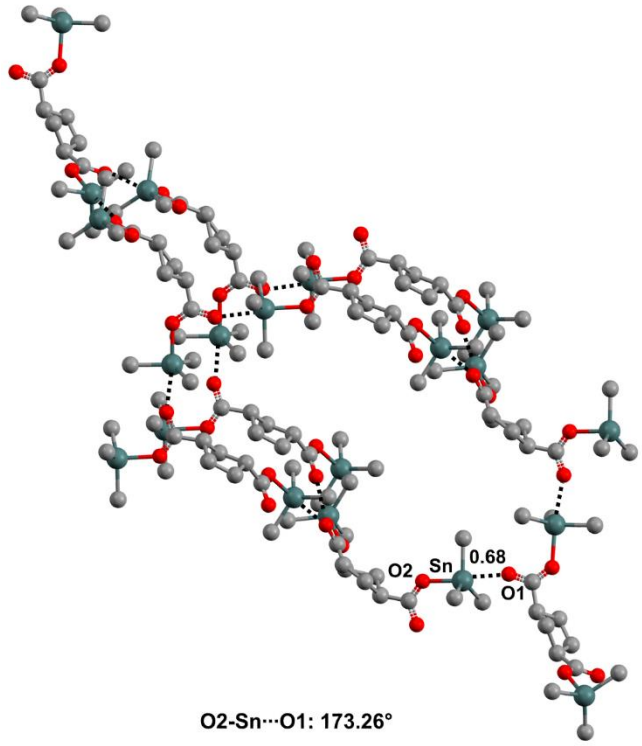

Fig. 9 Ball and stick representation (Mercury 3.9) of the three-dimensional network with adamantanoid topology formed by bis(tri-*n*-butyltin)-1,2,2-trimethylcyclopentane-1,3-dicarboxylate (DIYFIB). Three atoms of the butyl residues bound to tin and methyl pendants on cyclopentyl rings have been deleted for sake of simplicity. Color code: Grey, carbon; red, oxygen; dark teal, tin.

Various other oxygen functionalities can work as donors of electron density to organotin and germanium derivatives, e.g. water [63–65], sulfoxides and sulfones [66–69], phosphineoxides, hexamethylphosphortriamide and their analogues [70–76] (Fig. 10).

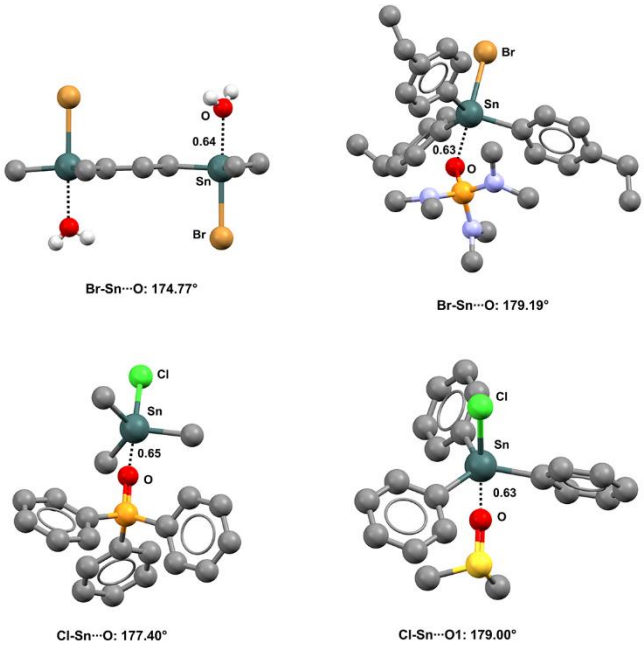

Fig. 10 Ball and stick representation (Mercury 3.9) of the trimer formed by 1,3-bis(bromo-dimethylstannyl)propane and water (XINROB, top left), of the dimer formed by bromo-tris(*p*-ethylphenyl)-tin and hexamethylphosphoramide (HEVQIJ, top right), of the dimer formed by chloro-trimethyl-tin and triphenylphosphine oxide (HIGRUK01, bottom left), and of the dimer formed by chloro-triphenyl-tin and dimethyl sulfoxide (RUGYOI, bottom right). Hydrogen atoms and 2,2'-bipyridine in XINROB have been deleted for sake of simplicity. TBs are black dotted lines. Color code: Grey, carbon; red, oxygen; blue, nitrogen; orange; phosphorus; green, chlorine, brown, bromine; yellow, sulphur; dark teal, tin.

Nitrogen atoms as TB acceptors

Several structures are available in the CSD where the nitrogen atom of amine, pyridine, and cyano moieties forms a short contact with tin or germanium atoms (Fig. 11) thus showing that, similar to oxygen atoms, nitrogen atoms can act as TB acceptors and this can be the case when adopting both the sp^3, and sp^2 or *sp* hybridization.

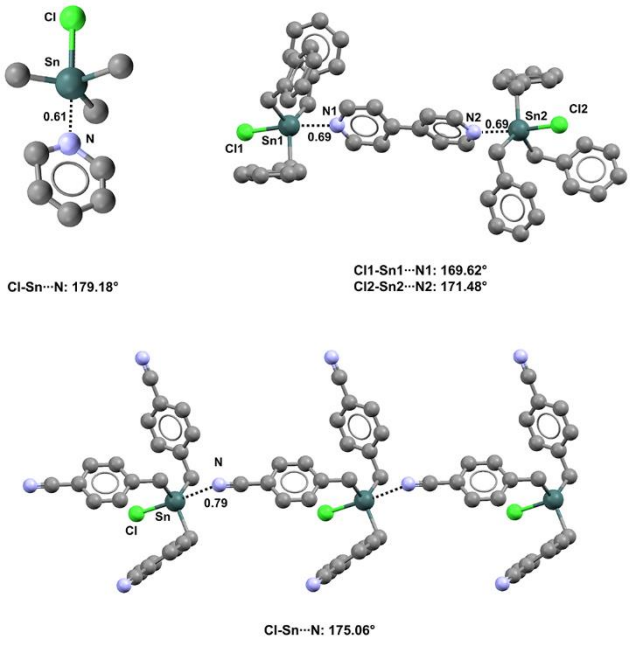

Fig. 11 Ball and stick representation (Mercury 3.9) of the dimer formed by chloro-(trimethyl)-tin and pyridine (CMEPSN, top left), of the trimer formed by chloro-tribenzyl-tin and 4,4'-bipyridyl (FEJFUW, top right), and of the 1D chain formed by chloro-tris(4-cyanobenzyl)-tin (BIBQIN, bottom). Hydrogen atoms have been deleted for sake of simplicity. TBs are black dotted lines. Color code: Grey, carbon; blue, nitrogen; green, chlorine, dark teal, tin.

The ability of nitrogen atoms of tertiary amines to form short contacts with organogermanium and -tin derivatives is particularly well-documented. For instance, two symmetrically non-equivalent molecules are present in crystals of tris(2-((dimethylamino)methyl)phenyl)-germane (Refcode

GAGYIW) [77] and the conformation of both molecules is influenced by three intramolecular C–Ge···N TBs (Fig. 12, left) (Nc values span the range 0.82 - 0.84 and C–Ge···N angles vary between 172.45° and 176.79°). C–N–C Angles vary between 109.70° and 113.25° indicating that nitrogen atoms of the tertiary amine moieties adopt a nicely tetrahedral conformation and the lone pairs point to the elongation of C–Ge covalent bonds as expected for a σ-hole interaction (C–N···Ge angles span the range 82,34° - 120.39°).

Imine nitrogen atoms behave similar to amine nitrogens. A short and linear C–Ge···N interaction affects the conformation adopted by 1-(trimethylsilylimino(diphenyl)phosphoranyl)-2-(triphenylgermyl)benzene (Nc for Ge···N separation is 0.85, C–Ge···N angle is 173.79°) (Refcode VIQXIC) [78] (Fig. 12, right). In the crystal of this compound the P=N···Ge angle is 96.80° and the germanium atom is approximately in the iminophosphoranyl plane (the distance between the tetrel bonded germanium atom and the mean square plane through phosphorous, nitrogen, and silicon atoms is 263 pm) suggesting that the lone pair at nitrogen points to the elongation of C–Ge covalent bond.

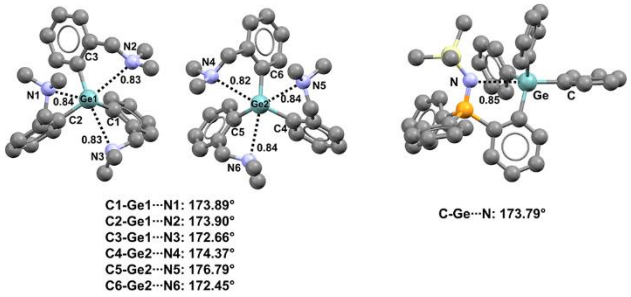

Fig. 12 Ball and stick representation (Mercury 3.9) of tris(2-((dimethylamino)methyl)phenyl)-germane (GAGYIW, left) and 1-(trimethylsilylimino(diphenyl)phosphoranyl)-2-(triphenylgermyl)benzene (VIQXIC, right) derivatives. TBs are black dotted lines, hydrogen atoms have been omitted for clarity. Nc values are reported close to the respective interactions. Color code: Grey, carbon; light blue, nitrogen; yellow, sulphur; pearl white; silicon; orange; phosphorus; light teal, germanium.

Short and intramolecular Ge···N contacts affect the conformation of a family of 4,6,11-trioxa-1-aza-5-germa-bicyclo[3.3.3]undecanes (germatrane derivatives). 5-(*t*-Butyl)-germatrane (Refcode BUWBUQ) [79] adopts in the solid an *endo*-conformation (Fig. 13, left) where the C–Ge···N separation is as short as 223.6 pm (Nc = 0.61). 5-Bromo-germatrane (Refcode BUWCUR) [80] behaves similarly (Fig. 13, mid) and the Br–Ge···N separation is even shorter (208.4 pm, Nc = 0.57) than in BUWBUQ, consistent with the fact that bromine is more electronegative than carbon and the σ-hole opposite to the Br–Ge covalent bond is probably more positive than opposite to the C–Ge

bond. Analogous *endo* conformations and Ge···N distances much shorter than the sum of van der Waals radii of germanium and nitrogen atoms are observed in other germatrane derivatives [81–83] and related systems [84, 85] (Fig. 13, right). A similar behaviour is encountered in the crystals of tin analogues. 5-Methyl-1-aza-5-stanna-bicyclo[3.3.3]undecane (Refcode FEWXOU) [74], and 5-fluoro [86], 5-chloro [87], 5-bromo [86], and 5-iodo [86] analogues (Refcodes ZANKEE, DAYMUL, ZANKOO, ZANKUU, respectively) all show short Sn···N contacts (Fig. 14).

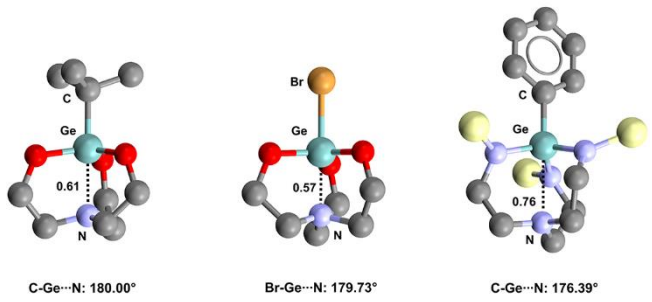

Fig. 13 Ball and stick representation (Mercury 3.9) of 5-(*t*-butyl)-germatrane (BUWBUQ, left), 5-Bromo-germatrane (BUWCUR, mid) and phenyl-(tris(2-(trimethylsilylamido)ethyl)amine-N,N',N")-germanium (XUSLOM , right). TBs are black dotted lines, hydrogen atoms and methyl substituents on silyl moieties of XUSLOM have been omitted for clarity. Nc values are reported close to the respective interactions. Color code: Grey, carbon; red, oxygen; light blue, nitrogen; bronze; bromine; pearl white, silicon; light teal, germanium.

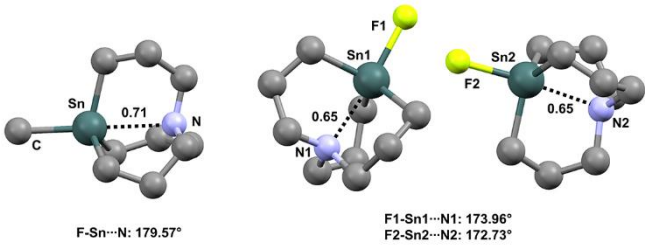

Fig. 14 Ball and stick representation (Mercury 3.9) of 5-methyl-1-aza-5-stanna-bicyclo(3.3.3)undecane (FEWXOU, left) and 5-fluoro-1-aza-5-stannatricyclo(3.3.3.$0^{1,5}$)undecane (ZANKEE, right). TBs are black dotted lines, hydrogen atoms have been omitted for clarity. Nc values are reported close to the respective interactions. Color code: Grey, carbon; light blue, nitrogen; yellowish green, fluorine; dark teal, tin.

As in organogermanium derivatives, the nitrogen atom of the 2-(dimethylaminomethyl)phenyl-stannyl moiety forms, in the solid, an intramolecular TB which affects the conformation of the respective compound. This is the case for (cyclopenta-2,4-dien-1-yl)-(2-(dimethylaminomethyl)phenyl)-diphenyl-tin (Refcode IHOZAH) [88] (Fig. 15, left) where the intramolecular C–Sn···N distance corresponds to an Nc value of 0.74 and the C–Sn···N angle is 171.08°, congruent with an attractive interaction between the lone pair of the tertiary amine nitrogen

and the σ-hole on the elongation of C–Sn covalent bond. Analogous Sn···N interactions are present in structurally related derivatives [89–91]. A five membered and tetrel bonded ring similar to that of IHOZAH is afforded by (3-aminopropyl)-triphenyl-tin (Refcode COKVUV) [92] (Fig. 15, right) which shows an Sn···N interaction where Nc is 0.74 and C–Sn···N angle is 175.81°.

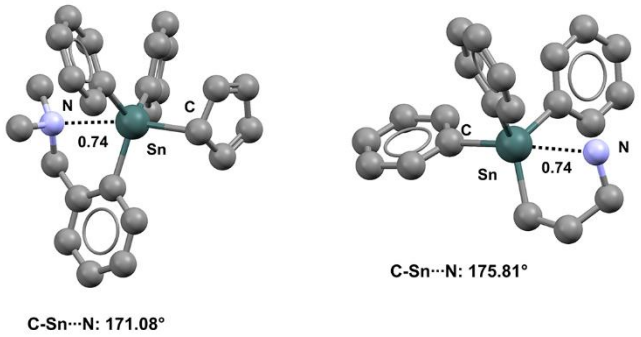

Fig. 15 Ball and stick representation (Mercury 3.9) of (cyclopenta-2,4-dien-1-yl)-(2-(dimethylaminomethyl)phenyl)-diphenyl-tin (left) and of (3-aminopropyl)-triphenyl-tin (IHOZAH, right). TBs are black dotted lines, hydrogen atoms have been omitted for clarity. Nc values are reported close to the respective interactions. Color code: Grey, carbon; light blue, nitrogen; dark teal, tin.

The tin atom of R_3Sn–OC(O)R' derivatives is a good TB donor and frequently forms interactions with the oxygen atom of carbonyl groups (Figs. 7-9) or to the nitrogen atom of pyridine moieties. The intermolecular Sn···N interaction is formed opposite to the Sn–O covalent bond and discrete trimers [93] (Fig. 16, top), one-dimensional [94–97] (Fig. 16, bottom) or two-dimensional [98] networks (Fig. 17) are formed depending on the ability of the tin derivative to function as a mono-, bi-, or polydentate tecton.

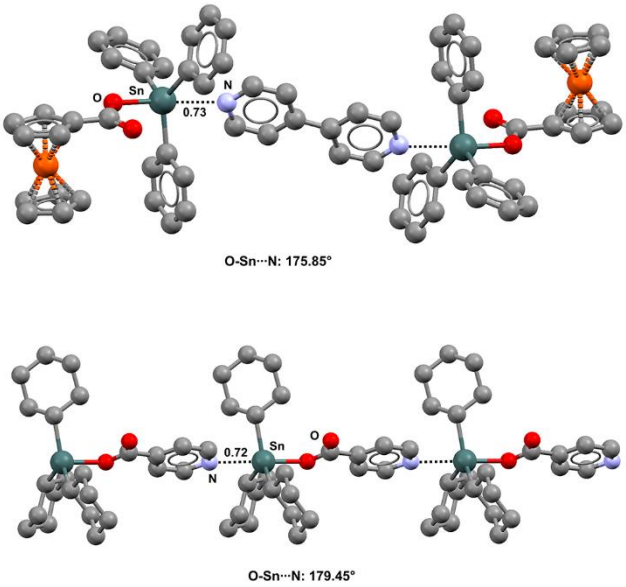

Fig. 16 Ball and stick representation (Mercury 3.9) of the trimer formed by (ferrocene-1-carboxylato)-triphenyl-tin and 4,4'-bipyridine (IVUVUR, top) and of the infinite chain formed by (pyridine-4-carboxylato)-tricyclohexyl-tin (UZAVUN, bottom). TBs are black dotted lines and hydrogen atoms have been deleted for sake of simplicity. Nc values are reported close to the respective interactions. Color code: Grey, carbon; red, oxygen; orange, iron; light blue, nitrogen; dark teal, tin.

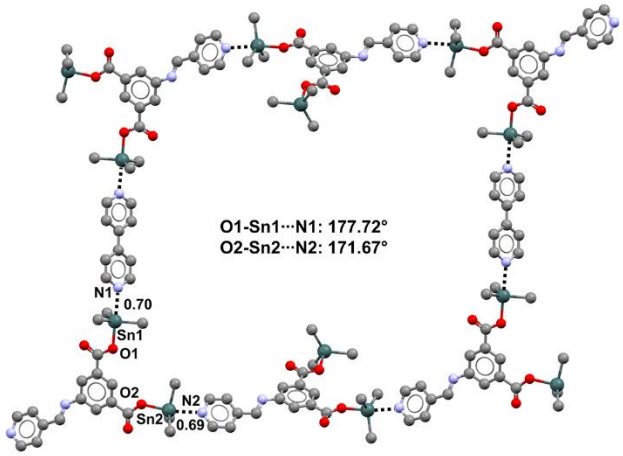

Fig. 17 Ball and stick (Mercury 3.9) of the network generated by di(tri-*n*-butyl)-stannyl 5-((pyridin-4-ylmethylene)amino)isophthalate with 4,4'-bipyridine (TISVEY). TBs are black dotted lines; three atoms of the butyl residues at tin and hydrogen atoms have been deleted for sake of simplicity. Nc values are reported close to the respective interactions. Color code: Grey, carbon; red, oxygen; light blue, nitrogen; dark teal, tin.

The nitrogen atom of pyridine derivatives forms short contacts with tin on the elongation not only of O–Sn covalent bonds, but also of C–Sn, Cl–Sn, Br–Sn, I–Sn, and S–Sn bonds [94, 96, 99, 100]. In all cases the geometric features of the adducts indicate that the nitrogen lone pair points to the elongation of one of the tin covalent bonds. For instance, in the infinite chain formed by the dithiocarbamate reported in Fig. 18 (Refcode UGEFIX), the S–Sn···N angle is 174.50°, the geometry around nitrogen is strictly trigonal planar, and tin is nearly in the pyridine plane (the two C(sp^2)N···Sn angles are 121.18° and 122.40° and the distance of tin from the mean square plane through the pyridine ring is 85 pm).

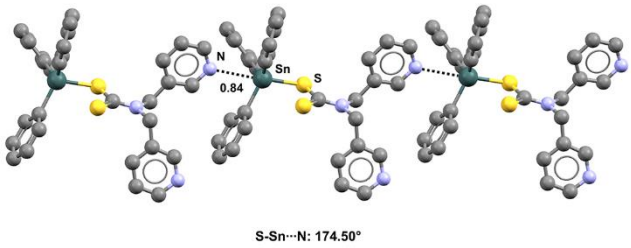

Fig. 18 Ball and stick representation (Mercury 3.9) of the one-dimensional network formed by (bis(pyridin-3-ylmethyl)carbamodithioato)-triphenyl-tin (UGEFIX). TBs are black dotted lines and hydrogen atoms have been deleted for sake of simplicity. Nc values are reported close to the respective interactions. Color code: Grey, carbon; yellow, sulphur; light blue, nitrogen; dark teal, tin.

The cyano group seems a profitable TB acceptor group *via* the lone pair at nitrogen. Moreover, thanks to its high electron withdrawing ability, it is expected that when the cyano group is directly bound to a tin or germanium atoms, the σ-hole opposite to the NC–Sn/Ge covalent bond is particularly positive. Indeed, trimethyltin cyanide (Refcode TIMSNC01) and dimethyltin dicyanide (Refcode DMCYSN) both work as self-complementary modules and form infinite chains [101] and square 2D networks [102], respectively (Fig. 19) by pairing TB donor and TB acceptor sites. Dimethylgermanium dicyanide (Refcode DMCYGE) show a somewhat similar behavior.

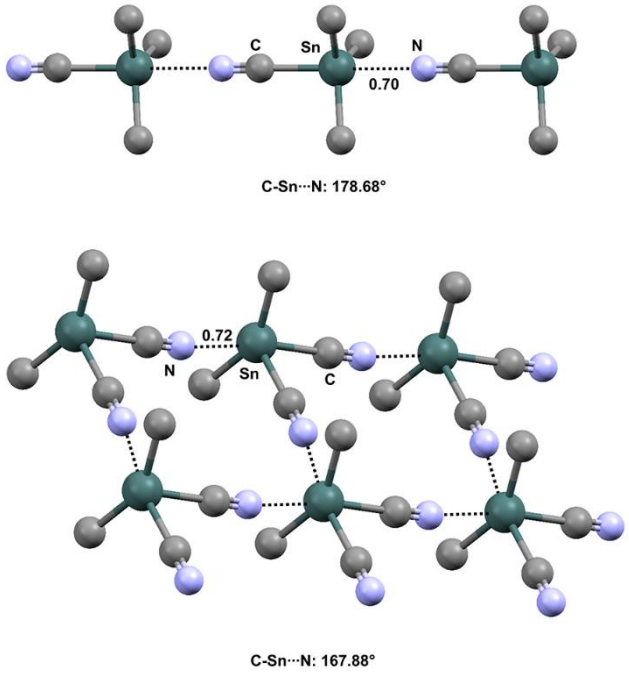

Fig. 19 Ball and stick representation (Mercury 3.9) of the 1D infinite chain formed by trimethyltin cyanide (TIMSNC01, top) and the 2D network generated by dimethyltin dicyanide (DMCYSN, bottom). TBs are black dotted lines and hydrogen atoms have been deleted for sake of simplicity. Nc values are reported close to the respective interactions. Color code: Grey, carbon; light blue, nitrogen; dark teal, tin.

Tetrakis(2-cyanobenzyl)-tin (Refcode JIWROX) [103] (Fig. 20) functions as a self-complementary tecton as the cyano group of one molecule enters the elongation of one of the C–Sn covalent bonds of an adjacent molecule and infinite tetrel bonded ribbons are formed (Nc = 0.96, the C–Sn···N angle is 178.46°).

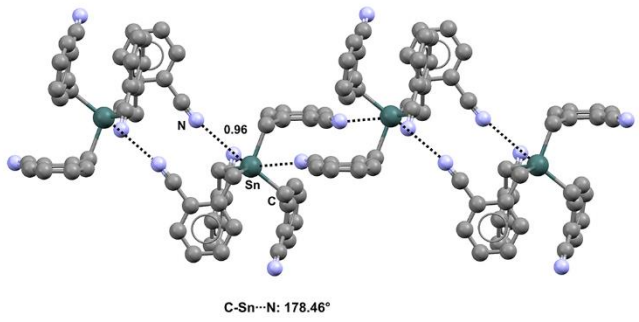

Fig. 20 Ball and stick representation (Mercury 3.9) of the network formed by tetrakis(2-cyanobenzyl)-tin (JIWROX). TBs are black dotted lines and hydrogen atoms have been deleted for sake of simplicity. Nc values are reported close to the respective interactions. Color code: Grey, carbon; light blue, nitrogen; dark teal, tin.

In 2-(dimethylaminomethyl)phenyl)-cyano-diphenyl-tin and bis(2-(dimethylaminomethyl)phenyl)-dicyano-tin (Refcodes WUVKOP and WUVLOQ, respectively) [104], one and two NC–Sn···N short contacts are present, respectively, and the amine nitrogen works as TB acceptor site in all cases (Fig. 21). This may suggest that, an N(sp^3) atom is a better TB acceptor than an N(*sp*) atom. The same relative ability to work as donors of electron density is observed in XB formation.

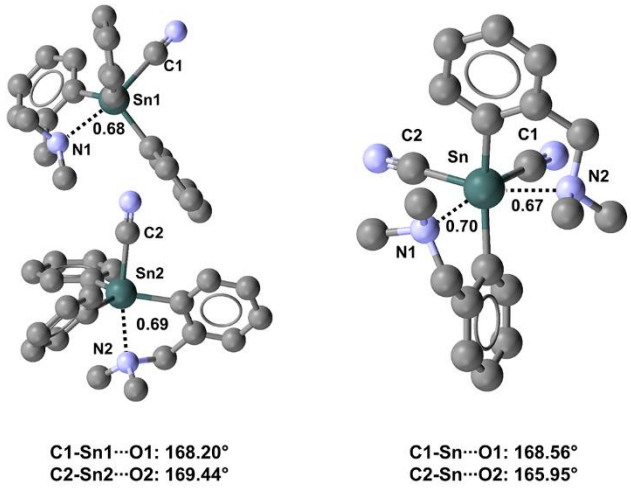

Fig. 21 Ball and stick representation (Mercury 3.9) of conformation adopted by cyano-2-(dimethylaminomethyl)phenyl)-diphenyl-tin (WUVKOP, left) and bis(2-(dimethylaminomethyl)phenyl)-dicyano-tin (WUVLOQ, right). TBs are black dotted lines and hydrogen atoms have been deleted for sake of simplicity. Nc values are reported close to the respective interactions. Color code: Grey, carbon; light blue, nitrogen; dark teal, tin.

Halogen atoms as tetrel bond acceptors

Structures in the CSD reveal that the four halogens can all form short contacts with tetravalent germanium and tin atoms comprised in organic derivatives. These interactions can be rationalized as TB due to the fact that the halogen atoms are approximately on the elongation of one of the covalent bonds formed by the germanium and tin, the bond with the most electron withdrawing group being involved preferentially in the formation of these short contacts.

For instance, crystals of bis(2,5-bis(trifluoromethyl)phenyl)(dichloro)germane (Refcode ZAVCUW) have two symmetrically non-equivalent molecules in the unit cell [105]. Both these molecules show two fairly short and linear TBs on the elongation of the Cl–Ge bonds (Nc values span the range 0.78 – 0.79; the C–Ge···F angles are between 176.15° and 174.93) (Fig. 22, left). Analogously, an intramolecular C–Ge···F short contact locks the conformation of (1,2,3,3,3-pentafluoroprop-1-en-1-

yl)-triphenyl-germanium (Refcode ADUKUH) [106] in the solid and allows for the formation of a tetrel bonded five member ring (the Nc value of the Ge···F separation is 0.86, the C–Ge···F angle 166.80°). The tin analogue of ADUKUH (Refcode ADUKOB) behaves similarly as, in both independent molecules present in the unit cell of the crystal, an intramolecular C–Sn···F TB is present and enables for a tetrel bonded ring (Fig. 22, right).

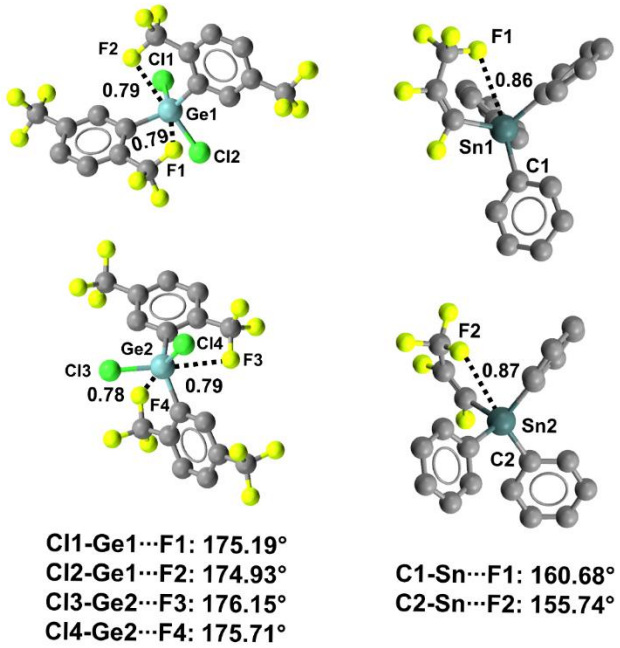

Fig. 22 Ball and stick representation (Mercury 3.9) of the conformation adopted by bis(2,5-bis(trifluoromethyl)phenyl)(dichloro)germane (ZAVCUW, left) and (1,2,3,3,3-pentafluoroprop-1-en-1-yl)-triphenyl-tin (ADUKOB, right). TBs are black dotted lines and hydrogen atoms have been deleted for sake of simplicity. Nc values are reported close to the respective interactions. Color code: Grey, carbon; yellowish green, fluorine; light teal, germanium; dark teal, tin.

Interestingly, tricyclohexyl-tin fluoride (Refcode BAJWOY) [107] works as a self-complementary module as the fluorine atom of one molecule forms a short and remarkably linear TB on the elongation of the F–Sn covalent bond of an adjacent molecule and infinite chains are formed (Fig. 23, top) (Nc value for the Sn···F separation is 0.91, the F–Sn···F angle is 178.85°). A similar behaviour is shown by several other organotin derivatives bearing one, two, or three halogen atoms at the heavy tetrel [108–111] (Fig. 23).

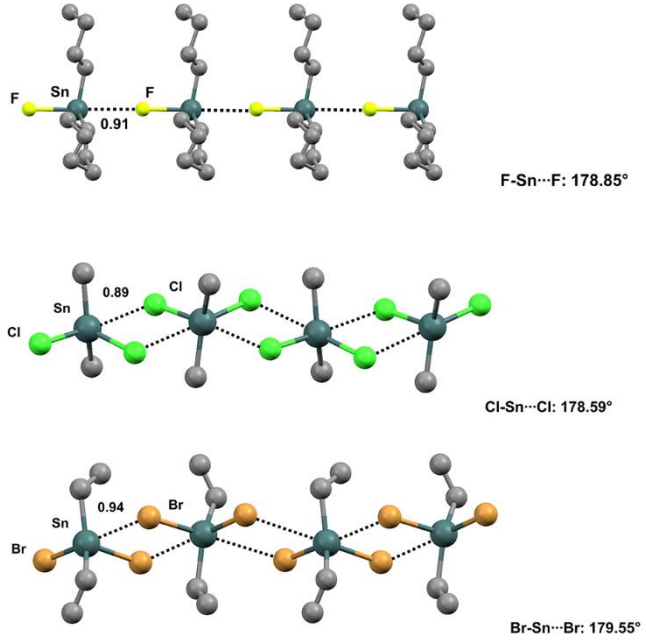

Fig. 23 Ball and stick representation (Mercury 3.9) of 1D chain generated by fluoro-tricyclohexyl-tin (BAJWOY, top), dichloro-dimethyl-tin (DMSNCL, mid) and dibromo-diethyl-tin (DESNBR, bottom). TBs are black dotted lines, hydrogen atoms have been omitted for clarity. Nc values are reported close to the respective interactions. Color code: Grey, carbon; brown, bromine; green, chlorine; yellowish green, fluorine; dark teal, tin.

Crystals of tetrakis(2-chlorobenzyl)-tin (Refcode CEWGEQ) [112] are a nice example of intramolecular C–Sn···Cl interactions as three such contacts (Nc spans from 0.94 to 0.97) lock the molecular conformation (Fig. 24, left). Interestingly, tetrakis(2-methoxybenzyl)-tin (Refcode HEVFOD) [113] and tetrakis(2-fluorobenzyl)-tin (Refcode VULSOM) [114] show in their respective crystals four intramolecular C–Sn···O and C–Sn···F TBs, respectively. Tetrakis(chloromethyl)-tin (Refcode UGATEB) [115] is a nice case of intermolecular C–Sn···Cl contacts. The molecule works as a self-complementary bidentate TB donor (at tin) and acceptor (at chlorine) (Fig. 24, right) and a tetrel bonded (4,4) network is formed wherein UGATEB sits at the nodes.

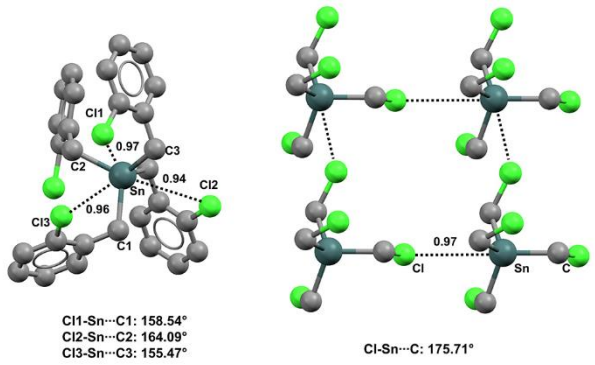

Fig. 24 Ball and stick representation (Mercury 3.9) of the conformation adopted by tetrakis(2-chlorobenzyl)-tin (CEWGEQ01, left) and the network generated by tetrakis(chloromethyl)-tin (UGATEB, right). TBs are black dotted lines, hydrogen atoms have been omitted for clarity. Nc values are reported close to the respective interactions. Color code: Grey, carbon; green, chlorine; dark teal, tin.

The conformation of diphenyl-(6-bromo-1,2-dihydroacenaphthylen-5-yl)-chloro-tin (Refcode VEKKUT) [116] is influenced by an intramolecular TB wherein the bromine atom enters the elongation of the Cl–Sn bond (Nc = 0.78, the Cl–Sn···Br angle is 172.06) (Fig. 25, bottom) [116]. Similar Cl–Sn···Br contacts are present in various other (6-bromo-1,2-dihydroacenaphthylen-5-yl)-tin derivatives. Bromine atoms can be involved also in intermolecular TBs. This is the case in steroid derivative 3β-(bromodimethylstannyl)-24-nor-5β-cholane (Refcode MISYAO) [117] (Fig. 25, top) which shows, in the crystals, 1D infinite chains assembled via Br-Sn···Br.

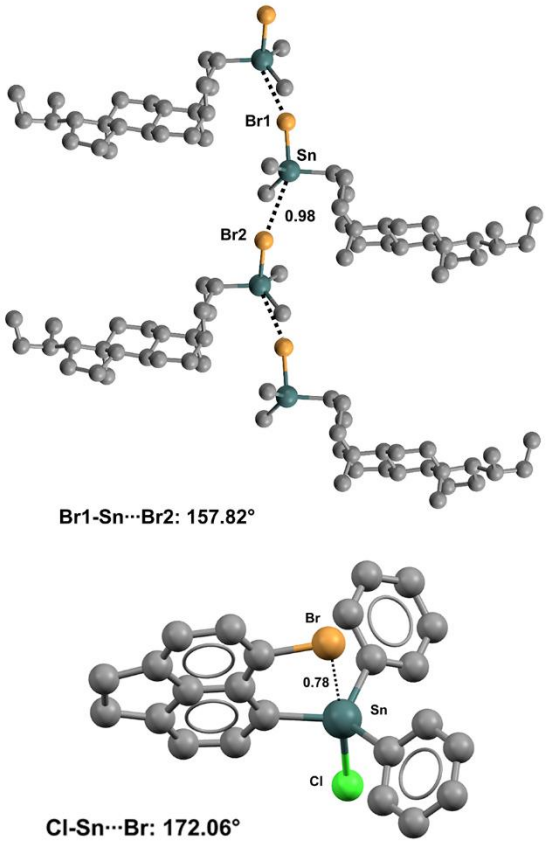

Fig. 25 - Ball and stick representation (Mercury 3.9) of the conformation adopted by chloro-(6-bromo-1,2-dihydroacenaphthylen-5-yl)-diphenyl-tin (VEKKUT, bottom) and the 1D chain generated by 3β-(bromodimethylstannyl)-24-nor-5β-cholane (MISYAO, rtop). TBs are black dotted lines, hydrogen atoms have been omitted for clarity. Nc values are reported close to the respective interactions. Color code: Grey, carbon; brown, bromine; dark teal, tin.

The covalent bonds pathway connecting iodine and tin in (8-iodo-1-naphthyl)-trimethyl-tin (Refcode AQIVUS) [118] recalls that connecting bromine and tin in VEKKUT and this translates into the supramolecular similarity between the C–Sn···I TB in the former compound and the Cl–Sn···Br TB in the latter. In the crystal structure of bromo-(4-iodo-1,2,3,4-tetraphenyl-1,3-butadienyl)-diphenyl-tin (Refcode SICSOM) (Fig. 26, bottom) [119] the iodine atom works as the TB acceptor and gets close to tin, the TB donor, on the elongation of the Br–Sn bond (Nc = 0.94 and the Br–Sn···I angle is 168.95°). This pattern is consistent with the fact that the more positive σ-hole on tin is expected in this position as bromine is more electron withdrawing than other atoms bound to tin. Finally, the Sn···I interactions present in crystals of tris(trimethylstannyl)ammonium iodide (Refcode RONDAZ) [120] give a nice example of charge assisted TB. The existence of this type of

TBs further confirms the analogy among the different subsets of σ-hole interactions, as charge assisted XBs [121] and charge assisted PBs [31] have already been observed. Specifically, two crystallographically independent salt units are present in the crystal of RONDAZ, in both of them the tris(trimethylstannyl)ammonium cations work as tridentate TB donors, the iodide anion as tridentate TB acceptors, and 3D networks are formed (one 3D net is reported in Fig. 26, top).

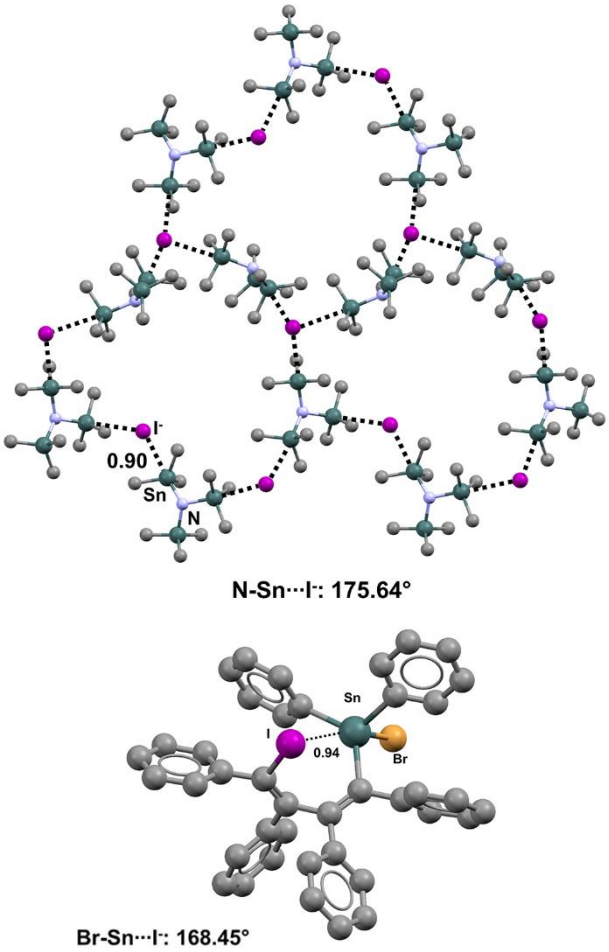

Fig. 26 Ball and stick representation (Mercury 3.9) of the conformation adopted by bromo-(4-iodo-1,2,3,4-tetraphenyl-1,3-butadienyl)-diphenyl-tin (SICSOM, bottom) and the network formed by tris(trimethylstannyl)ammonium iodide (RONDAZ, top). One layer of RONDAZ is reported and hydrogen atoms have been omitted for clarity. TBs are black dotted lines and Nc values are reported close to the respective interactions. Color code: Grey, carbon; purple, iodine; brown, bromine; light blue, nitrogen; dark teal, tin.

Conclusion

In this paper we report the results of an analyses of the CSD aimed at identifying crystal structures of organic derivatives of germanium and tin wherein these two elements form short contacts with lone pair possessing atoms.

Attention has been focused on short contacts where oxygen, nitrogen, and halogens are the lone pair possessing atoms as a wider set of examples was found in the CSD for these atoms. However, it may be worth mentioning that other heteroatoms (e.g., sulfur [122–124] and phosphorous [125–127]) also form similar interactions. Ether and carbonyl oxygens as well as amine, pyridine, and cyano nitrogens can all be involved in these interactions and the observed geometry indicates that the lone pair of these heteroatoms is directed towards the germanium/tin atom independent of the hybridization of the oxygen/nitrogen atom (which can be sp^3, sp^2, or sp). Short contacts are formed by derivatives where germanium and tin atoms bear four carbon residues or where halogen, oxygen, sulfur, or nitrogen substituents replace one, two, or three such carbon residues. Independent of the nature and hybridization state of the lone pair possessing atom and independent of the nature of the residues covalently bound to germanium and tin, the short contacts are preferentially formed on the elongation of the covalent bonds that germanium and tin form with strong electron withdrawing residues. Moreover, the more electron withdrawing the residue bound to germanium/tin is, the shorter the interaction on its elongation is.

All these features are typical for σ-hole interactions and we are thus proposing to rationalize the short contacts described in this review as *tetrel bonds*. Tetravalent germanium and tin atoms have a tetrahedral geometry. When these atoms form one or two short contacts with lone pair possessing atoms, the geometry around them tends to change into trigonal bipyramidal or octahedral, respectively. These changes have been explained through an $sp^3 \rightarrow dsp^3$ or $sp^3 \rightarrow d^2sp^3$ rehybridization at the tetrels. It seem possible to explain these changes also resorting to the *tetrel bond* [128], namely via an attractive interaction between lone pairs and the positive σ-holes on the extensions of the covalent bonds formed by these tetrels. The presence of σ-holes on all the four tetrels has been widely indicated by modelling [34–37] and the geometric features of the interactions discussed in this review offer experimental evidences consistent with this presence. The *tetrel bond* rationalization is congruent with other alternative explanations mentioned above. It may offer the profit that these interactions given by Group 14 elements are understood after the same mindset enabling for the rationalization of interactions formed when elements of Groups 15–18 function as electrophilic sites.

The examined dataset is too limited to draw general conclusions but it seems to suggest that deviations of the interaction from the elongation of one of the covalent bonds is usually smaller for

the TBs formed by germanium and tin than for most PBs and CBs [31], This is consistent with theoretical calculations which show that the region of most positive electrostatic potential opposite to a covalent bond deviates from the extension of the bond more in pnictogen derivatives and less in tetrel derivatives [129, 130]. The greater linearity of TB may be related to the fact that the electronic dissymmetry generated around germanium and tin atoms by the four bonded residues is usually smaller than the dissymmetry generated around pnictogen and chalcogen atoms by the residues bonded to the pnictogen/chalcogen and the lone pair(s).

It also seems that steric congestion around the tetrel atoms studied in this paper plays a quite influential role in *tetrel bonds* formation to the point that interaction formation may be prevented. For instance, tetrakis(2-fluorobenzyl)-tin (Refcode VULSOM) forms four intramolecular TBs and the tetrakis(2-chlorobenzyl) analogue (Refcode CEWGEQ) forms three intramolecular TBs; methyl-tris((2-methoxymethyl)phenyl)germane (Refcode IMUTEP) forms one TB and the phenyl-tris((2-methoxymethyl)phenyl) analogue (IMUTIT) forms no TB.

In conclusion, the crystal structures discussed in this paper afford reliable experimental evidences that the electrophilic character of germanium and tin in some organic derivatives can be high enough that the *tetrel bonds* formed with a lone pair possessing atom can become a structural determining factor in crystalline solids. Intra- and intermolecular *tetrel bonds* can be present in crystals and the interactions can affect the preferred conformation of a molecule and/or the network of intermolecular interactions in the crystal lattice. These interactions seem reliable enough to become useful tools in crystal engineering.

Acknowledgements Authors are pleased to recognize the seminal role of Prof. Dr. Peter Politzer to the understanding of the the interactions discussed in this paper and of sister interactions now encompassed by the term σ-hole bondings. Authors are also grateful to Prof. Politzer for the fruitful discussions and collaborations on the topic.

References

1. Scheiner S (2015) Noncovalent forces. Noncovalent Forces. doi: 10.1007/978-3-319-14163-3

2. Kollman PA (1977) Noncovalent Interactions. Acc Chem Res 10:365–371. doi: 10.1021/ar50118a003

3. Riley KE, Pitoňčák M, Jureččka P, Hobza P (2010) Stabilization and structure calculations for noncovalent interactions in extended molecular systems based on wave function and density functional theories. Chem Rev 110:5023–5063. doi: 10.1021/cr1000173

4. Arunan E, Desiraju GR, Klein RA, et al (2011) Definition of the hydrogen bond (IUPAC Recommendations 2011). Pure Appl Chem. doi: 10.1351/PAC-REC-10-01-02

5. Desiraju GR, Steiner T (1999) The Weak Hydrogen Bond in Structural Chemistry and Biology; Oxford University Press, 2001. doi: 10.1093/acprof:oso/9780198509707.001.0001

6. Swart M, van der Wijst T, Fonseca Guerra C, Bickelhaupt FM (2007) π-π stacking tackled with density functional theory. J Mol Model 13:1245–1257. doi: 10.1007/s00894-007-0239-y

7. Dougherty DA (2013) The Cation-π Interaction. Acc Chem Res 46:885–893. doi: 10.1021/ar300265y

8. Schottel BL, Chifotides HT, Dunbar KR (2008) Anion-π interactions. Chem Soc Rev 37:68–83. doi: 10.1039/b614208g

9. Jiang XF, Hau FKW, Sun QF, Yu SY, Yam VWW (2014) From $\{Au^{I}\cdots Au^{I}\}$-coupled cages to the cage-built 2-D $\{Au^{I}\cdots Au^{I}\}$ arrays: $Au^{I}\cdots Au^{I}$ bonding interaction driven self-assembly and their Ag^{I} sensing and photo-switchable behavior. J Am Chem Soc 136:10921–10929. doi: 10.1021/ja502295c

10. Cavallo G, Metrangolo P, Milani R, et al (2016) The halogen bond. Chem Rev 116:2478–2601. doi: 10.1021/acs.chemrev.5b00484

11. Politzer P, Murray JS, Clark T (2014) σ-Hole bonding: A physical interpretation. Top Curr Chem 358:19–42. doi: 10.1007/128_2014_568

12. Clark T, Hennemann M, Murray JS, Politzer P (2007) Halogen bonding: The σ-hole. J Mol Model 13:291–296. doi: 10.1007/s00894-006-0130-2

13. Murray JS, Lane P, Politzer P (2009) Expansion of the σ-hole concept. J Mol Model 15:723–729. doi: 10.1007/s00894-008-0386-9

14. Murray JS, Lane P, Clark T, Politzer P (2007) σ-hole bonding: Molecules containing group VI atoms. J Mol Model 13:1033–1038. doi: 10.1007/s00894-007-0225-4

15. Murray JS, Lane P, Politzer P (2007) A predicted new type of directional noncovalent interaction. In: Int. J. Quantum Chem. pp 2286–2292

16. Brinck T, Murray JS, Politzer P (1992) Surface electrostatic potentials of halogenated methanes as indicators of directional intermolecular interactions. Int J Quantum Chem 44:57–64. doi: 10.1002/qua.560440709

17. Brinck T, Murray JS, Politzer P (1993) Molecular surface electrostatic potentials and local ionization energies of Group V–VII hydrides and their anions: Relationships for aqueous and gas- phase acidities. Int J Quantum Chem 48:73–88. doi: 10.1002/qua.560480202

18. Politzer P, Murray JS, Clark T (2013) Halogen bonding and other σ-hole interactions: a perspective. Phys Chem Chem Phys 15:11178–11189. doi: 10.1039/C3CP00054K

19. Wang H, Wang W, Jin WJ (2016) σ-Hole Bond vs π-Hole Bond: A Comparison Based on Halogen Bond. Chem Rev 116:5072–5104. doi: 10.1021/acs.chemrev.5b00527

20. Bauzá A, Mooibroek TJ, Frontera A (2015) The Bright Future of Unconventional σ/π-Hole Interactions. ChemPhysChem 16:2496–2517. doi: 10.1002/cphc.201500314

21. Politzer P, Murray JS, Clark T (2013) Halogen bonding and other σ-hole interactions: a perspective. Phys Chem Chem Phys 15:11178. doi: 10.1039/c3cp00054k

22. Cavallo G, Metrangolo P, Pilati T, et al (2014) Naming interactions from the electrophilic site. Cryst Growth Des 14:2697–2702. doi: 10.1021/cg5001717

23. Terraneo G, Resnati G (2017) Bonding Matters. Cryst Growth Des 17:1439–1440. doi: 10.1021/acs.cgd.7b00309

24. Metrangolo P, Pilati T, Resnati G, Stevenazzi A (2003) Halogen bonding driven self-assembly of fluorocarbons and hydrocarbons. Curr Opin Colloid Interface Sci 8:215–222. doi: 10.1016/S1359-0294(03)00055-4

25. Wang W, Ji B, Zhang Y (2009) Chalcogen bond: A sister noncovalent bond to halogen bond. J Phys Chem A 113:8132–8135. doi: 10.1021/jp904128b

26. Fick RJ, Kroner GM, Nepal B, et al (2016) Sulfur-Oxygen Chalcogen Bonding Mediates AdoMet Recognition in the Lysine Methyltransferase SET7/9. ACS Chem Biol 11:748–754. doi: 10.1021/acschembio.5b00852

27. Nayak SK, Kumar V, Murray JS, et al (2017) Fluorination promotes chalcogen bonding in crystalline solids. CrystEngComm 19:4955–4959. doi: 10.1039/C7CE01070B

28. Wonner P, Vogel L, Düser M, et al (2017) Carbon-Halogen Bond Activation by Selenium-Based Chalcogen Bonding. Angew Chemie - Int Ed 12009–12012. doi: 10.1002/anie.201704816

29. Legon AC (2017) Tetrel, pnictogen and chalcogen bonds identified in the gas phase before they had names: a systematic look at non-covalent interactions. Phys Chem Chem Phys 19:14884–14896. doi: 10.1039/C7CP02518A

30. Scheiner S (2013) The pnicogen bond: Its relation to hydrogen, halogen, and other noncovalent bonds. Acc Chem Res 46:280–288. doi: 10.1021/ar3001316

31. Scilabra P, Terraneo G, Resnati G (2017) Fluorinated elements of Group 15 as pnictogen bond donor sites. J Fluor Chem. 203: 62–74. doi: 10.1016/j.jfluchem.2017.10.002

32. (a) DeBackere JR, Bortolus MR, Schrobilgen GJ (2016) Synthesis and Characterization of $[XeOXe]^{2+}$ in the Adduct-Cation Salt, $[CH_3CN\text{-}\ \text{-}\ \text{-}XeOXe\text{-}\ \text{-}\ \text{-}NCCH_3][AsF_6]_2$. Angew Chemie - Int Ed 55:11917–11920; doi: 10.1002/anie.201606851, (b) Grabowski SJ (2014) Tetrel bond-σ-hole bond as a preliminary stage of the S_N2 reaction. Phys Chem Chem Phys 16:1824–1834. doi: 10.1039/c3cp53369g

33. (a) Jonsson B, Karlstrom G, Wennerstrom, H (1975) Ab initio molecular orbital calculations on the water-carbon dioxide system: Molecular complexes. Chem Phys Lett 30:58–59; doi.org/10.1016/0009-2614(75)85497-2. (b) Peterson KI, Klemperer W (1984) J. Structure and internal rotation of H_2O–CO_2, HDO–CO_2, and D_2O–CO_2 van der Waals complexes. J. Chem. Phys. 80:2439–2445; doi.org/10.1063/1.446993. (c) Peng YP, Sharpe SW, Shin SK, Wittig C, Beaudet RA (1992) Infrared spectroscopy of CO_2-D(H)Br complex: Molecular structure and its reliability. J. Chem. Phys. 97:5392–5402; doi: org/10.1063/1.463799. (d) Leopold KR, Fraser GT, Klemperer W (1984) Rotational spectrum and structure of the complex HCN-CO_2. J. Chem. Phys. 80:1039–1046; doi: org/10.1063/1.446830.

34. Mani D, Arunan E (2013) The X–C···Y (X = O/F, Y = O/S/F/Cl/Br/N/P) "carbon bond" and hydrophobic interactions. Phys Chem Chem Phys 15:14377–14383. doi: 10.1039/c3cp51658j

35. Bauzá A, Mooibroek TJ, Frontera A (2013) Tetrel-bonding interaction: Rediscovered supramolecular force? Angew Chemie - Int Ed 52:12317–12321. doi: 10.1002/anie.201306501

36. (a) Liu M, Li Q, Scheiner S (2017) Comparison of tetrel bonds in neutral and protonated complexes of pyridineTF_3 and furanTF_3 (T = C, Si, and Ge) with NH_3. Phys Chem Chem Phys 19:5550–5559; doi: 10.1039/C6CP07531B. (b) Alkorta I, Rozas I, Elguero J (2001) Molecular Complexes between Silicon Derivatives and Electron-Rich Groups. J. Phys. Chem. A 105: 743–749. doi: 10.1021/jp002808b.

37. Grabowski S, J. S (2017) Lewis Acid Properties of Tetrel Tetrafluorides—The Coincidence of the σ-Hole Concept with the QTAIM Approach. Crystals 7:43. doi: 10.3390/cryst7020043

38. Southern SA, Bryce DL (2015) NMR Investigations of Noncovalent Carbon Tetrel Bonds. Computational Assessment and Initial Experimental Observation. J Phys Chem A 119:11891–11899. doi: 10.1021/acs.jpca.5b10848

39. Mahmoudi G, Bauzá A, Frontera A (2016) Concurrent agostic and tetrel bonding interactions in lead(II) complexes with an isonicotinohydrazide based ligand and several anions. Dalt Trans 45:4965–4969. doi: 10.1039/c6dt00131a

40. Cheng F, Hector AL, Levason W, et al (2009) Preparation and structure of the unique silicon(IV) cation $[SiF_3(Me_3tacn)]^+$. Chem Commun (Camb) 1334–1336. doi: 10.1039/b822236c

41. Bondi A (1964) van der Waals Volumes and Radii. J Phys Chem 68:441–451. doi: 10.1021/j100785a001

42. The van der Waals radius of 210 pm was adopted for Germanium atoms as suggested by Batsanov in Batsanov SS (2001) Van der Waals Radii of Elements. Inorg Mater Transl from Neorg Mater Orig Russ Text 37:871–885. doi: 10.1023/A:1011625728803

43. Dostál L, Jambor R, Růžička A, et al (2007) Organotin(IV) derivatives of some O,C,O-chelating ligands. Part 2. Organometallics 26:6312–6319. doi: 10.1021/om700576n

44. Jambor R, Dostál L, Růžička A, Císařová I, Brus J, Holčapek M, Holeček J (2002) Organotin(IV) Derivatives of Some O,C,O-Chelating Ligands. Organometallics 21:3996–4004. doi: 10.1021/om020361i

45. Scheiner S (2017) Systematic Elucidation of Factors That Influence the Strenght of Tetrel Bonds. J Phys Chem A 121:5561–5568. doi: 10.1021/acs.jpca.7b05300

46. Sugiyama Y, Matsumoto T, Yamamoto H, et al (2003) Synthesis, solid-state and solution structures of tris[(2-methoxymethyl)phenyl]germanes with a substituent on germanium. Tetrahedron 59: 8689–8696. doi: 10.1016/j.tet.2003.09.053

47. Shindo M, Matsumoto K, Shishido K (2007) Hyperconjugative effect of C-Ge bonds: synthesis of multisubstituted alkenylgermanes via torquoselective olefination of acylgermanes with ynolates. Tetrahedron 63:4271–4277. doi: 10.1016/j.tet.2007.03.048

48. Jousseaume B, Villeneuve PM, Driiger Roller S, Chezeau JM (1988) Unique tin-oxygen coordination bond in a pentacoordinated tetraorganotin compound. First confirmation by X-ray crystal structure of (2-carbomethoxy-1,4-cyclohexadien-1-yl) trimethyltin. J Organomet Chem 349:C1–C3. doi: 10.1016/0022-328X(88)80459-5

49. Beak P, Lee WK (1993) α-Lithioamine Synthetic Equivalents: Syntheses of Diastereoisomers from Boc Derivatives of Cyclic Amines. J Org Chem 58:1109–1117. doi: 10.1021/jo00057a024

50. Cintrat JC, Léat-Crest V, Parrain JL, et al (2004) Identification of chiral *cis*- and *trans*-2-stannyloxazolidines by their NMR spectra and solid-state structures. European J Org Chem 4268–4279. doi: 10.1002/ejoc.200400203

51. Gurkova SN., Gusev AI., Alekseev NV., Gar TK, Viktorov NA (1984) Intramolecular interactions in germanium compounds. Crystal and molecular structures of the N,N'-dimethylamide of 2-methyl-3-(trichlorogermyl) propionic acid and 1-(1-trichlorogermyl) pyrrolid-2-one. J Struct Chem 25:825–828.

52. Deka DC, Helliwell M, Thomas EJ (2001) Synthesis of chiral organotin reagents: Synthesis and X-ray crystal structures of bicyclo[2.2.1]heptan-2-yl(diphenyl)tin chlorides with cis-disposed nitrogen containing substituents. Tetrahedron 57:10017–10026. doi: 10.1016/S0040-4020(01)01035-3

53. Tretyakov EV, Mareev AV, Demina MM, et al (2009) Silyl- and germylpropynals in the synthesis of azolyl-substituted 2-imidazoline 3-oxide 1-oxyls. Russ Chem Bull 58:1915–1920. doi: 10.1007/s11172-009-0261-6

54. Gurkova SN, Gusev AI, Alekseev NV. Gar, TK, Viktorov NA (1984) Intramolecular interactions in Germanium compounds. Crystal and molecular structure of 1,3-diphenyl-3-methyl-3-(trichlorogermyl)-butan-1-one. J Struct Chem 25:829–831.

55. Wang LB (2007) (μ-2,2′-biquinolinyl-4,4′-dicarboxylato-κ ^{2} *O* :*O*′)bis[(dimethylformamide-κ *O*)triphenyltin(IV)]. Acta Crystallogr Sect E Struct Reports Online 63:m1883–m1883. doi: 10.1107/S1600536807028048

56. Lorberth J, Shin S, Donath H, Wacadlo S, Massa W (1991) Crystal structure of trimethyltin diazoacetic ester. 407:167–171.

57. Lukevics E, Arsenyan P, Belyakov S, et al (1999) Cycloaddition Reactions of Nitrile Oxides to Silyl- and Germyl-Substituted Thiophene-1,1-dioxides. Organometallics 18:3187–3193. doi: 10.1021/om9902129

58. Chuprunov EV, Stolyarova NE, Shcherbakov VI, Tarkhova TN (1988) Crystal structure of N-triethylstannylsuccinimide. J Struct Chem Chem 28:797–799.

59. Jaray O, Pritzkow H, Jander J (1977) X-ray Structural Analysis of Organic N-Br Compounds for Making Visible General Structure Elements of Bromamines. Z Naturforsch 32b:1416–1420.

60. Adama MS., Du D-F, Zhu D-S, Xu L (2011) The One-Dimensional Chain: Synthesis, Crystal Structure and Biological Activities of Tricyclohexyl Tin Carboxylates. Chin J Struct Chem 27:107–113.

61. Kuang D-Z, Zhu X-M, Feng Y-L, Zhang F-X, Yu J-X, Jiang W-J, Tan Y-X, Zhang-JZ (2015) Syntheses, Crystal Structures and Biological Activities of Bis(tricyclohexyltin)dicarboxylates with Macrocyclic Building 2D Network. Chin J Struct Chem 31:2044–2050.

62. Ma C, Wang Q, Zhang R (2008) Self-Assembly of Triorganotin Complexes: Syntheses, Characterization, and Crystal Structures of Dinuclear, 1D Polymeric Chain, and 2D Network Polymers Containing Chiral (+)-(1*R*,3*S*)-Camphoric Acid andmeso-*cis*-4-Cyclohexene-1,2-dicarboxylic Acid Ligands. Eur J Inorg Chem 2008:1926–1934. doi: 10.1002/ejic.200701211

63. Uehara K, Nakao H, Kawamoto R, et al (2006) 2D-grid layered Pd-based cationic infinite coordination polymer/polyoxometalate crystal with hydrophilic sorption. Inorg Chem 45:9448–9453. doi: 10.1021/ic061393r

64. Taylor P, Poll E, Olbrich F, Fischer RD (2014) $[Sn_2(H_2O)_2Br_2(CH_3)_4\{\mu\text{-}(CH_2)_3\cdot 2bpy]$: A Layered, Hetero Bimolecular Composite (bpy=2,2-bipyridine). Supramol Chem 10:2014. doi: 10.1080/10610270290029344

65. Reeske G, Schürmann M, Costisella B, Jurkschat K (2005) Organotin-substituted crown ethers for ditopic complexation of anions and cations. Eur J Inorg Chem 2881–2887. doi: 10.1002/ejic.200500191

66. Mandolesi S, Studentkowski M, Preut H, Mitchell T (2001) A 1:1 adduct between 2,2-bis(chlorodimethylstannyl)propane and dimethyl sulfoxide. Acta Crystallogr Sect E Struct Reports Online 57:m543–m544. doi: 10.1107/S1600536801017603

67. Zhu FC, Shao PX, Yao XK, et al (1990) Stereochemistry and crystal structures of triphenyltin chloride complexes with bis(phenylsulfinyl)ethane. Inorganica Chim Acta 171:85–88. doi: 10.1016/S0020-1693(00)84669-1

68. Kumar S, Shadab SM, Idrees M (2009) Chlorido(dimethyl sulfoxide-κ*O*)triphenyltin(IV). Acta Crystallogr Sect E Struct Reports Online 65:m1602–m1603. doi: 10.1107/S1600536809048090

69. Howie RA,. Wardell JL (1994) Structures of $Ph_3SnCH_2CH_2CH_2SO_2C_6H_4Me$-p and $IPh2SnCH_2CH_2CH_2SO_2C_6H_4Me$-p. Main Group Met. Chem. 17:571–582. doi: org/10.1515/MGMC.1994.17.8.571

70. Lo KM, Ng SW (2011) Tribenzyl-chlorido(triphenyl-phosphine oxide-κO)tin(IV). Acta Crystallogr Sect E Struct Reports Online 67:112–122. doi: 10.1107/S160053681101957X

71. Lo KM, Ng SW (2004) [Chlorobis(*p* -chlorophenyl)(*p* -tolyl)tin]-μ-1,2-bis(diphenylphosphoryl)ethane-κ^2*O*:*O*′-[bromobis(*p*-chlorophenyl)(*p*-tolyl)tin]. Acta Crystallogr Sect E Struct Reports Online 60:m717–m719. doi: 10.1107/S1600536804010219

72. Preut H, Godry B, Mitchell TN (1992) [2-(bromodimethylstannyl)ethyl]diphenylphosphine sulfide. Acta Crystallogr Sect C 48:1491–1493. doi: 10.1107/S0108270191014750

73. Shariatinia Z, Mirhosseini Mousavi HS, Bereciartua PJ, Dusek M (2013) Structures of a novel phosphoric triamide and its organotin(IV) complex. J Organomet Chem 745–746:432–438. doi: 10.1016/j.jorganchem.2013.08.003

74. Jurkschat K, Tzschach A, Meunierpiret J (1986) Synthesis, Crystal and molecular structure of 1-aza-5-stanna-5-methyltricyclo[3.3.3.01,5]undecane. Evidence for a transannular donor-acceptor interaction in a tetraorganotin compound. J Organomet Chem 315:45–49. doi: 10.1016/0022-328X(86)80409-0

75. Jurkschat K, Hesselbarth F, Dargatz M, Lehmann J, Kleinpeter E, Tzschach A, Meunierpiret J (1990) 1,2-bis(organostannyl)ethanes as powerful bidentate Lewis acids. Crystal structures of $(Ph_2ClSnCH_2)_2\cdots(Me_2N)_2PO$ and $[Ph_3P{=}N{=}PPh_3][(Ph_2ClSnCH_2)_2\cdots Cl]$. J Organomet Chem 388:259–271. doi: 10.1016/0022-328X(90)85373-7

76. Lo KM, Ibrahim AR, Chantrapromma, S, Fun HK, Ng SW (2001) Main Gr Met. Chem. 24:301. doi: org/10.1515/MGMC.2001.24.5.301

77. Breliere C, Carre F, Corriu RJP, Royo G (1988) Synthesis and structures of hypervalent species of silicon and germanium: toward heptacoordination? Organometallics 7:1006–1008. doi: 10.1021/om00094a034

78. Wingerter S, Pfeiffer M, Stey T, et al (2001) The iminophosphorane Ph3P=NSiMe3 as a synthon for M-C_{aryl} σ bonds (M = In, Fe, Ge) implementing imino sidearm donation. Organometallics 20:2730–2735. doi: 10.1021/om0009738

79. Gurkova SN, Gusev AI, Alekseev NV, Segel'man RI, Gar TK, Khromova NYu (1983) Crystal and Molecular Structure of 1-(tert-Butyl)germatrane. J Struct Chem 24:155–157. doi: 10.1021/ic50138a020

80. Gurkova SN, Gusev AI, Alekseev NV, Segel'man RI, Gar TK, Khromova NYu (1983) Crystal and

molecular structure of 1-bromogermatrane. 24:238–241. doi: 10.1007/BF00747386.

81. Gurkova SN, Gusev AI, Alekseev NV, Segel'man RI, Gar TK, Khromova NYu (1981) Crystal and Molecular Structure of Iodomethylgermatrane. J Struct Chem 22:461–462.

82. Gurkova SN, Gusev AI, Alekseev NV, Gar TK, Khromova NYu (1981) Crystal and Molecular Structure of 1-methyl-2-carbagermatrane. J Struct Chem 22:924–926.

83. Gurkova SN, Gusev AI, Alekseev NV, Gar TK, Viktorov NA (1985) Crystal and molecular structure of 1-(germatranyl)-1-(2-pyrrolidonyl)ethane. J Struct Chem 26:124–127.

84. Shutov PL, Sorokin DA, Karlov SS, et al (2003) Azametallatranes of group 14 elements. Syntheses and X-ray studies. Organometallics 22:516–522. doi: 10.1021/om020708h

85. Karlov SS, Lermontova EK, Zabalov M V., et al (2005) Synthesis, X-ray diffraction studies, and DFT calculations on hexacoordinated germanium derivatives: The case of germaspirobis(ocanes). Inorg Chem 44:4879–4886. doi: 10.1021/ic048165m

86. Jurkschat K, Kolb U, Dräger M, Dargatz M (1995) Unusual Hexacoordination in a Triorganotin Fluoride Supported by Intermolecular Hydrogen Bonds. Crystal and Molecular Structures of 1-Aza-5-stanna-5-halogenotricyclo[3.3.3.01.5]undecanes $N(CH_2CH_2CH_2)_3SnF \cdot H_2O$ and $N(CH2CH_2CH_2)_3SnX$ (X = Cl, Br, I). Organometallics 14:2827–2834. doi: 10.1021/om00006a031

87. Jurkschat K, Tzschach A (1985) Crystal and Molecular Structure of 1-aza-5-stanna-5-chlorotricyclo[3.3.3]undecane, a 2,8,9-Tricarbastannatrane. J Organomet Chem 290:285–289.

88. Turek J, Padělková Z, Černošek Z, et al (2009) C,N-chelated hexaorganodistannanes, and triorganotin(IV) hydrides and cyclopentadienides. J Organomet Chem 694:3000–3007. doi: 10.1016/j.jorganchem.2009.04.043

89. Růžička A, Padělková Z, Švec P, et al (2013) Quest for triorganotin(IV) compounds containing three C,N- and N,C,N-chelating ligands. J Organomet Chem 732:47–57. doi: 10.1016/j.jorganchem.2013.02.018

90. Kawachi A, Tanaka Y, Tamao K (1999) Synthesis and structures of a series of Ge-M (M=C, Si, and Sn) compounds derived from germyllithium containing three 2-(dimethylamino)phenyl groups on germanium. J Organomet Chem 590:15–24. doi: 10.1016/S0022-328X(99)00386-1

91. Novák P, Císařová I, Jambor R, et al (2004) Coordination behaviour of the 2-(N,N-dimethylaminomethyl)phenyl ligand towards the di-t-butylchlorotin(IV) moiety. Appl Organomet Chem 18:241–243. doi: 10.1002/aoc.615

92. Pichler J, Torvisco A, Bottke P, et al (2014) Novel amino propyl substituted organo tin compounds. Can J Chem 92:565–573. doi: 10.1139/cjc-2013-0504

93. Zhu C, Yang L, Li D, et al (2011) Synthesis, characterization, crystal structure and antitumor activity of organotin(IV) compounds bearing ferrocenecarboxylic acid. Inorganica Chim Acta 375:150–157. doi: 10.1016/j.ica.2011.04.049

94. Winkelhaus D, Neumann B, Stammler H-G, Mitzel NW (2012) Bis(tetrafluorophenyl)borane. Dalt Trans 41:8609. doi: 10.1039/c2dt30924f

95. Hong M, Geng H, Niu M, Wang F, Li D, Liu J, Yin H (2014) Organotin(IV) complexes derived from Schiff base N'-[(1E)-(2-hydroxy-3-methoxyphenyl)methylidene]pyridine-3-carbohydrazone: Synthesis, in vitro cytotoxicities and DNA/BSA interaction. Eur J Med Chem 86:550–561. doi: 10.1016/j.jorganchem.2015.12.041

96. Gupta AN, Kumar V, Singh V, et al (2015) Influence of functionalities on the structure and luminescent properties of organotin(IV) dithiocarbamate complexes. J Organomet Chem 787:65–72.

doi: 10.1016/j.jorganchem.2015.03.034

97. Feng YL, Yu J-X, Kuang D-Z, Yin D-L, Zhang F-X, Wang J-Q, liu M-Q (2011) Synthesis, Crystal Structure and Quantum Chemistry of Tricyclohexyl Tin Pyridine-4-Carboxylate Polymer. Chin J Inorg Chem 27:1793–1797.

98. Chandrasekhar V, Mohapatra C (2013) 2D-coordination polymer containing interconnected 82-membered organotin macrocycles. Cryst Growth Des 13:4655–4658. doi: 10.1021/cg401363p

99. Ma CL, Han YF, Li DC (2004) Synthesis and crystal structures of diorganotin dicyanoethylene-1,2-dithiolate compounds and their derivatives with 4,4'-Bipy or Phen. Polyhedron 23:1207–1216. doi: 10.1016/j.poly.2004.01.019

100. Bajue SA, Bramwell FB, Charles M, et al (1992) Crystal and molecular structures of the adducts of tri-p-tolyltin chloride, bromide and iodide with 4,4'-bipyridine. Inorganica Chim Acta 197:83–87. doi: 10.1016/S0020-1693(00)85523-1

101. Avalle P, Harris RK, Hanika-Heidl H, Dieter Fischer R (2004) Magic-angle spinning NMR spectra and re-examined crystal structure of trimethyltin cyanide. Solid State Sci 6:1069–1076. doi: 10.1016/j.solidstatesciences.2004.06.001

102. Konnert JH, Britton D, Chow YM (1972) The crystal structures of the dimethyldicyano compounds of silicon, germanium, tin and lead. Acta Crystallogr Sect B Struct Crystallogr Cryst Chem 28:180–187. doi: 10.1107/S0567740872002043

103. Kuang DZ, Jiang JP, Feng YL, Zhang FX, Wang JQ, Luo JM (2008) Synthesis and crystal structure of tetra(o-cyanobenzyl)tin. Chin J Struct Chem 27:35–38.

104. Švec P, Růžičková Z, Vlasák P, et al (2016) Expanding the family of C,N-chelated organotin(IV) pseudohalides: Synthesis and structural characterization. J Organomet Chem 801:14–23. doi: 10.1016/j.jorganchem.2015.10.014

105. Coffer PK, Dillon KB, Howard JAK, et al (2012) Synthesis and characterisation of selected group 14 derivatives of the 2,5-$(CF_3)_2C_6H_3$ (Ar) ligand. Dalt Trans 41:4460–4468. doi: 10.1039/c2dt12369j

106. Brisdon AK, Pritchard RG, Thomas A (2012) Pentafluoropropenyl complexes of mercury, germanium, tin, and lead derived from (*Z*)-$CFH{=}CFCF_3$ and their use as transfer reagents. Organometallics 31:1341–1348. doi: 10.1021/om2009843

107. Calogero S, Ganis P, Peruzzo V, Tagliavini G, Valle G (1981) X-ray and mössbauer studies of tricyclohexyltin(IV) halides. The crystal structures of (cyclo-C_6H_{11})3SnX (X = F, Br and I). J Organometallic Chem 220:11–20.

108. Bilayet Hossain M, Lefferts JL, Molloy KC, Van der Helm D, Zuckerman JJ (1979) Crystal and Molecular Structure of Trimethyl- tin Chloride at 135 K. Inorganica Chim Acta 36:L409–L410.

109. Chaudhary P, Bieringer M, Hazendonk P, Gerken M (2015) The structure of trimethyltin fluoride. Dalton Trans. 44:19651–19658. doi: 10.1039/C5DT01994J

110. Alcock NW, Sawyer JF (1977) Secondary Bonding. Part 2. Crystal and Molecular Structures of Diethyltin Dichloride, Dibromide, and Diiodide. J Chem Soc Dalt Trans 1090–1095.

111. Frank W, Reiss GJ, Kuhn D (1994) Trichloromethyltin(IV). Acta Crystallogr Sect C Cryst Struct Commun 50:1904–1906. doi: 10.1107/S010827019400795X

112. Schürmann M, Silvestri A, Ruisi G, et al (1999) The structure and dynamics of Cl-substituted tetraphenyl- and tetrabenzyl-tin(IV). J Organomet Chem 584:293–300. doi: 10.1016/S0022-328X(99)00166-7

113. Ross JN, Wardell J, Ferguson G, Low JN (1994) Symmetrical tetrasubstituted tin compounds:

tetrakis(2-methoxyphenyl)tin and tetrakis(2-methoxybenzyl)tin. Acta Crystallogr Sect C Cryst Struct Commun 50:1703–1707. doi: 10.1107/S0108270194006815

114. Zhang FU, Kuang DZ, Feng YL, Wang JQ, Yu JZ, Jiang WJ, Zhu XM (2015) Synthesis, Crystal structure and Properties of the tetra(*o*-fluorobenzyl)tin and the tribenzyltin Ferrocenecarboxylate. Chin J Struct Chem 31:1194–1200. doi: 10.11862/CJIC.2015.157

115. Veith M, Agustin D, Huch V (2002) New synthetic approach and structural characterization of the chloroalkylstannanes $(Cl\text{-}CH_2)_n\ SnCl_{4-n}$ (n = 2,4) and the hydrolysis product $[(ClCH_2)_2Sn(Cl)\text{-}O\text{-}Sn(Cl)(CH_2Cl)_2]_2$. J Organomet Chem 646:138–145. doi: 10.1016/S0022-328X(01)01099-3

116. Lechner ML, Athukorala Arachchige KS, Randall RAM, et al (2012) Sterically crowded tin acenaphthenes. Organometallics 31:2922–2930. doi: 10.1021/om201253t

117. Schiesser CH, Skidmore MA, White JM (2001) Stannanes from cholic acid as enantioselective free-radical reducing agents. Aust J Chem 54:199–204. doi: 10.1071/CH01045

118. Meyer N, Sivanathan S, Mohr F (2011) Transfer of organic groups to gold using organotin compounds. J Organomet Chem 696:1244–1247. doi:l0.1016/jJorganchem.2010.10.060

119. Muchmore CRA, Heeg MJ (1990) Structure of bromo(4-iodo-1,2,3,4-tetraphenyl-1,3-butadienyl)diphenyltin(IV). Acta Crystallogr Sect C Cryst Struct Commun 46:1743–1745. doi: 10.1107/S0108270190003158

120. Hillwig R, Harms K, Dehnicke K, Muller U (1997) Organoelement substituted ammonia salts. Crystal structures of $[HN(SnMe_3)3]I$, $[H_2N(SnMe_3)_2][SnMe_3Cl_2]$, and $[N(AsMe_3)_2]Br$. Z Anorg Allg Chemie 623:676–682. doi: 10.1002/zaac.199762301107

121. Cavallo G, Murray JS, Politzer P, et al (2017) Halogen bonding in hypervalent iodine and bromine derivatives: Halonium salts. IUCrJ 4:411–419. doi: 10.1107/S2052252517004262

122. Affan MA, Salam MA, Ahmad FB, Hitam RB, White F 2012) Triorganotin(IV) complexes of pyruvic acid-N(4)-cyclohexylthiosemicarbazone (HPACT): Synthesis, characterization, crystal structure and in vitro antibacterial activity. Polyhedron 33:19–24. doi: 10.1016/j.poly.2011.11.021

123. Jurkschat K, Schmid B, Dybiona M, Baumeister U, Hartung H, Tzschach A (1988) Zur Struktur und Reaktivitat von stannylierten Propylaminen und -sulfiden. Kristall- und Molekulstruktur von Bis(3-dimethyl. chlorostannylpropy1)suIfid $S(CH_2CH_2CH_2SnMe_2CI)$. Z Anorg Allg Chem 560:110–118. doi: 10.1002/zaac.19885600113

124. Vargas-Pineda DG, Guardado T, Cervantes-Lee F, et al (2010) Intramolecular chalcogen-tin interactions in $[(o\text{-}MeEC_6H_4)CH_2]_2SnPh_{2-n}Cl_n$ (E = S, O, CH2; n = 0, 1, 2) and intermolecular chlorine-tin interactions in the meta- and para-methoxy isomers. Inorg Chem 49:960–8. doi: 10.1021/ic901800c

125. Seibert M, Merzweiler K, Wagner C, Weichmann H (2002) Synthesis and structural behavior of the P-functional organotin. J Organomet Chem 650:25–36. doi: 10.1016/S0022-328X(02)01116-6

126. Hoppe S, Weichmann H, Jurkschat K, et al (1995) Synthesis and structural studies of 2-stannyl-substituted ferrocenylmethylamine and -phosphine derivatives $2\text{-}Me_2RSnFcCH_2Y$ (R=Me, Cl; Y=NMe_2, PPh_2, $P(O)Ph_2$; Fc=$C_{10}H_8Fe$). J Organomet Chem 505:63–72. doi: 10.1016/0022-328X(95)05549-5

127. Baumeister U, Hartung H, Krug A, Merzweiler K, Schulz T, Wagner C, Weichmann H (2000) Ligand Behaviour of P-functional Organotin Halides: Nickel(II), palladium(II), and platinum(II) complexes with $Me\text{-}2(Cl)SnCH_2CH_2PPh_2$. Z Anorg Allg Chem 626:2185-2195.

128. Politzer P, Murray JS, Lane P, Concha MC (2009) Electrostatically driven complexes of SiF_4 with amines. In: Int. J. Quantum Chem. 109:3773–3780. doi: 10.1002/qua.22385

129. Scheiner S (2016) Highly Selective Halide Receptors Based on Chalcogen, Pnicogen, and Tetrel Bonds. Chem - A Eur J 22:18850–18858. doi: 10.1002/chem.201603891

130. Murray JS, Resnati G, Politzer P (2017) Close contacts and noncovalent interactions in crystals, Faraday Discuss. 203:113–130. doi: 10.1039/c7fd00062f

131. Politzer P, Murray JS, Clark T, Resnati G (2017) The σ-hole revisited. doi: 10.1039/C7CP06793C